THE UNIVERSITY OF CHICAGO

MACROPHAGE INFLAMMATION AND LIPID METABOLISM IN ATHEROSCLEROSIS

A DISSERTATION SUBMITTED TO

THE FACULTY OF THE DIVISION OF THE BIOLOGICAL SCIENCES

AND THE PRITZKER SCHOOL OF MEDICINE

IN CANDIDACY FOR THE DEGREE OF

DOCTOR OF PHILOSOPHY

COMMITTEE ON MOLECULAR METABOLISM AND NUTRITION

BY

VICTOR DANIEL MENDOZA

CHICAGO, ILLINOIS

AUGUST 2023

DEDICATION

To my ancestors - Benzaa, Benii-logeshi

……

Gu'subu quidad teh xi'gűish gaku tu shi gaku

TABLE OF CONTENTS

LIST OF FIGURES

LIST OF TABLES

ACKNOWLEDGEMENTS

Death is a prominent figure in my indigenous *Benzaa* community in the mountainous region of Oaxaca. My people live their everyday lives with the idea that we will all be *going back.* This foundational principle has influenced every aspect of my life and influenced my educational trajectory. I am cognizant that the only thing I will leave behind is impact I have made on others' lives. This desire to make an impact influenced me to be a part of the solution to diminish inequalities, particularly in metabolic health disorders and education, so that future generations do not have to go through what I did. For this reason, I pursued a doctoral degree in Molecular Metabolism & Nutrition to help close the health inequities in metabolic disorders and scientific literacy observed in disadvantaged minority populations.

Graduate school in the natural sciences is challenging for *everyone*. However, there are additional social, economic, and psychological barriers faced by disabled first-generation low-income underrepresented minority students to succeed (Redford, Hoyer, 2017). This is in contrast to most individuals who seek doctoral degrees as they usually have parents who received post-secondary education or are accustomed to the independent socioeconomic culture and can navigate the rough environment of academic science (Morgan et al., 2022). And I can attest to this, as the challenges I perceived being the first in my family to obtain a high school diploma, bachelor's degree, and doctoral degree were insurmountable. This included full time minimum wage employment, full time undergraduate workload while facing homelessness and institutional barriers. Nevertheless, I persevered. During my studies at The University of Chicago, I was tremendously privileged to have basic needs of shelter, food, and access to medical care which afforded me the time and resources to process the tremendous trauma that I had carried and

unfortunately this often hindered me in achieving my absolute best. Yet, I persisted, with the tremendous help of the faculty, friends, and family.

With that in mind, my academic and research journey can be summarized by two prominent African Proverbs:

'*If you want to go fast, go alone. If you want to go far, go together*'(*Were The African Proverbs Mentioned At The DNC Really African Proverbs? : Goats and Soda : NPR*, n.d.) and

'*It takes a village to raise a child.*' (Reupert et al., 2022)

The contents of this dissertation, including my academic and personal growth, would not have been possible if not for the contributions from countless individuals.

Emblematic of the Becker lab is the collaborative essence that each research project takes. Just like all others, this research endeavor here is no different. This dissertation and work portrayed here represents the culmination of community-like work both in the experiments performed and in the mentoring I received during my tenure at The University of Chicago.

First and foremost, I would like to extend my deepest gratitude to my thesis advisor, Dr. Lev Becker. His invaluable guidance, unwavering support, and expertise in the field have been instrumental in shaping this research and pushing me to achieve my best. His insightful feedback has been instrumental in refining this work and my scientific thinking. He has taught me countless scientific and life lessons, including to use everything in my power and not *luck* to

achieve my best. Furthermore, he believed in me even when I could not see what I could achieve. Words cannot express the impact he has made on my life.

I would also like to acknowledge Dr. Catherine Reardon for her exceptional teaching and meticulous research techniques. I was very fortunate to be her pupil in cardiovascular mouse techniques and animal husbandry that I performed in this dissertation. Her passion for education and commitment to fostering student scientific knowledge have inspired me to explore new avenues in my research. I am grateful for the valuable insights, contributions to the project, and knowledge she shared with me. Her previous published work with the LXR and apoE projects tremendously fueled and started this research. In addition, she provided her invaluable time throughout the entire process of writing this dissertation, which encompassed meticulous editing of the document's contents, and played an important role in bringing this thesis to its successful completion. I learned so much from her and I cannot express how thankful I am.

I am deeply indebted to Matthew Brady, the Chair of the Committee on Molecular Metabolism & Nutrition, for his tremendous support, encouragement, and mentorship. From the moment I interviewed to this program to the end of this graduate experience, I felt he truly cared about *me* as a person and my success. He extends this nurturing essence to the entire committee on Molecular Metabolism & Nutrition and has played a role in making sure all students succeed. His leadership and guidance have provided me with a nurturing academic environment in which to thrive, especially on the days where I felt like I did not belong. His willingness to allocate resources and facilitate learning opportunities have been instrumental in the successful completion of my thesis and my growth. Thank you, from the bottom of my heart.

I would also like to express my heartfelt appreciation to Kasturi Chakraborty, whose contributions have been invaluable to this project, my scientific development, and my

development as an individual. The DNA nanotechnology expertise she brought was paramount to the third chapter of this dissertation and for successful completion of my PhD and for the co-first author publication. She taught me a myriad of lessons I will never forget, including microscopy and scientific thinking. Her presence in the lab was key to my perseverance – I don't know where I would be without her constant support, mentorship, and absolute willingness to put science and truth above all else. She leads by example and constantly attempts to diminish bias in her thinking. As a woman of color in the sciences, she does not let institutional bias and perception interfere with her scientific goals and career aspirations. I am truly inspired, and I hope I could be a scientist like her one day. I wish to emulate her strength and her desire to mentor, nurture, and support students and subordinates.

I would like to thank Guolin Zhou and Xu Anna Tang, for their work in this dissertation. Their work ethic is tremendously inspiring, and they have been instrumental in every single project. They contributed significantly to the project by helping me run quantitative PCR and westerns. Their support and morale in the lab were crucial for my survival in obtaining this degree. To Kelly Schoenfelt who provided me invaluable lessons in bone marrow isolations and primary hepatic isolations and worked with me side by side on those long days of dissecting the aortas from mice, each which took about 2 hours per mice so they could be completed in one day. Her spirit immediately lightened the lab environment. To Kasia Kurylowicz, having joined recently joined the Lab, her spirit and dedication to work are truly inspiring, I am grateful to call her my friend.

I would like to thank past lab members including visiting Ph.D. scholar Gustavo Davanzao, who inspired me to be better and spent time with me teaching various biological techniques. His enthusiasm for science was infectious. To Kierstin Webster, who joined the lab

alongside me and was my support buddy, I cherish the times we spent together and getting through it.

To Dean Nancy Schwartz and Dr. Laurie Risner for their incredible support throughout this process and providing me with guidance. To Melissa Lindberg and Dean Victoria Prince who opened their doors and welcomed me with open arms.

To my chosen family Andrew Schuman who has been through a lot with me for the past ten years, Elena Cortés, Juan Ibarra, Jessica Priest, Fabian Bylehn, and Jonathan Salmeron – thank you for your support during this process. I could have not done it without you all. Lastly, I would like to extend my gratitude to all the professors, friends, and family members who have provided support, encouragement, and motivation throughout this journey. Your belief in my abilities and unwavering encouragement have been a constant source of inspiration. Your feedback and insights have helped shape this thesis into its final form.

Without the support and guidance of these exceptional individuals, this thesis would not have been possible. I am truly grateful for their contributions and the impact they have had on my academic and personal growth.

ABSTRACT

Atherosclerosis, a complex vascular disease, is increasingly recognized as an immunometabolic disorder due to the intricate interplay between inflammatory cytokines, blood-borne leukocytes, hyperlipidemia, and vascular cells during lesion development. During my doctoral studies, I focused on investigating cholesterol metabolism and inflammation within atherosclerotic macrophages, aiming to develop novel therapeutic methods. In chapter two, my research aimed to uncover a non-canonical signaling pathway triggered by interferon gamma, which plays a role in excessive cholesterol uptake by macrophages in individuals with obesity and insulin resistance. This excessive cholesterol uptake leads to larger atherosclerotic lesions and contributes to the increased risk of cardiovascular disease observed in patients with obesity and insulin resistance. To explore this pro-atherogenic pathway, I utilized in vivo models of atherosclerosis, conducted phosphoproteomic analyses, and employed small molecule inhibitors. In Chapter Three, my study focused on leveraging the activation of liver X receptor (LXR) in macrophages to promote cholesterol efflux, thereby reducing the size of atherosclerotic lesions. To accomplish this, I used a DNA nanodevice that conjugated to an LXR agonist, enabling targeted modulation of LXR activation to macrophages without the typical side effect of hypertriglyceridemia in the liver. Through this innovative approach, I demonstrated the potential of new therapeutic strategies in addressing atherosclerosis. Additionally, I investigated the mechanism of metabolism and drug release of the DNA nanodevice, confirmed its targeting of LXR, and demonstrated its efficacy in vivo. Overall, this research enhances our understanding of the intricate connections between cholesterol metabolism, inflammation, and atherosclerosis, while also highlighting promising strategies for targeted intervention in this prevalent cardiovascular disease.

CHAPTER ONE: INTRODUCTION

1.1 Cardiovascular disease is the leading cause of death.

Cardiovascular disease (CVD) is the leading cause of death worldwide (*Heart Disease Facts | cdc.gov*, n.d.; Mc Namara et al., 2019). Atherosclerosis is the most common underlying cause of CVD and is characterized by the formation of a plaque or lesion in the arterial wall. Lesion formation and development are perpetuated by chronic inflammation, hyperlipidemia, and biomechanical stressors (Libby, 2021b). Symptomatic patients usually present with lesions that are large enough to obstruct the lumen of the arteries, inducing ischemic pain, or ruptured lesions. Ruptured lesions can result in stroke, myocardial infarction (MI), or death (Burke et al., 1999). Most patients with atherosclerotic lesions, however, are typically asymptomatic for years, as the lesion takes decades to mature (Gisterå & Hansson, 2017).

Atherosclerosis can be classified as a chronic inflammatory and lipid metabolism disorder that culminates in the formation of atherosclerotic lesions (Gisterå & Hansson, 2017; Libby, 2012, 2021a; Libby et al., 2002). One of the epidemiological drivers of atherosclerosis is obesity. Since the 1980's, the worldwide incidence of obesity has nearly doubled (Rakhra et al., 2020; Valenzuela et al., 2023). Currently, over 1.9 billion individuals are classified as overweight or obese, and it includes over 50 million children under the age of five (Rakhra et al., 2020; Valenzuela et al., 2023). While obesity is linked to several physiological, psychological, and psychosocial comorbidities (such as depression, anxiety, discrimination, neurological, digestive, respiratory, musculoskeletal, and inflammatory disorders), atherosclerotic CVD is the leading burden on patients with obesity (Campos-Vazquez & Gonzalez, 2020; Kivimäki et al., 2017; Puhl & Suh, 2015; Tomiyama et al., 2018). Patients with obesity have an almost fivefold

higher risk of developing coronary heart disease (CHD), stroke, or diabetes mellitus, which increases to almost 15-fold for those with obesity class 2 and 3 (Kivimäki et al., 2017; Powell-Wiley et al., 2021) . Comorbidities that are common in both obesity and atherosclerosis are hyperlipidemia, hypertension, chronic inflammation, and insulin resistance (which presents as type 2 diabetes (T2D)) (GBD 2015 Obesity Collaborators et al., 2017). Patients with obesity and T2D have an additional increased risk of cardiac events, even when traditional CVD risk factors such as hyperlipidemia (statins), hypertension (blood pressure medications), and diabetes (insulin and metformin) are under control (Beckman et al., 2002; Gore et al., 2015; Martín-Timón et al., 2014; Wong & Sattar, 2023). Identifying this link is of critical importance to mediate the disease burden. Our lab has found the inflammatory cytokine interferon gamma (IFNγ) to be upregulated in obesity and insulin resistant mice which exacerbates atherosclerotic lesions *in vivo.* Furthermore*,* we found that IFNγ promotes increased cholesterol uptake in macrophages, leading to foam cell formation. Foam cell macrophages are causally linked to all stages of atherosclerotic development and may be a critical cellular link between obesity/IR and atherosclerosis (Reardon et al., 2018). Our work adds to the growing body of evidence highlighting the intricate interplay between inflammation and lipid metabolism that drives atherosclerosis. Targeting IFNγ may be beneficial to decrease atherosclerotic disease; however, this cytokine is crucial for host defense, and antagonizing IFNγ may leave patients immunocompromised (McLaren & Ramji, 2009; Moss & Ramji, 2015).

My doctoral work aims to further understand the link between inflammation and lipid metabolism in macrophages of atherosclerotic lesions. This chapter provides a framework for my doctoral research, which consists of identifying an IFNγ signaling pathway in macrophages that influences lipid uptake, and later employing a DNA-nanodevice to selectively deliver the small

molecule LXR agonist T0-901317 to promote cholesterol efflux in macrophages to decrease atherosclerotic lesion size. I will start with an introduction to macrophages and their contribution to atherosclerosis, then talk about the history of atherosclerosis in the context of lipid metabolism and inflammation.

1.2 Atherosclerosis is an immunometabolic disorder driven by chronic inflammation and hyperlipidemia.

Prior to the 1900s, atherosclerosis was thought to be a dull disease driven by aging. However, in 1913 physician-scientist Nikolai Anitschkow showed that atherosclerosis can be induced in rabbits fed a high cholesterol diet (Konstantinov et al., 2006) . His studies linked hyperlipidemia as the main driver of atherosclerosis. However, Anitschkow's contemporaries were skeptical of his conclusions and erupted in fierce debate (Steinberg, 2004). Many cardiologists and nutritionists of the era were extremely skeptical of the idea that lipids were the causative agent of atherosclerosis (McMichael, 1979) (Peters & Van Slyke, 1947). For example, in a 1976, an excerpt from the *British Heart Journal* stated "The view that raised plasma cholesterol is per se a cause of coronary heart disease is untenable" (Steinberg, 2004). It was not until 70 years after Anitschkow's 1913 studies in cholesterol-fed rabbits that the NIH published its seminal 1984 *Coronary Prevention Trial* showing a significant decrease in CVD incidences in humans as a result of reduced cholesterol intake, providing robust epidemiological evidence linking hypercholesterolemia to atherosclerosis (Rifkind, 1984). This allowed the atherosclerotic field to move from a 'dull aging disease' to a 'lipid storage disease' dogma. Nevertheless, currently (40 years since the 1984 NIH CPT studies) we have overwhelming experimental evidence that shows atherosclerosis is a disease driven by hyperlipidemia (specifically elevated

LDL or ‘bad’ cholesterol) and inflammation, most specifically by macrophages which comprise a large portion of the immune cell population in the atherosclerotic lesion (Bäck & Hansson, 2015; Tabas & Bornfeldt, 2016). Interestingly, the interplay of immunity and metabolism is strongly intertwined, where infectious pathogens hijack the metabolic state of the host, using host resources to reproduce (Gehre et al., 2016; Lee & Bensinger, 2022; Olive & Sassetti, 2016; Sviridov & Bukrinsky, 2014). Consequently, the host responds to this insult by altering its metabolic state as defense. Over millions of years, this has spawned an evolutionary tug-of-war of resources between host and pathogens. Each selects metabolic mechanisms to outwit one another (Olive & Sassetti, 2016). Take the dengue virus and hepatitis C virus, for example, they induce lipophagy in hepatocytes and hijack the Golgi as its own reproductive hub (Chatel-Chaix & Bartenschlager, 2014; Randall, 2018). In mammalian hosts, we observe immune cells changing their metabolic landscape to combat pathogens. Macrophages, cells of the innate immune system, switch to glycolysis when faced with bacterial components (such as bacterial cell wall factor lipopolysaccharide, or LPS) and self-induced inflammatory signals (cytokines) (N. C. Williams & O’Neill, 2018) (Viola et al., 2019). Similarly, T cells also use their glycolytic system to perform essential functions (Buck et al., 2015).

This evolutionary interplay has influenced immunometabolic diseases such as obesity and atherosclerosis (Schipper et al., 2012) (Rocha & Libby, 2009). A significant population of cells that make up the atherosclerotic lesion are immune cells, largely macrophages but also T cells and dendritic cells. This in combination of a hyperlipidemic environment lead to the implication that atherosclerosis is an immunometabolic disorder (Gisterå & Hansson, 2017). Two phenomena were observed in the 1980’s that provided insight of atherosclerosis as an inflammatory disease. One was a correlational study of inflammatory markers in patients’ serum

presenting with MI and the second was an investigation involving cholesterol fed rabbits infected with *Chlamydia pneumoniae*.

In 1982 physicians observed a significant increase in plasma levels of C-reactive protein (CRP), and acute phase reactant, in patients presenting with MI, acute inflammation with myocardial ischemia. Elevated CRP levels were later recognized as a serum biomarker that could predict cardiovascular events (Wang et al., 2015). Later that decade in 1988, Seikku et al. showed serological data strongly correlating the presence of the *Chlamydia pneumoniae,* the etiologic agent of most acute respiratory infections in humans, in patients suffering from chronic CHD and acute MI (Saikku et al., 1988) (Moazed et al., 1997). This led to the hypothesis that atherosclerotic CVD might be driven by pathogenic bacteria.

Indeed, *Chlamydia pneumoniae* could exacerbate experimental atherosclerotic lesions in cholesterol-fed rabbits but it was later found that the pathogen alone did not induce atherogenesis. Moreover, findings from germ-free mice indicate that they can develop atherosclerosis, indicating that bacteria are not required for atherogenesis (Caligiuri et al., 2001)(Moazed et al., 1997). In addition, a meta-analysis of randomized controlled trials showed no beneficial effect of antichlamydial antibiotic therapy on mortality or the incidence of cardiovascular events in patients with coronary artery disease (Andraws et al., 2005; Caligiuri et al., 2001). These findings suggest no causal link between an infectious agent and atherosclerosis. However, what these studies *do* suggest is a link between the host *response* to infection to the size of atherosclerotic lesions.

The host's defense against pathogens and damage relies heavily on inflammatory cytokines. In the context of atherogenesis, early research by Gimbrone and colleagues in the 1990s demonstrated that vascular wall cells have the ability to produce adhesion molecules, which are

factors that attract immune cells to the arterial wall(Bevilacqua et al., 1987; Cybulsky & Gimbrone, 1991). Subsequent studies revealed that human endothelial cells and smooth muscle cells not only respond to cytokines but also produce their own proinflammatory molecules (Braun et al., 1995; Cybulsky & Gimbrone, 1991; Gargalovic et al., 2006) (Loppnow & Libby, 1990; Nilsson, 1993). These investigations provided valuable insights into the connection between the inflammatory response triggered by infection and the development of atherosclerosis.

The regulation of the inflammatory process in the vascular wall involves cytokines. Cytokines are a diverse group of over 100 proteins identified to date. They can be classified into various classes, including interleukins (IL), chemokines, colony stimulating factors (CSF), tumor necrosis factor (TNF), interferons (IFN), and transformation growth factors (TGF) (Ait-Oufella et al., 2011; Zernecke & Weber, 2014). Initially, chemokines were primarily associated with the recruitment of leukocytes to sites of inflammation. However, it is now known that they have additional properties that extend beyond cell recruitment, and they can also influence vascular homeostasis (da Luz et al., 2018). In the case of hyperlipidemic individuals, the presence of excessive apoB-containing lipoproteins stimulates cytokine and chemokine production in the endothelial cells of the vascular wall. These lipoproteins enter the subendothelial space, where they undergo modifications, likely oxidation, acting as damage signals that trigger cytokine production. Besides lipoproteins, biomechanical stressors resulting from hypertension or disturbed blood flow can also induce the expression of inflammatory cytokines (Steffensen et al., 2015)(Barvitenko et al., 2022)(Mullick et al., 2008).

The discovery of inflammatory cytokines and adhesion molecules expressed by endothelial cells, and consequently the recruitment of immune cells, has provided valuable insights into the

initiation of atherosclerotic lesions (Bevilacqua et al., 1987). Extensive research has demonstrated that the presence of vascular cell adhesion molecule-1 (VCAM-1) plays a crucial role in the development of early atherosclerotic plaques. This molecule is expressed by endothelial cells that have been stimulated by cytokines, and it exhibits a specific affinity for inflammatory cells that gather in these plaques, including monocytes and T lymphocytes. As a result, VCAM-1 contributes to the accumulation of immune cells within the damaged vascular wall, exacerbating the inflammatory response (Cybulsky & Gimbrone, 1991; H. Li et al., 1993). This finding builds upon the observations made by Poole and Florey in 1958, who noticed the adherence of mononuclear cells to intact endothelium in hypercholesterolemic rabbits (Poole & Florey, 1958). Immune cells, such as blood-borne monocytes, exhibit a remarkable affinity for the adhesion molecules expressed on the surface of endothelial cells. Once attached, these cells receive chemoattractant signals that propel them towards the subendothelial space. Among the key players in this intricate interplay are monocyte chemoattractant protein-1 (MCP-1) and a group of chemokines induced by IFN-γ. Together, they selectively recruit T lymphocytes to participate in the formation of atherosclerotic plaques, contributing to their development (Mach et al., 1999).

Once monocytes have taken up residence in the arterial intima, they differentiate into macrophages. These mononuclear phagocytes in the plaque express scavenger receptors, which are necessary for the uptake of modified lipoproteins and subsequent foam cell formation. These findings have revolutionized the understanding of atherosclerosis by revealing it as a complex and interactive process involving both vascular wall cells, blood-borne immune cells, and hypercholesterolemia (*Cellular and molecular pathobiology of cardiovascular disease*, 2014). This contradicts previous notions that vascular cells were passive in arterial inflammation and

that foam cells were inert recipients of lipid debris. The involvement of the innate and adaptive immune system in the development of atherosclerosis has provided a more nuanced understanding of lesion development, integrating both the cholesterol and endothelial cell injury hypotheses.

1.3 Macrophages contribute to all pathological phases of atherosclerotic lesion development.

Observations of lipid-loaded cells or "foam cells" have been a critical feature of atherosclerotic lesions since the 1800s (Steinberg, 2004). The development of monoclonal antibodies allowed for the confirmation that most foam cells are derived from the monocyte lineage, although it is speculated that other cell types such as smooth muscle cells and endothelial cells can also become foamy (Yu et al., 2013). At first, macrophages were viewed as the place where lipids went to die within the plaque, rather than as active participants in atherogenesis. However, with the characterization of macrophage-derived cytokines, the concept of dynamic interplay between mononuclear phagocytes and vascular cells during atherogenesis emerged. Macrophages make up the majority of inflammatory cells in atherosclerotic plaques, while T and B lymphocytes exist in much lower numbers but play a decisive roles in regulating inflammation during atherogenesis(Cochain et al., 2018; Koelwyn et al., 2018; Lichtman et al., 2013).

1.4 Macrophage Origin and Function

Macrophages act as guards of the innate immune system and are ubiquitous in all tissues. They exquisitely detect and respond to fluctuations in their microenvironment to maintain tissue

homeostasis (Ginhoux & Jung, 2014; Rasheed & Rayner, 2021)(Wynn et al., 2013). These cells perform various essential functions, such as removing dying cells (efferocytosis) and harmful microbes from tissues (phagocytosis), promoting tissue repair, and producing cytokines to combat pathogens (inflammatory response). Through lineage tracing methods, researchers have identified two primary macrophage populations: tissue-resident macrophages (TRMs) originating from the yolk during early development, and monocyte-derived or blood-borne macrophages (MDMs) derived from monocyte precursors in the bone marrow (Schulz et al., 2012)(Hoeffel et al., 2012).

Both TRMs and MDMs share similar functions as phagocytic cells, which can respond to invading pathogens, promote repair and maintain homeostasis. However, TRMs have the unique ability to self-renew and exhibit tissue-specific characteristics (Hashimoto et al., 2013). In contrast, MDMs primarily originate from hematopoietic stem cells in the bone marrow and spleen and differentiate into monocytes and then macrophages under specific conditions.

MDMs exist in low levels within tissues and are replenished through the recruitment and differentiation of monocytes via growth factors like macrophage colony-stimulating factor (M-CSF). Classical monocytes, marked by high expression of Ly6C (in mice) or CD14 (in humans), can be recruited into the subendothelial space (Blagov et al., 2023). Depending on the stimulus received, these monocytes can become polarized towards either pro-inflammatory M1 or anti-inflammatory M2 macrophages. However, it is important to note that MDMs in vivo exhibit a more dynamic state and can take on a range of phenotypes based on specific stimuli from their microenvironment (Rasheed & Rayner, 2021).

In vitro, M1-like macrophages are polarized through engagement of Toll-like receptor 4 (TLR4) by pathogen-associated molecular patterns (PAMPs), such as lipopolysaccharide (LPS)

from Gram-negative bacteria, in parallel with the pro-inflammatory cytokine IFN-γ (Yunna et al., 2020). Upon polarization, M1-like macrophages exhibit increased bactericidal capacity, increased production of reactive oxygen species (ROS), a preference for glycolytic metabolism, release of numerous inflammatory cytokines like TNF-α and IL-1β, and expression of inducible nitric oxide synthase (iNOS) (Shi & Pamer, 2011).

On the other hand, macrophages become polarized to M2-like phenotype upon stimulation with IL-4 or IL-13 and promote increased phagocytic capacity, a preference for oxidative metabolism, and release of pro-resolving factors that promote angiogenesis, tissue repair, and immunoregulation, such as IL-10 and TGF-β.

Our current understanding of the distinct properties of TRMs and MDMs, including their polarization, has greatly contributed to our comprehension of macrophages in various diseases, including atherosclerosis. M1-like or proinflammatory macrophages are typically observed in progressing plaques with active inflammation, whereas M2-like or reparative macrophages are more frequently seen in regressing and stable plaques during repair (Blagov et al., 2023; Moore & Tabas, 2011). Although macrophages are a potential source of inflammation within plaques, they are also capable of adapting and shifting their phenotype according to the requirements of the tissue and are crucial for the stabilization and resolution processes that accompany plaque regression in mice. Macrophages exhibit complex and intricate dynamics within all the different components of an atherosclerotic plaque (Moore et al., 2013).

1.5 Steps of Atherosclerotic Lesion Development and Macrophage Involvement.

Atherosclerosis develops at specific sites in the aorta that are characterized by disturbed blood flow and low oscillatory shear stress such as is found at curved regions or branch points of

the artery (Tamargo IA 2023). These biomechanical stressors promote endothelial dysfunction by increasing EC permeability and exposure to circulating cells and lipoproteins. Lesions tend to develop at these sites due to increased cell loss, differential gene expression, and prolonged contact with circulating cells and lipoproteins. Atherogenesis can be divided into three critical steps: 1) lesion initiation or fatty streak, 2) lesion progression, and 3) plaque disruption, which includes the symptomatic stage, where most patients present at the clinic (*Vascular medicine: A companion to braunwald's heart disease*, 2013; Zipes MD & Libby MD PhD, 2018) (Stary et al., 1994).

1.6 Lesion initiation

The arterial vessel is composed of three distinct layers: the intima, media, and outer adventitia (Netter MD, 2018). The intima, located closest to the arterial lumen, is composed of a single layer of endothelial cells with connective tissue including collagen and proteoglycans and a few smooth muscle cells in the subendothelial space. The intima is separated from the medial layer composed of smooth muscle cells and elastin by the internal elastic lamina. The adventitia layer is composed of connective tissue, nerves, and small blood vessels. (Netter MD, 2018). The endothelium acts as a metabolic barrier and transporter between the blood and arterial wall, playing a critical role in atherosclerosis. Occasionally, the intima in normal vessel may also contain lymphocytes, macrophages, and other types of inflammatory cells (Schenkel et al., 2004).

In a hyperlipidemic environment, apoB-containing lipoproteins, such as very low density lipoprotein (VLDL) and LDL, accumulate in the vascular wall, increasing the risk of lesion development in atherosclerosis susceptible regions of the aorta (Borén et al., 2022; Yu et al.,

2013). The first step in this process is the movement of LDL into the subintimal space, (Rader & Puré, 2005). Once in the intima, LDL particles are susceptible to structural modifications, including lipolysis, proteolysis, aggregation, and oxidation by ROS (Vance & Vance, 2008). These modified LDL particles have multiple effects that contribute to the initiation and progression of atherosclerosis. They act as inflammatory molecules inducing endothelial cells to upregulate the expression of adhesion molecules such as ICAM-1, VCAM-1, E-selectin, and P-selectin (Gisterå & Hansson, 2017; Parthasarathy & Rankin, 1992). Adhesion molecules induce circulating monocytes and lymphocytes to stick and tether to the endothelial surface (Schenkel et al., 2004). Mouse models lacking ICAM-1, P-selectin, or E-selectin demonstrate the pro-atherogenic effects of adhesion molecules, highlighting their significance in lesion development (Collins et al., 2000; da Luz et al., 2018; H. Li et al., 1993; Mach et al., 1999).

With continuous elevated levels of LDL in the blood, further accumulated and modified LDL stimulates ECs to express monocyte chemotactic protein-1 (MCP-1), a chemokine that attracts adhesive monocytes to migrate into the intima. Demonstrating the role of MCP-1 in lesion development, mice lacking MCP-1, or its receptor CCR2, had reduced atherosclerotic lesions (Gosling et al., 1999). Finally, the modified LDL in the intima also stimulates the production of macrophage colony-stimulating factor (M-CSF) that induces monocyte proliferation and differentiation into mature and activated macrophages that express scavenger receptors (Moore & Tabas, 2011). The absence of M-CSF has been shown to dramatically reduce lesion sizes in LDL receptor (LDLR) knockout and apolipoprotein (apo)E knockout mice (Getz & Reardon, 2012). These early lesions composed primarily of lipid loaded macrophages are referred to as fatty streaks.

1.7 Lesion progression

Activated macrophages also secrete cytokines that stimulate ECs expression of adhesion molecules to attract more monocytes and other immune cells. Thus, the movement and accumulation of LDL in the intima results in a local inflammation in the vessel wall, characterized by the cycle of increased adhesion molecule expression, immune cell recruitment, cytokine release and foam cell formation(Tabas & Bornfeldt, 2016; H. Xu et al., 2019). As the lesion progresses, a chronic inflammatory situation is created by the interaction of macrophages foam cells and T-cells, which secrete a variety of cytokines and chemokines that exert both pro- and anti-atherogenic effects among the cells of the arterial wall. One such effect is the migration of vascular smooth muscle cells (SMC) from the medial layer into the intima, where exposure to growth factors secreted by macrophages foam cells and T-cells stimulate the normally quiescent SMC to proliferate and synthesize extracellular matrix protein(Inaba et al., 1996)s (Shah, 2014). These SMC are an important component of the fibrous cap that forms underneath the EC over the growing atherosclerotic lesion. The SMC secrete extracellular matrix proteins that provides stability to the lesion. The thickness of the cap is associated with the stability of the lesion, where thinner caps are more vulnerable to ruptures (Bentzon et al., 2014; Koenig & Khuseyinova, 2007).

1.8 Lesion rupture & clinical manifestations

Plaque rupture, the lethal symptomatic phase of the disease, occurs when the fibrous cap covering the plaque becomes extremely thin. Van Der Wal et al. have shown that the majority of ruptured fibrous caps in post-mortem individuals who have died from a MI, are less than 65 μm thick (van der Wal et al., 1994) compared to stable plaques.

A higher concentration of macrophages has been shown to be present in ruptured plaques in post-mortem analyses. Lesion macrophages significantly contribute to the thinning of the fibrous cap by secreting metalloproteinases, which degrade the extracellular matrix proteins in the fibrous cap (composed of collagen and proteoglycans) (Thim et al., 2008). Ruptured caps exhibit a higher density of macrophages and a lower density of smooth muscle cells compared to intact caps (Thim et al., 2008).

Unstable plaques, also known as vulnerable or high-risk plaques, are a significant underlying cause of cardiovascular events, particularly acute coronary syndromes like heart attacks. These plaques are characterized by a combination of factors, one of which is the presence of necrotic cores (Bentzon et al., 2014; Thorp & Tabas, 2009). Unstable plaques are often also associated with the presence of necrotic cores. Necrotic cores are areas within atherosclerotic plaques where cell death and tissue degeneration have occurred. They are composed of a mixture of cellular debris, lipids, cholesterol crystals, and extracellular matrix components (Thorp & Tabas, 2009). The necrotic core is an important histopathological feature of unstable plaques and contributes to their vulnerability (Bentzon et al., 2014).

Once the fibrous cap ruptures, plaque lipids are exposed to blood components that initiate coagulation and platelet adhesion mechanisms (*Vascular medicine: A companion to braunwald's heart disease*, 2013; Zipes MD & Libby MD PhD, 2018). Activation of the coagulation cascade can result in a thrombus that adds to the blood vessel obstruction, or it can detach and become trapped in micro-vessels leading to clinical events such as MIs or strokes.

1.9 Macrophage Cholesterol Homeostasis and Reverse Cholesterol Transport

Cholesterol is a critical lipid and signaling molecule in cells. It is used to maintain cell-membrane integrity and can act as a signaling messenger. As such, cholesterol is tightly regulated to prevent lipotoxicity (Afonso et al., 2014; Luo et al., 2020). This intricate regulation in the macrophage involves several transcriptional and post-transcriptional mechanisms. Dysregulation of cholesterol homeostasis is a hallmark of foam cell macrophages in atherosclerosis. Post-transcriptional mechanisms involve the uptake of lipid-carrying proteins LDL/VLDL by scavenger receptors and the efflux of cholesterol to HDL by membrane bound transporters. An important regulator of macrophage cholesterol homeostasis are the Liver X Receptors (LXRs) transcription factors.

1.10 Macrophage cholesterol accumulation

Foam cell macrophages form due to excessive uptake of modified apoB containing lipoproteins, such as LDL and consequently the accumulation of cholesteryl esters. It is important to note that native (unmodified) LDL present in the bloodstream of healthy individuals does not cause the buildup of cholesteryl esters in cultured macrophages (Chistiakov et al., 2017). However, some investigators have shown modified LDL obtained from individuals with atherosclerosis significantly increases the intracellular levels of cholesteryl esters (Chistiakov et al., 2016, 2017), suggesting that modification influences cholesterol uptake *in vitro.* Cells express various scavenger receptors (SR), including SR-A1, CD36, and lectin-like oxLDL receptor-1 (LOX-1), which have an affinity for oxidized LDL (oxLDL). Additionally, macrophages possess key enzymes such as acyl coenzyme A:cholesterol acyltransferase-1 (ACAT1), which is essential for cholesteryl ester formation. Cholesteryl esters can be

hydrolyzed by two enzymes, namely neutral cholesteryl ester hydrolase 1 (NCEH1) and lysosomal acid lipase (LAL), resulting in the production of free fatty acids and cholesterol. Furthermore, macrophages express various membrane transporters, including the ATP-binding cassette (ABC) transporters A1 (ABCA1) and G1 (ABCG1), as well as the scavenger receptor SR-BI, which are involved in reverse cholesterol (RCT) transport.

Macrophages have low levels of LDL receptor but possess several scavenger receptors, including SR-A1, CD36, SR-BI and lectin-like oxLDL receptor-1 (LOX-1), which bind various molecules such as oxidized LDL, advanced glycation end products, and inflammatory mediators (de Villiers & Smart, 1999). Uptake by scavenger receptors is not regulated and as such in an environment of excess lipids there is increased accumulation of lipid in macrophages. Phagocytosis and micropinocytosis also contribute to uptake of apoB-containing lipoproteins in the intima (Moore and Tabas 2011). Additionally, macrophages engulf apoptotic cells, which contain lipids, contributing to macrophage lipid loading (Luo et al., 2020). The cholesteryl esters of the lipoproteins are hydrolyzed in late endosomes to free cholesterol and free fatty acids and the free cholesterol is trafficked to the endoplasmic reticulum (ER). The ER is an important site for lipid metabolism regulation. When intracellular free cholesterol levels exceed physiological concentrations, the ER enzyme acyl coenzyme A:cholesterol acyltransferase-1 (ACAT1) esterifies the excess cholesterol, forming cytosolic lipid droplets, a prominent feature of foam cell macrophages. This compartmentalizes intracellular cholesterol, preventing lipotoxicity.

1.11 Macrophage cholesterol efflux

While compartmentalizing intracellular cholesterol preventing lipotoxicity, efficient removal of excess cholesterol from the macrophage is crucial to prevent macrophage foam cell formation and subsequent dysfunction that contribute to atherosclerotic plaque progression. The process of removing excess macrophage cholesterol and delivering it to the liver for processing or elimination is called “reverse cholesterol transport” or RCT. In this process, the stored cholesteryl esters are hydrolyzed to free cholesterol and free fatty acids by the enzyme neutral cholesteryl ester hydrolase (NCEH) and the free cholesterol traffics to the plasma membrane and is transferred to the outer leaflet. ABCA1 is a transmembrane domain protein that mediates the ATP-dependent efflux of cholesterol and phospholipid in the membrane to lipid-free apoA-I, the major apoprotein on high density lipoproteins (HDL), in the subendothelial space. This generates nascent discoidal HDL (pre-HDL) that can be acted upon by lecithin cholesterol acyltransferase (LCAT) in the plasma to generate spherical HDL. In addition, ABCG1 in macrophages mediates the efflux of cholesterol and phospholipids to spherical HDL. Together they reduce the cholesterol content of the macrophages(Lund-Katz & Phillips, 2010) (Takahashi & Smith, 1999)(Nandi et al., 2009). Apolipoprotein E (apoE), secreted by macrophages, also contributes to cholesterol efflux by acting as a cholesterol acceptor to form nascent discoidal apoE-containing HDL which is also a substrate for LCAT (Getz & Reardon 2018). These are the initial steps in RCT pathway.

1.12 Liver Uptake and Cholesterol Elimination

The cholesterol in HDL can be transferred to LDL in the plasma by the enzyme cholesteryl ester transfer protein (CETP) and the cholesterol delivered to the liver via the LDL

receptor. However, HDL cholesterol is also taken up by hepatocytes by selective cholesteryl ester uptake mediated by SR-B1. In hepatocytes the cholesterol can be transformation into bile acids, a more hydrophilic version of cholesterol that plays a role in absorption of dietary lipids and fat-soluble vitamins in the intestine. Some of the bile acids secreted into the intestine can be eliminated through feces. The liver plays a crucial role in eliminating cholesterol from the body, thereby contributing to overall cholesterol homeostasis.

1.13 LXR is an important regulator of macrophage cholesterol efflux and inflammation.

Liver X receptor (LXR) is a member of the nuclear receptor family of ligand activated transcription factors. LXR is activated by oxysterols, which are cholesterol derivatives that act as second messengers. Upon activation, LXRα and LXRβ interact with RXRs to form specific heterodimers that bind to promoters of downstream genes involved in lipid metabolism. LXR plays a crucial role in macrophage cholesterol efflux, The expression of ABCA1 and ABCG1 is mainly regulated by LXR, which enhances macrophage cholesterol efflux. LXR also upregulates the expression of apoE (*see next section*) and ADP-ribosylation factor-like 7 (ARL7) which promotes cholesterol efflux, perhaps by facilitating transport of cholesterol to the plasma membrane for ABCA1 mediated efflux (Hong & Tontonoz, 2014). LXR upregulates the expression of other participants in RCT transport (e.g. LCAT and CETP) in the liver and upregulates the expression of a rate limiting gene in bile acid synthesis (i.e. CYP7A1) as well as ABCG5 and ABCG8 that promote excretion of cholesterol in the bile (Calkin & Tontonoz, 2010). Thus, LXR is an important regulatory of RCT transport.

Beyond macrophages and RCT transport, LXR influences other aspects of lipid homeostasis (Jeong et al., 2017). LXR activation in hepatocytes increases lipogenesis by

inducing the expression of lipid related genes including the transcription factor sterol regulatory element binding protein 1c (SREBP1c), a transcription factor that increases fatty acid synthesis, and fatty acid synthase and the lipogenic regulator carbohydrate response element ChREBP leading to increased synthesis of triglycerides and the secretion of VLDLs (Cha & Repa, 2007)(X. Xu et al., 2013)(Trapani et al., 2012). LXR also functions in the intestine to limit cholesterol absorption into the body. It down-regulates Niemann-Pick C1-like 1 (NPC1L1), a membrane protein that promotes cholesterol uptake into enterocytes and increases ABCG5 and ABCG8 expression to promote excretion of absorbed cholesterol back into the intestine (Duan et al., 2006)(Brown & Yu, 2009)(Skov et al., 2011).

LXR activation can also inhibit the expression of inflammatory mediators, thereby modulating the inflammatory states of related inflammatory cells, including vessel endothelial cells, macrophages, T lymphocytes, and smooth muscle cells (Im & Osborne, 2011; J. Xu et al., 2009). LXR activation can suppress inflammatory genes in foam cells of atherosclerotic plaques, inhibit the nuclear factor kappa B signaling pathway, and inhibit the production of pro-inflammatory factors stimulated by bacteria, LPS, TNF-α, and IL-1β (Kong et al., 2022; Rigamonti et al., 2008). LXR agonists also inhibit the expression of proinflammatory genes in macrophages and other types of cells(Im & Osborne, 2011; Rigamonti et al., 2008). Furthermore, LXR agonists can promote the expansion of regulatory T cells and inhibit the differentiation of Th17 cells that secrete proinflammatory factor IL-17 in mice and humans (J. Xu et al., 2009).

1.14 Apolipoprotein E

Apolipoprotein E (apoE) on remnants of chylomicron and VLDL mediates the hepatic uptake of these lipoproteins from the plasma by serving as a high affinity ligand for the LDL receptor and the LDL receptor related protein (Ishibashi et al., 1994). ApoE is expressed by many cell types including hepatocytes, macrophages and adrenal cells, but not enterocytes(Q. Xu et al., 2006) (Getz & Reardon, 2016). The majority of the plasma apoE is derived from hepatocytes (Raffaï et al., 2003). The importance of apoE as a regulator of plasma lipid levels is demonstrated by the hyperlipidemia in *Apoe-/-* mice due to the accumulation of remnant particles (Zsigmond et al., 1998)(Kypreos et al., 2001). Unlike wild type C57BL/6 mice, A*poe-/-* mice develop complex atherosclerotic lesions on low fat chow diet and accelerated atherosclerosis on a WTD (Curtiss, 2000). Much of the accelerated atherosclerosis in *Apoe-/-* mice is likely due to the hyperlipidemia (Nakashima et al., 1994). However, the absence of apoE expression in macrophages may also contribute. The absence of apoE in macrophages leads to accelerated atherosclerosis in wild type mice (Linton et al., 1995) and conversely reconstituting *Apoe-/-* with macrophages expressing apoE without impacting plasma lipid levels reduced atherosclerosis (Bellosta et al., 1995 and Hasty 1999).

While the primary function of apoE is thought to be the normalization of plasma cholesterol levels, recent studies suggest that it may have additional protective mechanisms independent of cholesterol regulation. Possible mechanisms for apoE's protective effects include facilitating cellular cholesterol efflux, modifying the inflammatory responses of T lymphocytes and smooth muscle cells, and exhibiting antioxidant activity (Curtiss, 2000; Mahley & Rall, 2000). ApoE is a critical protein involved in maintaining macrophage cholesterol balance. Studies have shown that the expression of apoE in cholesterol loaded cells enhances cholesterol efflux (Linton et al., 1995). Bioinformatic studies of control and sterol-loaded peritoneal

macrophages from WTD fed *Ldlr-/-* mice identified expressed by foam cells that form a network that was named the macrophage sterol responsive network (MSRN) that includes apoE (Becker et al. 2010). ApoE is down regulated in the cholesterol loaded macrophages and is a primary regulator of the MSRN. Peritoneal macrophages from WTD fed *Apoe-/-* mice are enriched in cholesterol compared to peritoneal macrophages from WTD fed *Ldlr-/-* mice and the response of the MSRN proteins to sterol accumulation was attenuated in the absence of apoE. siRNA down regulation of apoE lowered the expression of several MSRN proteins. Treatments that restore the MSRN in peritoneal macrophages in WTD fed *Ldlr-/-* mice (statin and rosiglitazone) are also associated with increased levels of macrophage apoE in the atherosclerotic lesions. These studies highlight the potential importance of understanding the regulation of apoE expression in macrophages and the impact this may have on atherosclerosis.

1.15 The Inflammatory Cytokine Interferon Gamma (IFNγ) is a Key Regulator of Atherogenesis.

One of the decisive cytokines that T cells secrete in atherogenesis is IFNγ. This particular cytokine is a powerful inflammatory modulator involved in multiple steps of atherosclerotic plaque development, including foam cell formation, leukocyte recruitment, and plaque instability (McLaren & Ramji, 2009). *In vitro* experiments show IFNγ accelerates macrophage foam cell formation by downregulating the machinery involved in cholesterol removal (cholesterol efflux) and upregulating cholesterol influx genes (McLaren & Ramji, 2009). IFNγ has been shown to play a role in leukocyte recruitment by inducing the expression of cytokines and chemokines attracting other immune cells and expanding the lesion size (H. Li et al., 1995). In later stages of atherosclerosis IFN-γ has also been shown to be able to weaken the fibrous cap around atherosclerotic plaques by inhibiting collagen I and III production in smooth muscle cells (Gupta

et al., 1997). Furthermore, IFNγ promotes the expression of metalloproteinase proteins, whose expression has been correlated with plaque ruptures, the symptomatic and often fatal consequence of the disease (McLaren & Ramji, 2009). Finally, in animal models, administration of IFNγ in atherogenic-prone mice aggravates atherosclerosis, while deficiency in IFNγ or its receptor attenuates it. These *in vivo* and *in vitro* studies largely support IFNγ as a key regulator of atherogenesis.

1.16 Summary

To summarize, atherosclerosis can be classified as an immunometabolic disorder, as there is extensive evidence delineating the clear interaction between inflammatory cytokines, blood-borne macrophages, hyperlipidemia, and vascular cells in all aspects lesion pathogenesis. My doctoral work integrates cholesterol metabolism and inflammation in the context of atherosclerotic macrophages. In chapter one we attempt to discover a non-canonical signaling pathway that governs excess cholesterol uptake in macrophages because of obesity and insulin resistance. In chapter three I capitalize on the activation of LXR in macrophages to promote cholesterol efflux reducing atherosclerotic lesion size using a DNA nanodevice.

CHAPTER 2: PRO-ATHEROGENIC NON-CANONICAL INTERFERON GAMMA SIGNALING IN MACROPHAGES

2.1 Introduction

Insulin-resistant and obese individuals face a considerably elevated risk of CVD. This risk remains substantial even when conventional factors like hypertension, hypercholesterolemia, and hyperinsulinemia are managed through lifestyle modifications and pharmaceutical interventions (Beckman et al., 2002; Gore et al., 2015). Alarmingly, approximately 70% of deaths related to type 2 diabetes (T2D) are attributed to cardiac events such as heart attack or stroke (Martín-Timón et al., 2014) (Bazmandegan et al., 2023; Virani et al., 2020) (Beckman et al., 2002). It is crucial to understand the basis for this increased risk to reduce unnecessary deaths associated with this manageable chronic disease. Despite the increased risk of CVD associated with T2D, the underlying mechanism connecting the two remains unclear. This is because most murine models that induce atherosclerosis (*Ldlr-/-* and *Apoe-/-*) and insulin resistance through a western-type diet also led to hypercholesterolemia, which is a significant contributor to atherogenesis (Getz & Reardon, 2012) (Reardon et al., 2018). This complicates the analysis of the effects of T2D on atherosclerosis, making it difficult to isolate the specific mechanisms that link the two conditions. To circumvent this, our lab used several dietary and genetic interventions in wild type and atheroprone *Ldlr-/-* mice to study the effects of obesity and insulin resistance (obesity/IR) on macrophage function and atherogenesis (Reardon et al., 2018). Using this approach, we demonstrated that in the presence of obesity/IR the inflammatory cytokine interferon gamma (IFNγ) targets macrophages to promote foam cell formation and exacerbate atherosclerotic lesion size (**Figure 2.1**). Mechanistically, obesity/IR-induced IFNγ promotes enhanced lipid loading in macrophages by disrupting extracellular levels of the ‘Macrophage

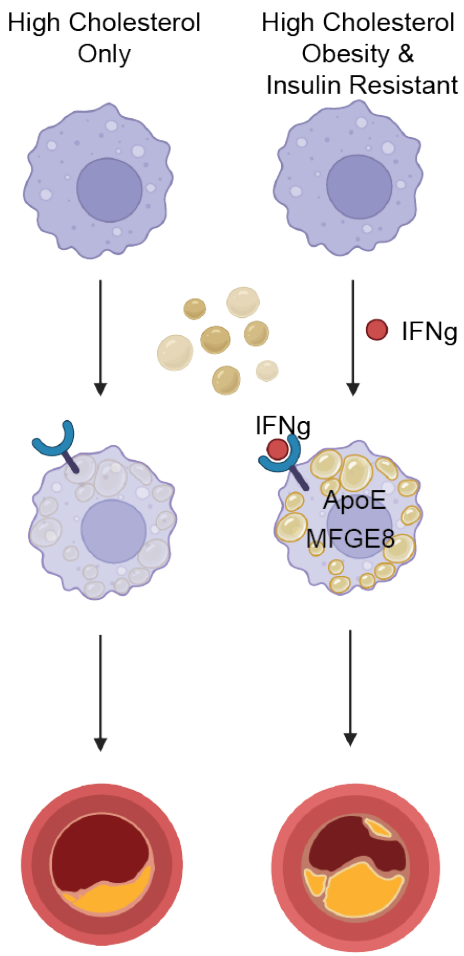

Figure 2.1 Interferon gamma (IFNγ) induced by metabolic inflammation exacerbates atherosclerosis. Cholesterol loaded or foam macrophages are a hallmark and driver of atherogenesis. In the context of obesity/IR IFNγ promotes cholesterol uptake by downregulating MSRN proteins most notable apoE in macrophages to enhance atherosclerosis.

Sterol Responsive Network' or MSRN (Reardon et al., 2018). Apolipoprotein E (apoE) is one of the most critical atheroprotective proteins present in the MSRN, as it serves as a cholesterol acceptor and is involved cholesterol efflux (L. Becker et al., 2010; Getz & Reardon, 2018; Reardon et al., 2018). Reardon & Lingaraju et al. found that obesity/IR in mice promoted dysregulation of nine MSRN proteins, including reduced apoE, C3 and MFEG8 levels, and increased macrophage cholesterol accumulation independently of cholesterol and lipid metabolism genes as these remained unaffected (*Cd36, Sra1, Srepb2*) or were upregulated to oppose cholesterol accumulation (*Abca1, Abcg1, Lxra*). *In vitro* studies with macrophages lacking apoE and C3 showed enhanced cholesterol accumulation relative to wild-type macrophages after incubation with serum from the obese/IR hypercholesterolemic *Ldlr-/-* mice suggesting that reduced expression of apoE and C3 likely contributed to the increased cholesterol loading in macrophages in obese/IR mice (Reardon et al., 2018).

Given the presence of low-grade inflammation in patients with type 2 diabetes (T2D), the impact of various inflammatory cytokines on MSRN expression in peritoneal macrophages was examined. *In vitro* treatment of IFNγ reduced the expression of apoE and MFEG8 and promoted the accumulation of cholesterol in wild type macrophages incubated with the serum from hypercholesterolemic obese/IR mice. To examine if IFNγ may have a role in obesity/IR promotion of atherosclerosis, *Ldlr-/-* mice were transplanted with bone marrow from wild type or interferon gamma receptor 1 (*Ifngr1-/-)* mice and fed a high fat, high cholesterol western type diet that results in hypercholesterolemia and obesity/IR or a low fat, high cholesterol diet that results in hypercholesterolemia but not obesity/IR. In the absence of myeloid *Ifngr1* peritoneal macrophage foam cell formation was reduced and MSRN protein levels restored without affecting cholesterol and lipid metabolism genes. Atherosclerosis was reduced in *Ldlr-/-* mice

transplanted with bone marrow from *IFNγr1-/-* mice with obesity/IR but not in mice without obesity/IR. IFNγ production by T cells was moderately increased in obesity/IR. These findings suggest that IFNγ produced in response to obesity/IR regulates the MSRN to exacerbate foam cell formation and atherosclerosis.

This study also provided evidence that the proatherogenic action of IFNγ on macrophages in obesity/IR is independent of the canonical IFNγ-STAT1-IRF signaling pathway that is known to be important for the host defense against pathogens. In this pathway IFNγ binding to IFNΓR1 induces heterodimerization with IFNΓR2 leading to phosphorylation and nuclear translocation of the transcription factor STAT1 and the expression of interferon regulatory factors (IRFs) that regulate the expression of genes involved in the host defense response (**Figure 2.2**).

First, IFNγ target genes (*Irf1, Irf8, Ibp1*) and phosphorylated STAT1 (pSTAT1) were not increased in peritoneal macrophages from obese/IR mice. Second, when BMDMs were treated with a range of IFNγ doses (0.03-12 ng/ml) extracellular apoE levels were reduced at low concentrations of IFNγ (0.03–1.2 ng/ml) without increases in pSTAT1 or *Irf8*. Furthermore, these low doses of IFNγ were not able to induce the macrophages to kill bacteria. Bacterial killing, phosphorylation of Stat1, and increased Irf8 were observed only at higher doses of IFNγ. This is consistent with the idea that obesity/IR is associated with low level of inflammation than is associated with bacterial infection. Finally, IFNγ was still able to reduce extracellular apoE levels in wild type BMDMs with STAT1 downregulated by siRNA or BMDMs from *Irf1-/-* mice.

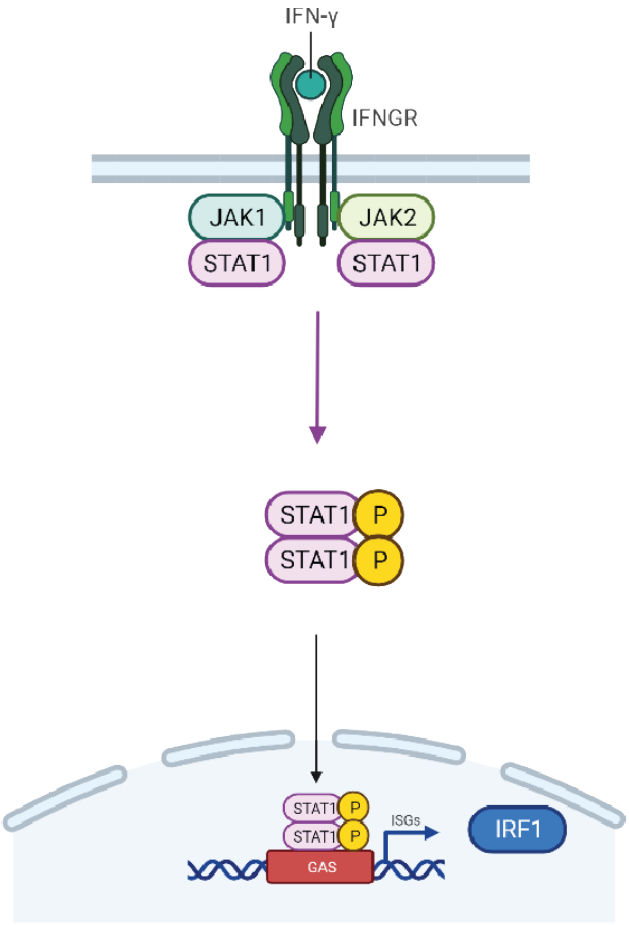

Figure 2.2 Canonical IFNγ signaling promotes the host defense response. Following binding to the IFNGR, IFNγ elicits its host defense activity on macrophages through the canonical pathway IFNγ-JAK-STAT pathway. This promotes the expression of host defense genes including IRF1.

Taken together, these findings suggest the pro-atherogenic actions of IFNγ on macrophages is likely not dependent on the canonical host defense signaling, alluding to an alternate pro-atherogenic and defense-independent pathway. This hypothesis is further supported by previous investigations showing that IFNγ modulates the expression of numerous genes in *Stat1−/−* macrophages (Ramana et al., 2002), indicating that STAT1-independent mechanisms play a significant role in the cytokine's impact on macrophage gene expression and function. Elucidating this novel pro-atherogenic pathway that is independent of host-defense could lead to the development of therapeutic targets that antagonize IFN*γ* without compromising the host-defense system in patients.

This chapter aims to find a non-canonical signaling pathway induced by obesity/IR and builds upon previous research conducted by the Becker group, which identified IFNγ as a cellular link between obesity/IR and atherosclerosis. My findings demonstrate that STAT1 and IRF1, canonical host-defense signaling proteins downstream IFNGR1, do not contribute to the obesity/IR enhancement of atherosclerosis in mice fed a WTD. This gave us the confidence to pursue the identification of a pro-atherogenic non-canonical IFNγ signaling pathway using a two-pronged approach. First, we sought to understand the fate of apoE in macrophages in response to IFNγ, and second, to narrow down the signaling pathway using unbiased phosphoproteomics. Our results show that IFNγ downregulates intracellular and extracellular apoE levels at the protein level, as mRNA apoE levels remained unchanged in response to IFNγ.

Furthermore, we showed that IFNγ increases the degradative machinery of the macrophage, giving us an insight that apoE may trafficked to degradation. Phosphoproteomics of

IFNγ treated bone-marrow derived macrophages (BMDMs) show signaling pathways involved in vesicle trafficking, autophagy, and degradation. Inhibitor studies may imply that IFNγ modulates both trafficking and degradation of apoE. However, further studies are needed to make firm conclusions on the specific mechanism in which IFNγ regulates apoE. While these targets uncovered by phosphoproteomics may be independent of the canonical host defense response, they are fundamental proteins involved in normal cell function, and targeting them therapeutically to address atherogenesis remains challenging. This work underscores the intricate interplay between inflammation and lipid metabolism in macrophages.

Impact. Overall, this work aims to identify a novel IFNγ pathway that plays a host defense independent role in atherogenesis. Targeting this pathway elicited by IFNγ may lead to the development of new therapeutics, especially for patients who are obese and insulin resistant, as they have an increased susceptibility for CVD mortality.

2.2 Methods

Mice: The University of Chicago IACUC (ACUP# 72209) approved all animal studies. Wild-type C57BL/6J (stock no. 000664), *Ptprca Pepc^{b}/BoyJ* (stock no.002014), *Ldlr-/-* (stock no. 002207), *Irf1-/-* (stock no 002762), LysM-Cre (stock no. 004781) and *Stat fl/fl* (stock no. 032054-JAX) and *Ldlr-/-* mice were purchased from Jackson Laboratory. All knockout and transgenic mice were on the C57BL/6 background. LysM-Cre, *Stat1 fl/fl* and *Ldlr-/-* mice were crossed to obtain *Ldlr-/-* mice with myeloid specific deletion of STAT1 (*mStat1-/-*) and control *Ldlr-/- Stat1 fl/fl* mice (*Stat1 fl/fl*). *Tfeb fl/fl* mice on the C57BL/6 background were obtained from Dr. Andrea Ballabio (Telethon Institute of Genetics and Medicine, Naples, Italy) and crossed with LysMCre mice to obtain m*Tfeb*-/- mice(Cui et al., 2021). For atherogenic studies, 7-

week-old male m*Stat1-/-* and *Stat1fl/fl* mice were placed on a western-type diet (WTD) (TD96121, Envigo: 21% milk fat, 1.25% cholesterol) diet for up to 16 weeks. Eight-week-old male *Ldlr-/-* mice were lethally irradiated (2 times 500 Gy separated by 16 hours) and transplanted with 5 x10^6 bone marrow cells from *Irf1-/-* mice or *Ptprca Pepc^b/BoyJ* mice (coisogenic C57BL/6 strain expressing CD45.1 allele) by Dr. Catherine Reardon. They were placed on the WTD 8 weeks post-transplantation to allow for bone marrow reconstitution and sacrificed after 12 weeks on diet.

Metabolic measurements: Blood glucose levels were measured with a *One Touch Ultra 2* glucometer (Lifescan) following a 3h fast. Total plasma cholesterol levels were measured on fast blood by the Amplex Red Cholesterol Assay kit (Invitrogen). Mice and spleen weight was determined at the time of sacrifice.

Quantification of atherosclerosis: Tribromoethanol anesthetized mice were perfused with PBS for 5 min, followed by 4% paraformaldehyde with 5% sucrose in PBS for 10 mins. The heart and upper vasculature were excised, cleaned of non-cardiac and vascular debris, and imbedded in optimal cutting temperature (OCT). Serial 10-µm sections of the innominate artery and the aortic root were collected using the Leica Cryocut 1800 cryostat as previously described (Reardon et al., 2018). Atherosclerosis in the innominate artery was assessed by averaging the lesion area in four sections between 150-450 mm above the junction of the innominate artery with the greater curvature of the aortic arch. Atherosclerosis in the aortic root was assessed by averaging the lesion area in three sections beginning at the appearance of the coronary artery and aortic valve leaflets. All sections were 100 mm apart. Sections were co-stained with Oil-Red-O and Fast green, and digital images were captured using a Nikon Eclipse Ti2 widefield microscope using 20x magnification for the innominate artery and 2x magnification for the aortic root using

brightfield. Atherosclerosis lesion area was quantified using NIS Elements AR software and expressed as mm^2.

Isolation of bone marrow-derived macrophage isolation: Bone marrow cells were isolated from the femur and tibia of mice and pooled. Cells were plated in Roswell Park Memorial Institute medium (RPMI) containing 10% FBS and 30% L-conditioned media as previously described (Reardon et a., 2018)). Media was changed on day 3 and 5, with activation occurring on day 6. BMDSs were treated with IFNγ (12ng/mL; R&D Biosystems) in 30% L-conditioned media.

Conditioned media and cell lysates: BMDSs were treated with IFNγ (12ng/mL; R&D Biosystems) in 30% L-conditioned media (DMEM) made with 10% FBS and 1% P/S, for 24h. Macrophage-conditioned media was prepared by the washing cells with PBS, and incubating them in serum-free RPMI media containing 1% P/S and M-CSF (20 ng/ml, R&D) for an additional 24 hr. The media was centrifuged to remove floating cells. Protein lysate was collected in 1% SDS containing protease inhibitors (Sigma) and quantified using a Pierce BCA protein assay kit (ThermoScientific).

Compound inhibitor studies: In studies with cotreatment with IFNγ and inhibitors, the inhibitors were added 2 hrs before IFNγ. The inhibitors included: D609 (PEBP1 inhibitor), INI-43 (importin beta inhibitor), Importazole (importin beta inhibitor), EKB-569 (GAK inhibitor), Doramapimod (p38 MAPK inhibitor), Trametinib (MEK1/MEK2 inhibitor), and SCH-772984 (ERK1/ERK2 inhibitor). All these compounds were purchased from MedChemExpress. Chloroquine and MG-132 were obtained from SelleckChem.

Viability Assay: BMDMs were seeded in 24 well plates (Corning) at 250,000 cells/well and differentiated using the method mentioned above. On day 5, BMDMs were treated with varying

concentrations of compounds for 24h. Following that cells were treated with cell permeant dye CalceinAM that fluoresces green in a live cell (ThermoFisher C1430; ex: and em:). Cells were incubated with 10 uM of Calcein AM for 15 mins at 37C following which they were washed 3 times in PBS. Cells were imaged in PBS using Sartorius Incucyte S3 for using the green excitation settings.

Immunoblot analysis: Macrophage-conditioned medium (normalized to protein concentration) and cell lysates (7 ug) (normalized to tubulin) were subjected to SDS-PAGE on 4%–12% gradient gels, transferred to PVDF membranes (Millipore), blocked with 5% milk and probed with rabbit anti-mouse apoE antibody (0.5 μg/mL) (abcam) and anti-mouse a-tubulin antibody (Cell Signaling Technology) and HRP-linked goat anti-rabbit antibody (abcam). Proteins were visualized using ECL detection kit (BioRad) and the LiCor Odyssey Imaging system and quantified by densitometry using ImageJ software. ApoE level in intracellular immunoblots were normalized to a-tubulin levels.

In Cell Western: BMDMs were seeded in black walled/clear bottom 96 well plates (Corning) at 20,000 cells/well. After differentiation, cells were treated with or without IFNγ (R&D biosystems) at 12 ng/mL. After 24h, cells were washed 3x with PBS and fixed using 4% PFA (ThermoFisher) and blocked with 5% NGS probed with rabbit anti-mouse apoE antibody (0.5 μg/mL) (abcam) and anti-mouse a-tubulin antibody (Cell Signaling Technology) near infra-red goat anti-rabbit or donkey anti-mouse antibody (abcam). Signal was detected and quantified using the LiCor Odyssey Imaging system.

DQ-OVA Assay for degradative capacity: The degradative capacity of macrophages was evaluated using a DQ-OVA degradation assay by measuring fluorescence with a plate reader.

BMDMs were plated in a black wall/clear bottom 96 well plates at 20,000 cells/well. Fully differentiated macrophages were treated with 12 ng/mL IFNγ (R&D Biosystems) for 1, 2, 6, 12, and 24h. Following IFNγ treatment, BMDMs were treated with 10 μg/mL of DQ-OVA at 37°C for 15 minutes, washed with PBS, and then incubated at 37°C for an additional 15 minutes. The fluorescence of DQ-OVA was measured using an Agilent Syntex Microplate Reader.

qRT-PCR: RNA was isolated using QIAGEN Midi-Prep Kits and RT with Quantiscript

(QIAGEN) using random hexamers (Invitrogen). mRNA levels were measured with specific primers (IDT) using SYBR green on a One Step Plus system (Applied Biosystems). Relative levels of each target gene were calculated using the ΔΔCt formula and 18S RNA as a control.

Primer sequences are:

Mouse *Apoe*: Forward: CGCAGGTAATCCCAGAAGC

Reverse: CTGACAGGATGCCTAGCCG

Mouse *18s*: Forward: GCCGCTAGAGGTGAAATTCTT

Reverse: CGTCTTCGAACCTCCGACT

Phosphoproteomics: Triplicate wild type BMDMs in 15 cm dishes were treated with 12 ng/ml IFNγ for 30 or 120 minutes. The IFNγ treated cells and untreated MO cells were lysed in 1 ml Lysis buffer (0.1% Rapigest (Waters Corp.), 10 mM Tris-HCl, pH 7.5, 1mM EDTA, 1 mM sodium fluoride, 1 mM b-glycerophosphate, 1 mM sodium orthovanadate, 1 mM sodium pyrophosphate, 1 mM PMSF, and 1 Complete mini-proteinase inhibitor cocktail, EDTA free per

10 ml lysis buffer) (Paulo et al., 2015; Possemato et al., 2017). The cell lysate was sonicated, centrifuged to remove cell debris and then reduced, alkylated, and digested overnight at 37°C with sequencing-grade trypsin (1:50, w/w, trypsin/protein; Promega). Tryptic digests were adjusted to 0.4% trifluoracetic acid and subjected to solid-phase extraction on a Sep-Pack tC18 column (HLB, 100 mg; Waters Corp.) and eluted with 0.3% formic acid/80% acetonitrile. Fractions containing peptides were dried under vacuum and resuspended in 50% acetonitrile/2M lactic acid (5 mg protein/mL). Titansphere TiO 5 um beads (GL Sciences) were added to the peptides (1:8 peptide:bead w/w) and rotated for 1 hour. After washing the beads with 50% and 25% acetonitrile with 0.1% TFA, the phosphopeptides were eluted with 50 mM K_2HP0_4/NH_4OH pH 10, neutralized in an equal volume of 50% acetonitrile/5% formic acid, desalted on Sep-Pack tC18 column (50 mg), eluted with 0.3% formic acid/80% acetonitrile and speed vac dried. Peptides were sent to Dr. Tomas Vaisar at the Quantitative and Functional Proteomics Core, University of Washington for liquid chromatography-electrospray ionization-tandem MS (LC-ESI-MS/MS). Differentially expressed proteins were identified using a combination of the t-test ($p<0.05$) and G-test ($G>1.5$) as previously described (Heinecke et al., 2010). Differentially changed phosphoproteins were placed on a literature search using PubMatrix (K. G. Becker et al., 2003).

2.3 Results

2.4 The canonical IFNγ-STAT1-IRF1 signaling pathway does not play a role in atherogenesis *in vivo*.

Previously, we observed that STAT1 downregulation or IRF1 knockout failed to restore extracellular apoE levels in macrophages treated with IFNγ in vitro. We next wanted to establish If the IFNγ-STAT1-IRF1 signaling pathway in myeloid cells also did not have a role in obesity/IR promotion of atherosclerosis. Our first investigation involved performing bone marrow transplantation (BMT) of either *wt* (*wt* BMT) or *Irf1-/-* (*Irf1-/-* BMT) bone marrow cells to *Ldlr-/-* mice to ablate *Irf1* expression in the myeloid cell lineage (**Figure 2.3**). After successful transplantation, mice were placed on a WTD for 12 weeks to induce obesity/IR and hyperlipidemia and evaluated for metabolic parameters such as glucose, body weight, and cholesterol. Our results showed that *Irf1-/-* BMT did not significantly affect these parameters compared to *wt* BMT (**Figure 2.4**). Additionally, spleen weights between both genotypes were unremarkable, indicating the absence of systemic inflammation at the time of sacrifice. Cross-sectional analysis of the innominate artery and aortic root revealed no significant differences in lesion size in both anatomical regions (**Figure 2.4**). These *in vivo* results, combined with the *in vitro* data previously published (Reardon et al., 2018), strongly suggest that IRF1 in the canonical IFNΓR1-STAT1-IRF1 pathway is not involved in atherogenesis in obesity/IR.

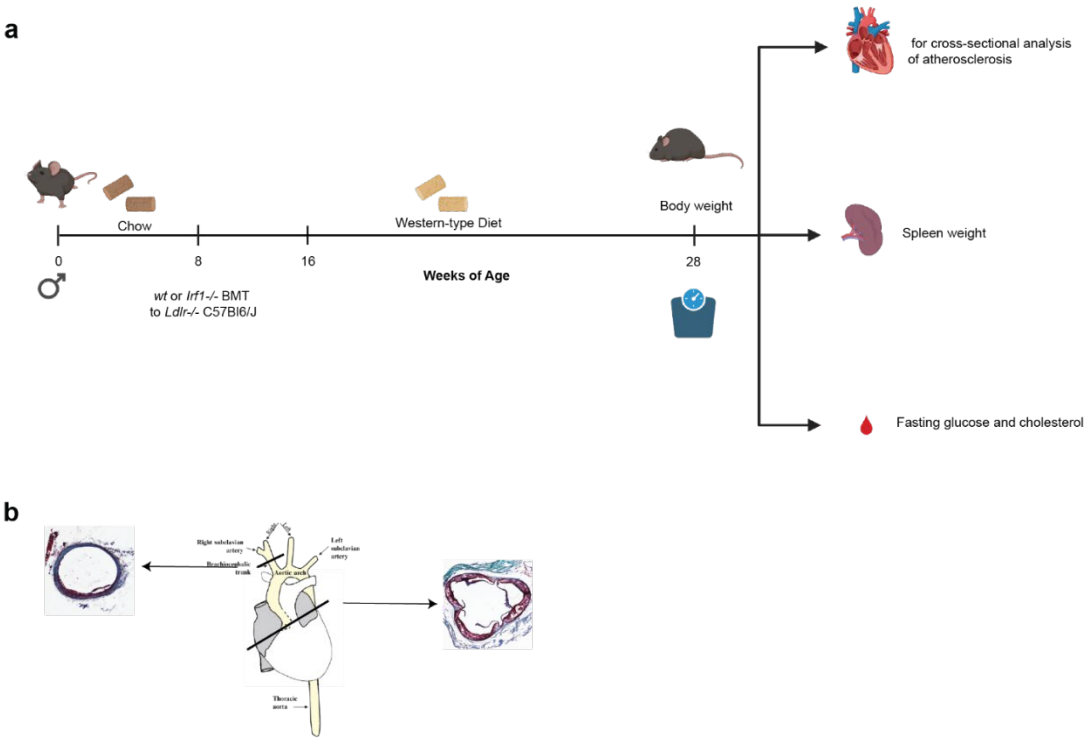

Figure 2.3 Genetic and dietary models to study the impact of myeloid IRF1 on atherosclerosis. (a) 16-week-old C57BL/6J *Ldlr-/-* male mice transplanted with *Irf1-/-* or *wt* bone marrow at 8 weeks of age were placed on a western-type diet (WTD; 21% milk fat, 1.25% cholesterol) for 12 weeks. Prior to sacrifice mice were weighed and fasted for at least 3h to collect blood for glucose and cholesterol levels. At sacrifice the heart and upper vasculature were collected for cross sectional analysis of atherosclerotic lesions and spleen weight was observed as a proxy for inflammation. (b) Anatomical cross sectional analysis schematic of innominate artery (brachiocephalic artery) and aortic root.

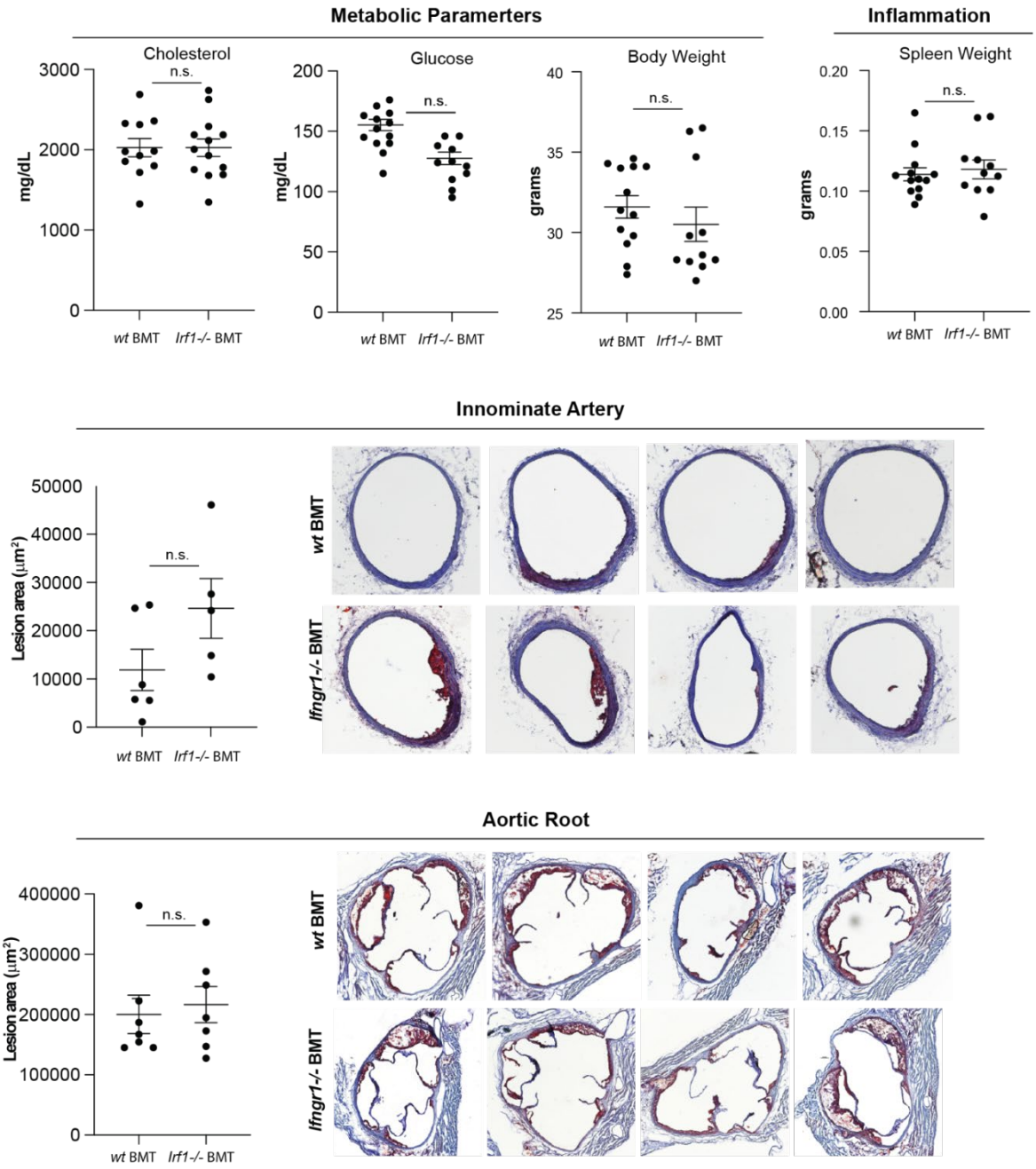

Figure 2.4 Deficiency of myeloid *Irf1* does not influence metabolic parameters, spleen weight and lesion size in obese/IR *Ldlr-/-* male mice fed a WTD. (Top) Metabolic parameters and spleen weight in *Ldlr-/-* mice transplanted with *Irf1-/-* or *wt* bone marrow. (Middle) Innominate artery lesion area and representative images. (Bottom) Aortic root lesion area and representative images. Results are mean ± SEM. No significant differences were observed (student's *t*-test); *n*=6-12/group

Next, we wanted to evaluate the effects of macrophage STAT1, which is upstream of IRF1 and downstream of IFNγ (**Figure 2.2**), on atherosclerosis in obesity/IR mice. For this we knocked out *Stat1* in myeloid cells (m*Stat1-/-*) using the Stat1*fl/fl* LysMCre system in *Ldlr-/-* mice (**Figure 2.5**). After 16 weeks of WTD, metabolic parameters such as glucose levels, weight, and cholesterol levels were not significantly different between m*Stat1-/-* and *fl/fl Ldlr-/-* mice. Further, spleen weights of both *fl/fl* and m*Stat1-/-* mice were of typical size, suggesting systemic inflammation from myeloid deficiency of *Stat1* was not present (**Figure 2.6**). Cross sectional analysis of the innominate artery and aortic root revealed no significant differences in lesion size in both anatomical regions, indicating that STAT1 in macrophages does not play a role in atherosclerosis in the context of obesity/IR (**Figure 2.6**). Taken together, these data suggest that the canonical IFNΓR1-STAT1-IRF1 signaling cascade is not involved in exacerbating atherosclerosis in obesity/IR *in vivo* (**Figure 2.1**).

These *in vivo* and previous *in vitro* findings indicate the mechanism of action of IFNγ on atherogenesis may be independent of the host defense pathway (**Figure 2.7**). To identify this novel pathway, we decided to use a hybrid approach that includes a top-down (phosphoproteomics) and bottom-up (observing the fate of apoE) tactics to understand the pro-atherogenic effects of IFNγ. In the top-down approach unbiased phosphoproteomics was utilized to find potential signaling protein pathways and the bottom-up approach to understand the fate of apoE to allow us to narrow down the pathway involved.

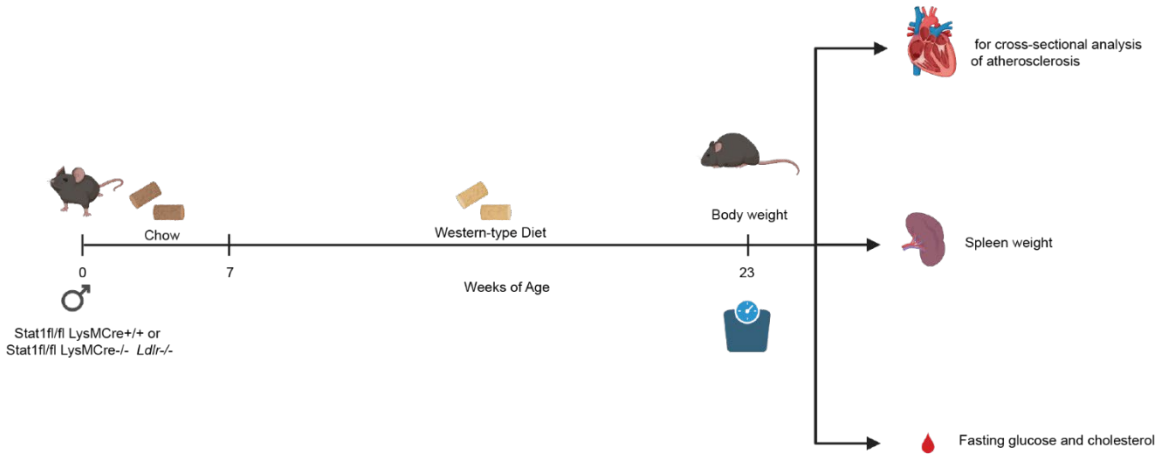

Figure 2.5 Genetic and dietary models to study the impact of myeloid *Stat1* KO on atherosclerosis. 7-week-old *Ldlr-/-* male mice with myeloid specific *Stat1-/-* deficiency *(*m*Stat1-/-) or Stat1fl/fl* were placed on a WTD for 16 weeks. Prior to sacrifice mice were weighed and fasted for at least 3h to collect blood for glucose and cholesterol levels. At sacrifice the heart and upper vasculature were collected for cross sectional analysis of atherosclerotic lesions and spleen weight was observed as a proxy for inflammation.

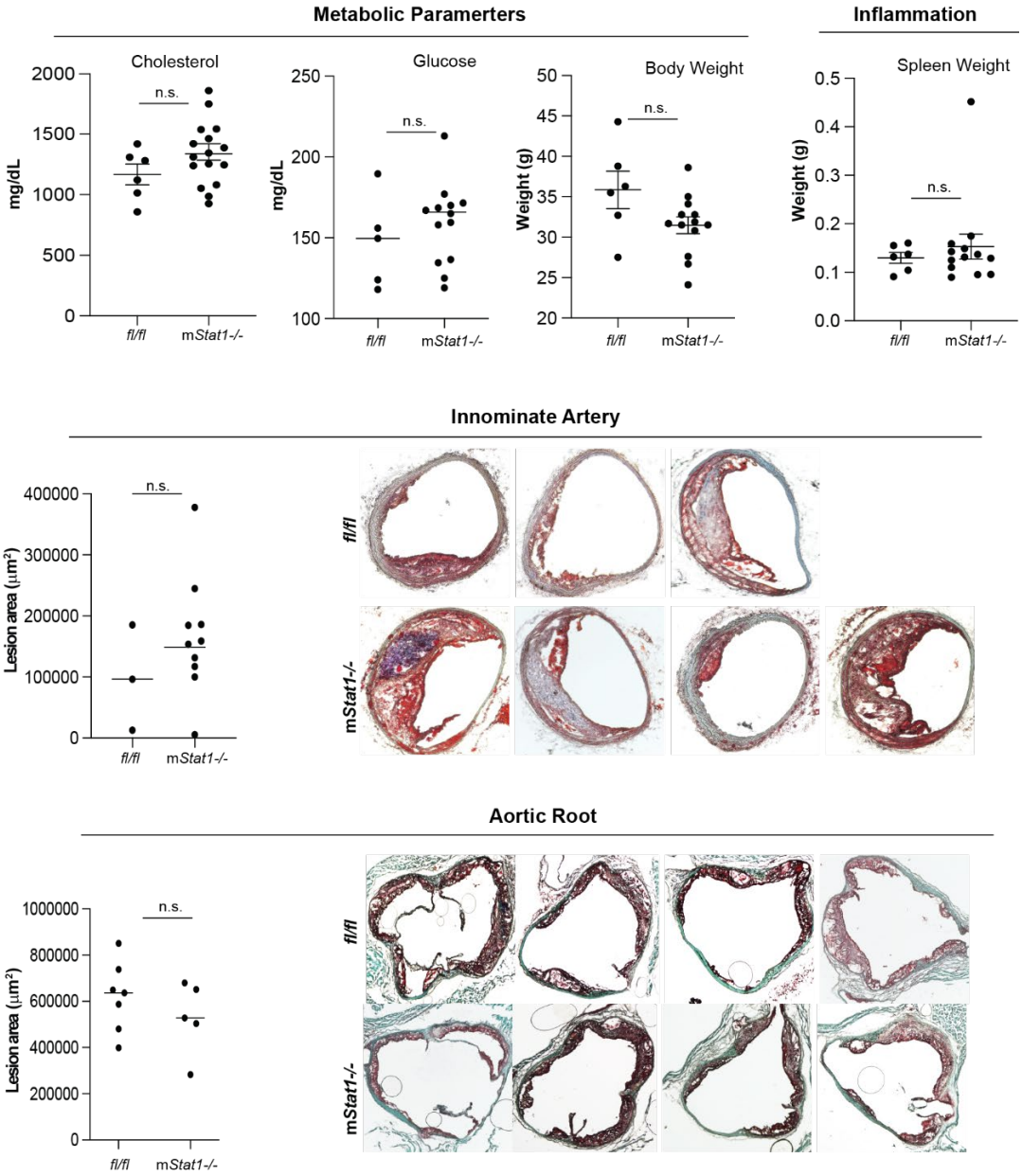

Figure 2.6 *mStat1-/-* does not influence metabolic parameters, spleen weight and lesion size in obese/IR *Ldlr-/-* male mice fed a WTD. (Top) Metabolic parameters and spleen weight of *Ldlr-/- Stat1* $^{fl/fl}$ or m*Stat1-/-*mice. (Middle) Innominate artery lesion area and representative images. (Bottom) Aortic Root lesion area and representative images. Results are mean ± SEM. No significant differences were observed (student's *t*-test); *n*=6-12/group

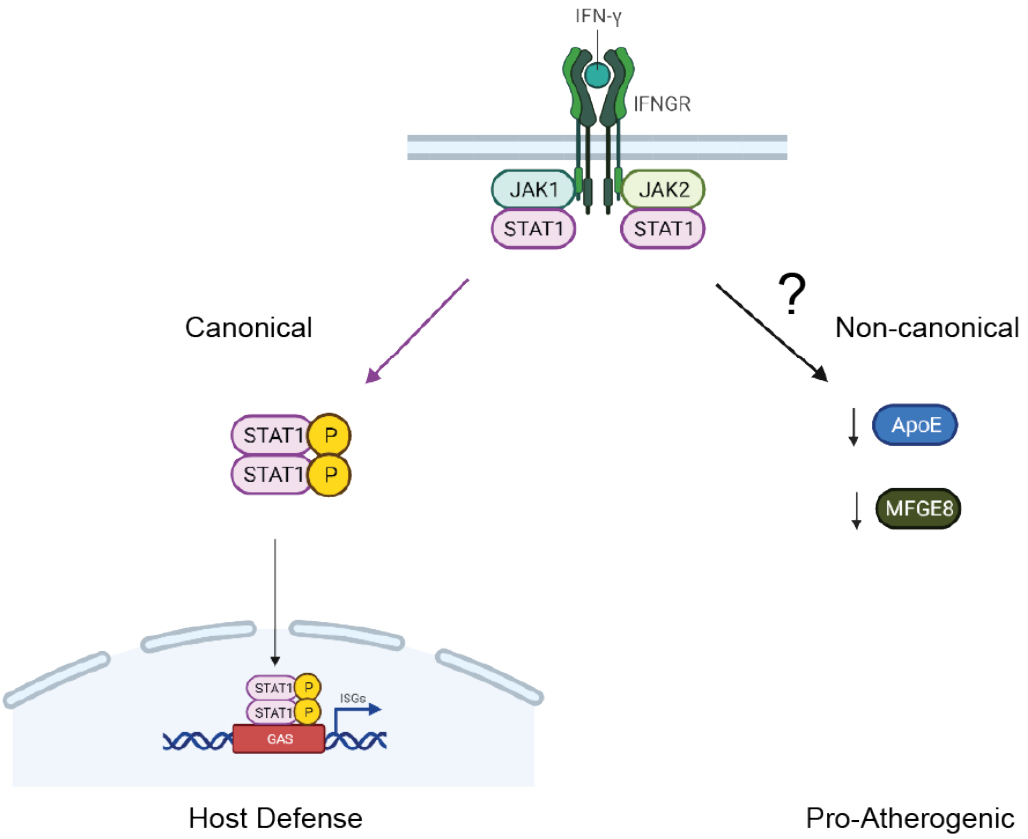

Figure 2.7 Canonical IFNγ signaling is not involved in exacerbating atherosclerosis in obesity/IR. IFNγ elicits its host defense activity on macrophages through the canonical IFNγ-STAT1-IRF pathway. Collectively, our data suggest that these proteins are not involved in regulating the MSRN proteins and exacerbating atherosclerosis in obesity/IR, pointing to an alternative, host-defense independent and pro-atherogenic pathway.

2.5 IFNγ regulates macrophage apoE expression at the protein level.

Previously, we observed that extracellular apoE levels were significantly decreased in response to IFNγ in peritoneal macrophages (Reardon et al., 2018). While peritoneal macrophages are a suitable model to study aortic macrophages, we sought to use bone-marrow derived macrophages (BMDMs) for our studies as the number of macrophages we can obtain is significantly larger from BMDMs and phosphoproteomics demanded a large scale of cells. To validate the IFNγ effects on apoE in BMDMs, we treated the cells with IFNγ for 24h and observed that IFNγ significantly downregulates extracellular apoE, corroborating the findings on peritoneal macrophages (**Figure 2.8a**). Significant reduction (~75%) was observed by 4 h and almost complete reduction by 8 h post-IFNγ treatment (**Figure 2.8b**) indicating a rapid response. We next examined the effect of IFNγ on intracellular apoE levels and apoE mRNA levels to help understand how extracellular apoE levels are reduced. We observed that IFNγ also significantly decreases intracellular apoE with a similar time course as extracellular apoE (Figure 2.8c and d). The decrease in intracellular apoE and another MSRN protein MFGE8 was confirmed by proteomic analysis of cellular lysates (**Figure 2.8e**). These two events occur independent of mRNA transcription, as the apoE mRNA levels in response to IFNγ were unchanged (**Figure 2.8f**), consistent with previous results (Brand et al., 1993). These findings suggest the effects of IFNγ on apoE occurred post-transcriptionally.

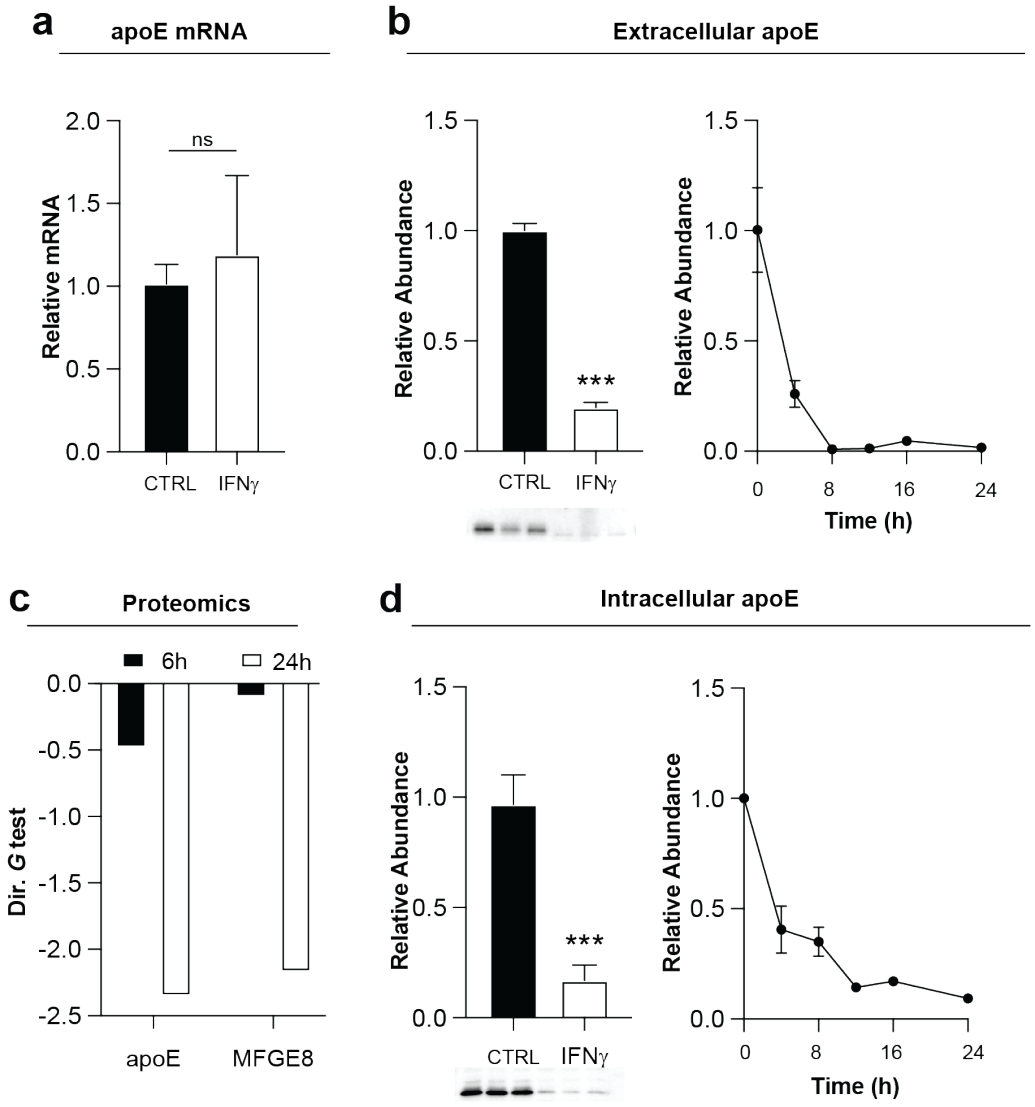

Figure 2.8 IFNγ post-transcriptionally decreases intracellular and extracellular apoE levels in BMDMs. (a) Bone-marrow-derived macrophages were treated with 12 ng/mL IFNγ for 24h. apoE mRNA was quantified and control was compared to IFNγ. (b) Immunoblot detection of extracellular apoE following 24h of 12 ng/mL IFNγ treatment (top left) immunoblot of extracellular apoE (bottom left). Time course of IFNγ-mediated reduction of extracellular apoE in BMDMs (right). (c) Proteomic detection of apoE and MGFE8 in BMDMs treated with 12 ng/mL IFNγ for 6 and 24h. (d) Time course of IFNγ-mediated reduction of intracellular apoE in BMDMs treated with IFNγ. Quantification of immunoblot (top left). Intracellular apoE immunoblot (top bottom). Results are mean ± SEM. ns ($p > 0.05$), * ($p \leq 0.05$), ** ($p \leq 0.01$), *** ($p \leq 0.001$), **** ($p \leq 0.0001$) (student's *t*-test). All experiments were $n = 3$

Since transcription (DNA to mRNA) was unaffected, we reasoned that the change in apoE observed could be due to changes in the translation machinery (**Figure 2.9a**). To test if apoE mRNA to protein translation is affected in response to IFNγ, we treated BMDMs with 20 uM Brefeldin A (BFA). This compound halts the trafficking of newly synthesized proteins to the Golgi and to the normal secretory pathway (**Figure 2.9a**) by inhibiting COPI vesicle formation from endoplasmic reticulum (ER) to the Golgi (Chardin & McCormick, 1999). Since apoE is translated in the ER and follows the normal secretory pathway (ER to Golgi and then secretion), we reasoned that if IFNγ decreases apoE translation (mRNA to protein), then the decrease of intracellular apoE in response to IFNγ would occur even with BFA treatment. On the other hand, if translation is not affected, then we would expect to not see difference in intracellular apoE levels between IFNγ-treated and control macrophages. BMDMs treated with Brefeldin A 'rescue' the intracellular downregulation of apoE by IFNγ. in macrophages but not its extracellular levels (**Figure 2.9b**), suggesting that IFNγ does not alter translation of apoE and IFNγ post-translationally regulates apoE levels.

The data so far suggests that extracellular apoE is downregulated in response to IFNγ. This downregulation is not a result of aberrant intracellular apoE trafficking, because we don't see accumulation of intracellular apoE in response to IFNγ. Instead, proteomics and western blot analysis of macrophages treated with IFNγ show significant decrease of intracellular apoE. IFNγ treated macrophages do not change their mRNA levels of apoE nor is translation affected. These data may point to an IFNγ-mediated degradation of IFNγ.

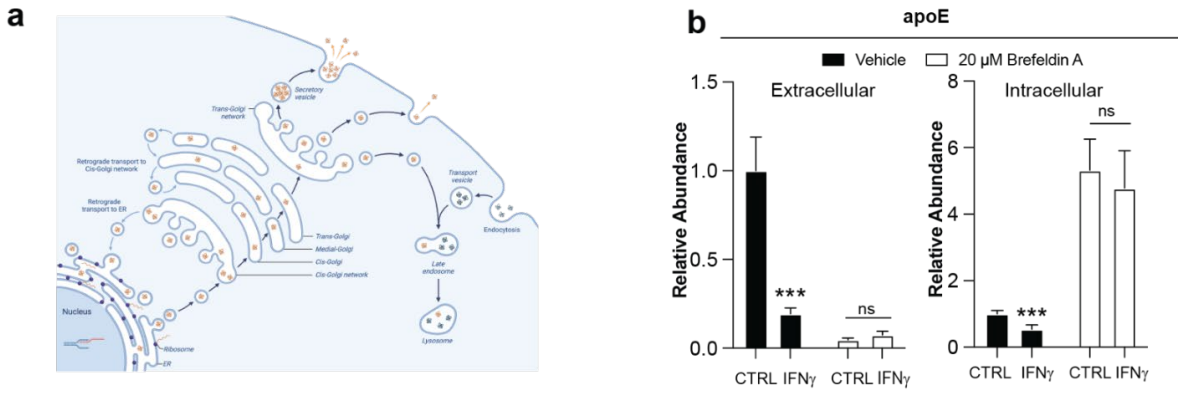

Figure 2.9 IFNγ post-translationally affects apoE in macrophages. (a) apoE follows the normal endocytic pathway where mRNA transcripts are synthesized in the nucleus, protein is translated in the ER and translocated to the Golgi for additional modifications and secreted to the extracellular milieu. (b) BMDMs pre-treated for 2 h with 20 Brefeldin A before treating with IFNγ for 24 h. Results are mean ± SEM. *$p < 0.05$ (student's *t*-test) n=3

We hypothesized that IFNγ may downregulate apoE by degradation. There are two main machineries that the cell uses for protein and organelle clearance, these are the autophagy-lysosome and ubiquitin–proteasome pathways. The autophagy- lysosome system degrades a variety of large and small substrates such as protein complexes and organelles. This bulk degradation of cytoplasmic proteins or organelles is largely mediated termed autophagy. The ubiquitin-proteasome system is formed from multiprotein complexes and degrade short-lived nuclear and cytosolic proteins that are tagged with ubiquitin for degradation.

To pursue this degradation hypothesis, we wanted to understand the degradative state of the IFNγ-activated macrophage. To this regard, previous investigators have shown increased Cathepsin B and Cathepsin L lysosome protease activity in macrophages as a result of IFNγ activation (Beers et al., 2003) (Lah et al., 1995) (Q. Li & Bever, 1997). Additionally, others have shown IFNγ to induce autophagy via the p38 pathway (Hardy et al., 2009) (Matsuzawa et al., 2014). To recapitulate these literature findings in our lab, we probed for the degradative activity of IFNγ activated BMDMs using a DQ-OVA degradation assay. DQ-OVA is a self-quenched conjugate of ovalbumin with a BODIPY dye that is released upon proteolytic digestion and exhibits bright green fluorescence We measured DQ-OVA degradation at various times after IFNγ treatment of BMDMs (2, 4, 8, 10, and 24h) and show that IFNγ promotes degradation of DQ-OVA (**Figure 2.10a**). To confirm these results, we the lysosome acidification inhibitor Bafilomycin A1 (inhibitor of vATPase) and the protease inhibitor MG-132 and observed decrease in DQ-OVA degradation. These data support the degradative assay, and our results suggest the degradative activity of BMDMS is increased with IFNγ (**Figure 2.10b**). Similarly, we see that LAMP1 expression is increased in IFNγ treated BMDMs, suggesting the lysosome numbers are increased (**Figure 2.10c**). Together these data show that the degradative machinery

of the IFNγ-treated macrophage measured by DQ-OVA is elevated compared to naïve macrophages, providing us confidence to pursue our IFNγ mediated degradation of apoE in macrophage hypothesis.

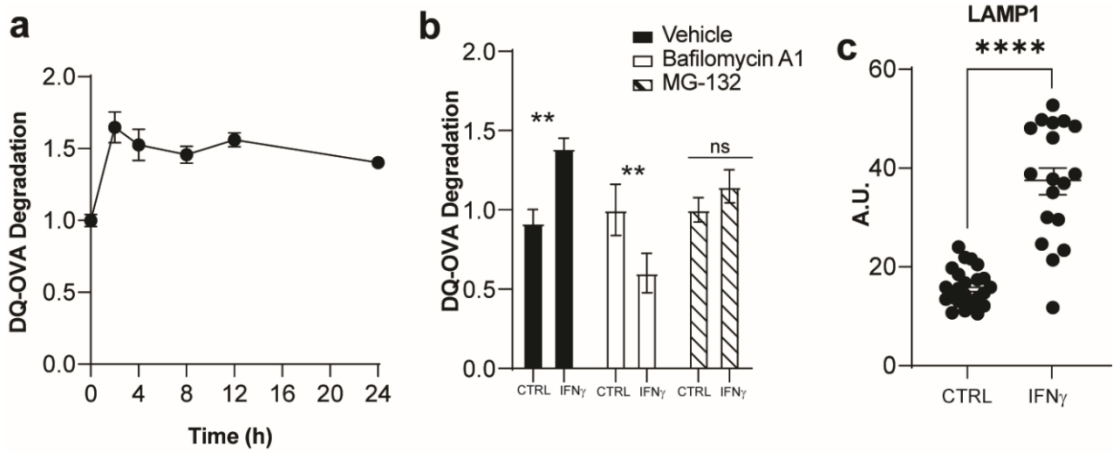

Figure 2.10 IFNγ enhances protease activity in BMDMs. (a) BMDMs treated with IFNγ for various times were incubated with 10 μg/mL DQ-Ova to measure degradation. (b) Degradative activity induced by IFNγ is attenuated by vATPase inhibitor Bafilomycin A1 (500 nM) and MG-132 (5 μM). (C) Confocal microscopy of LAMP1 in BMDMs treated with IFNγ for 60-min. Results are mean ± SEM. ns ($p > 0.05$), * ($p \leq 0.05$), ** ($p \leq 0.01$), *** ($p \leq 0.001$), **** ($p \leq 0.0001$) (student's *t*-test) $n=3$

To test our hypothesis, we used commercially available autophagy (chloroquine) and proteasome (MG-132) small molecule inhibitors. Chloroquine inhibits autophagy by impairing autosome fusion with lysosomes and by increasing lysosome pH (Klionsky et al., 2016) (Mauthe et al., 2018). MG-132 inhibits the degradation of ubiquitinated proteins by the 26S proteosome (Mroczkiewicz et al., 2010; Tsubuki et al., 1996). If IFNγ promotes apoE degradation via autophagy or proteasome pathways, then adding small molecule inhibitors would restore apoE levels. We observed that the proteasome inhibitor and autophagy inhibitor 'rescues' apoE intracellular decrease by IFNγ but does not rescue the extracellular decrease (**Figure 2.11a** and **b**). To confirm that the chloroquine compound indeed interfered with autophagy we measured LC3-II levels, which accumulates in when autophagy is compromised (Runwal et al., 2019; Yorimitsu & Klionsky, 2005). In addition to small molecules, we used a genetic approach to examine the role of lysosomes-autophagy on intracellular apoE levels. Transcription factor EB (TFEB) is a major regulator of genes involved in lysosomal biogenesis and function and autophagy (Cui et al., 2021; Napolitano & Ballabio, 2016). In the absence of *Tfeb* lysosomal proteins are reduced. Intracellular apoE levels were "rescued" in IFNγ treated BMDMs from *mTfeb-/-* mice (**Figure 2.11c**). So far, we have shown that IFNγ-treated macrophages increase proteolytic activity, and that treating macrophages with autophagy and proteasome inhibitors restore intracellular apoE levels but not extracellular apoE. Together, these data may support the hypothesis that in macrophages, IFNγ may modulate trafficking of newly synthesized apoE for degradation. Whether to the proteasome, the lysosome, or both is yet to be determined. Furthermore, restoring intracellular apoE by autophagy and proteasome inhibitors does not promote its extracellular expression. It is noteworthy to mention that rescuing extracellular apoE from IFNγ mediated downregulation is imperative for modulating obesity/IR mediated enhanced

atherosclerosis. ApoE is a cholesterol acceptor and helps efflux cholesterol from lipid loaded macrophages in the atherosclerotic lesions back to the liver for excretion (Getz & Reardon, 2018).

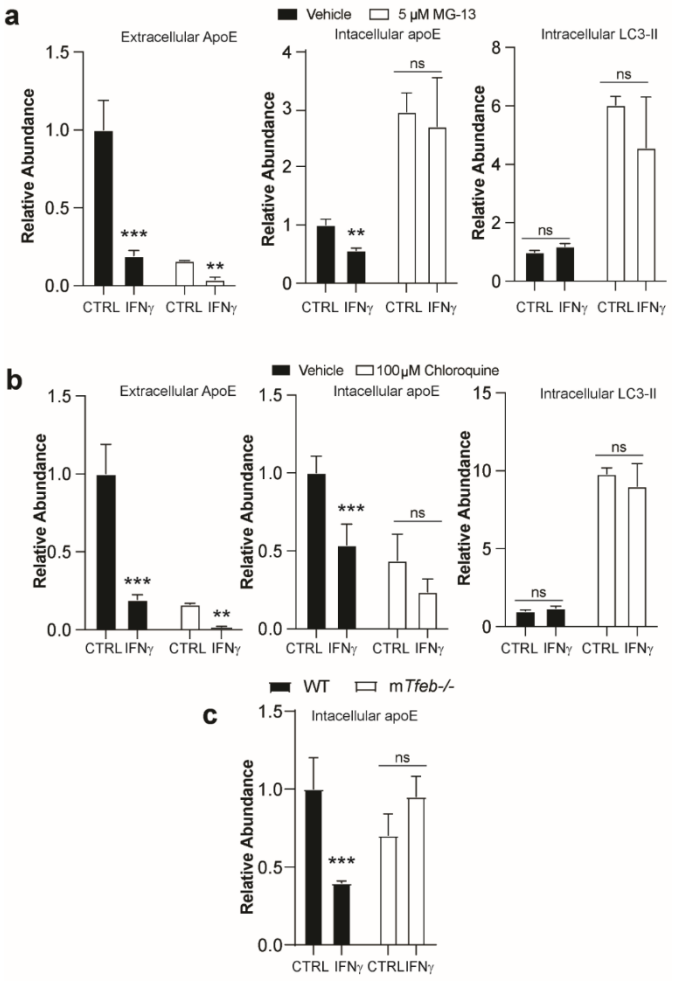

Figure 2.11 Small molecule or genetic (m*Tfeb-/-*) inhibitors of degradation restore intracellular apoE levels but do not restore extracellular apoE in BMDMs. BMDMs treated with IFNγ 24h with or without (a) lysosome acidification inhibitor chloroquine (100 uM) or (b) proteasome inhibitor MG-132 (5 uM). (c) Tf*eb-/-* BMDMs treated with IFNγ. Results are mean ± SEM. ns ($p > 0.05$), * ($p \leq 0.05$), ** ($p \leq 0.01$), *** ($p \leq 0.001$), **** ($p \leq 0.0001$) (student's *t*-test) n=3

2.6 Phosphoproteomics Approach for Uncovering Non-Canonical IFNγ Signaling Pathway

Since IFNγ signaling involves phosphorylation of proteins, we have chosen to use a phosphoproteomics approach to identify proteins differentially phosphorylated in the presence of IFN□ followed by verification of their role in regulating apoE expression in macrophages. To explore the potential signaling pathways involved in the dysfunction of the MSRN pathway mediated by IFNγ, we employed an unbiased phosphoproteomics approach. For this, we used bone marrow-derived macrophages (BMDMs) obtained from wild-type mice. The BMDMs were treated with IFNγ for 30 minutes and 120 minutes. We included an additional control group without IFNγ treatment (M0). To investigate the phosphorylation events that occur during these conditions, we isolated phosphoproteins from the BMDM cell lysates. These phosphoproteins were then subjected to analysis using LC-ESI-MS/MS (Liquid Chromatography-Electrospray Ionization Tandem Mass Spectrometry) (**Figure 2.12a**). This analytical technique allowed us to identify and characterize the specific proteins that undergo phosphorylation, shedding light on the signaling cascades associated with IFNγ-induced dysfunction in the MSRN pathway. As expected, phosphorylated Stat1 was enriched in the phosphoproteins isolated from the IFNγ treated cells relative to the M0 cells confirming phosphoprotein enrichment.

Using unbiased phosphoproteomics, we found 136 phosphoproteins to be significantly modulated by IFNγ (**Figure 2.12b**). Most of these proteins were known to have diverse biological functions (**Figure 2.12c**). To narrow these to a workable list of candidates we performed a literature search using PubMatrix software (K. G. Becker et al., 2003) where we compared our list of differentially phosphorylated proteins against a selection of relevant

biological functions such as ‘apoE, interferon, trafficking, atherosclerosis, secretion’ (**Figure 2.12d**).

Statistical analysis, literature mining, and our *in vitro* assays of apoE guided the list of candidate proteins. Our candidate proteins overwhelmingly represent proteins involved in autophagy, MAPK signaling cascades, and vesicle trafficking. Interestingly, these three distinct ‘pathways’ dynamically interact with one another, the common node of interaction being autophagy. For example, MAPK signaling pathways have been shown to modulate autophagy (p38). Vesicle trafficking proteins such as GAK and VAMP3 have been implicated in regulating autophagy and exocytosis(Bajno et al., 2000; He et al., 2020; C. Hu et al., 2007; Jović et al., 2014; Korolchuk & Banting, 2002; Kovackova et al., 2015; Miyazaki et al., 2021).

While these candidates may be intricately related, for the purposes of organization, we propose three conceptual frameworks in which we pursued subsequent experiments. The first is the concept of degradation, this could be by autophagy and/or proteasomes (ATG13, ZFAN5). Indeed some investigators have shown that apoE can be degraded by serine proteases in the lysosome while others have shown that apoE is degraded through autophagy post-Golgi trafficking (Fote et al., 2022)). In addition, our previous results with genetic and small molecule inhibitors of autophagy implicates IFNγ may influence apoE for degradation, corroborating published literature.

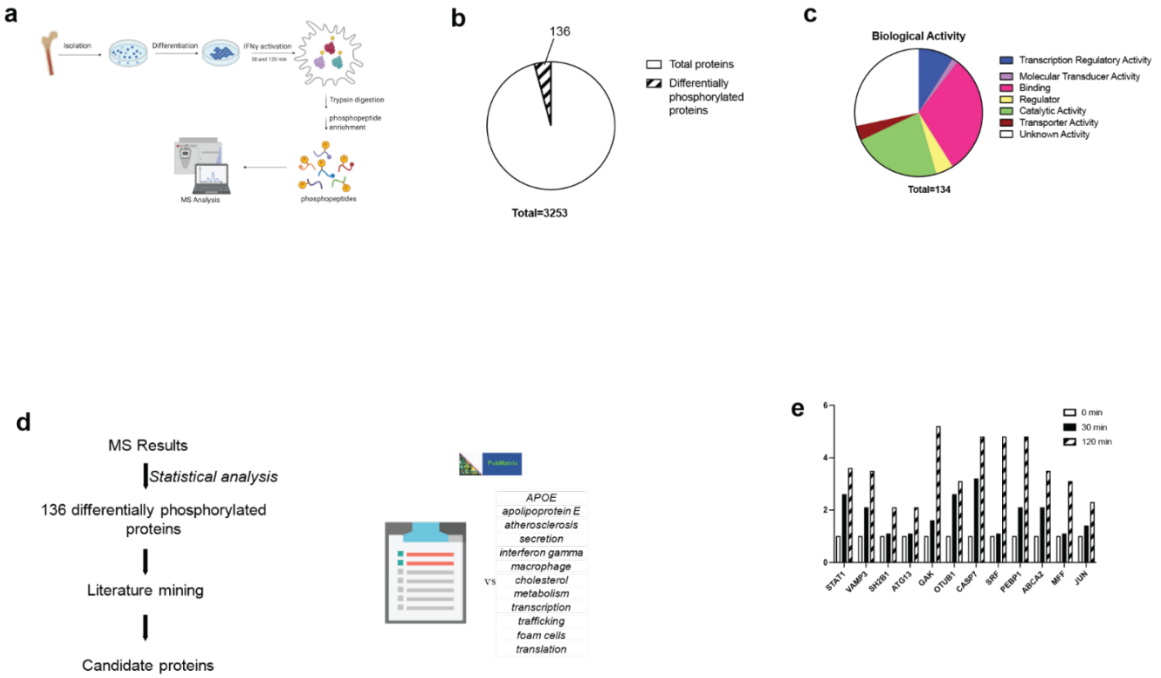

Figure 2.12 Phosphoproteomic analysis of IFNγ treated BMDM. (a) BMDMs were harvested from 7-week-old C57BL/6J male mice and plated in 15 cm dishes at 13 million per dish. Following 6 days of differentiation using 30% L-conditioned medium (DMEM) in RPMI supplemented with 10% FBS and 1% P/S cells were treated with 12 ng/mL IFNγ for 30 or 120 mins (n=3 plates/time point). IFNγ treated and naïve (M0) cells were harvested and digested with trypsin and subjected to phosphopeptide enrichment. Samples were dried using speed vac and sent to The University of Washington for LC-MS/MS. (b) Proteomic results were analyzed and revealed 136 differentially phosphorylated proteins in response to IFNγ. (c) Pie chart depicting known biological activity of the differentially phosphorylated proteins. (d) Candidate proteins were subjected to PubMatrix literature search to see their relationship to atherosclerosis and macrophages. (e) Relative spectral counts of candidate phosphorylated proteins induced by IFNγ.

Table 2.1. Candidate proteins

Candidate Name	Function	Major Associated Pathway
ATG13	Scaffold	Autophagy
ABCA2	Transporter	Cholesterol Metabolism
PEBP1	inhibitor protein /binds LC3	MAPK
C-JUN	Transcription Factor	MAPK
SRF	Transcription Co-Activator	MAPK
RGS3	Inhibitor protein	MAPK
MAPK2	kinase	MAPK
PEBP1	Scaffold/Inhibitor	MAPK
ZFAN5	effector protein	Proteasomal System
VAMP3	v-SNARE	Vesicle Transport
GAK	Kinase	Vesicle Transport

The second conceptual framework is the mitogen-activated protein kinase (MAPK) signaling cascades (PEBP1, transcription factor c-Jun, transcription co-activator SRF, RGS3, and MAPK2). MAP Kinases are a family of protein kinases that regulate a wealth of cellular processes like cell growth, differentiation, and survival through distinct signaling cascades. These include ERK, JNK/SAPK, and p38 MAPK. Consistent with this, there are investigations that show modulation of the MAPK pathway promote autophagy and degradation of specific proteins(Noh et al., 2016).

Finally, the third framework is vesicle transport (VAMP3 and GAK). Candidate proteins in this pathway have been implicated in inducing exocytosis and regulation of autophagy (Zhang et al. 2021). (**Table 2.1** and **Figure 2.12e**). To probe the contributions of the candidate proteins to the apoE effects of IFNγ we utilized commercially available small molecule inhibitors. We pursued this approach for two reasons. One, the compounds were readily available; and two, the screening would be resource-effective regarding time and reagents. We reasoned that if IFNγ activates these candidate proteins to exert downregulation of extracellular apoE then inhibition would restore extracellular apoE levels.

2.7 MAPK signaling pathway inhibition – Transcription Factors

Two of our candidate phosphoproteins were reported to be transcription factors under the MAPK signaling cascade (c-Jun and SRF) (Shaulian & Karin, 2002; Wagner & Nebreda, 2009). Their function largely relies on cytosolic activation and subsequent translocation to the nucleus where it binds to promoter sequences to initiate transcription of target genes. We reasoned that if these transcription factors, or others, are involved in the IFNγ effects on apoE then inhibition of nuclear import should block the IFNγ mediated reduction of apoE. Karyopherin Beta 1 (Kpnβ1), serves as a primary nuclear import receptor responsible for facilitating the transportation of cellular cargoes into the nucleus and holds a significant position as the primary importin protein involved in the nuclear import mechanism (Mosammaparast & Pemberton, 2004). We investigated the inhibition of Kpnβ1 by using commercially available small molecule inhibitors of the nuclear pore INI-43 and Importazole (Ajayi-Smith et al., 2021). We first assessed viability on BMDMs to determine a non-lethal dose of INI-43 and Importazole. BMDMs were then pre-treated with the compounds for 2 hours prior to adding IFNγ. We hypothesized if IFNγ exerted its effects on apoE through a transcription factor then we would see a rescue of apoE. However, both compounds did not show such rescue of intracellular or extracellular apoE suggesting that a transcription factor may not be involved (**Figure 2.13**).

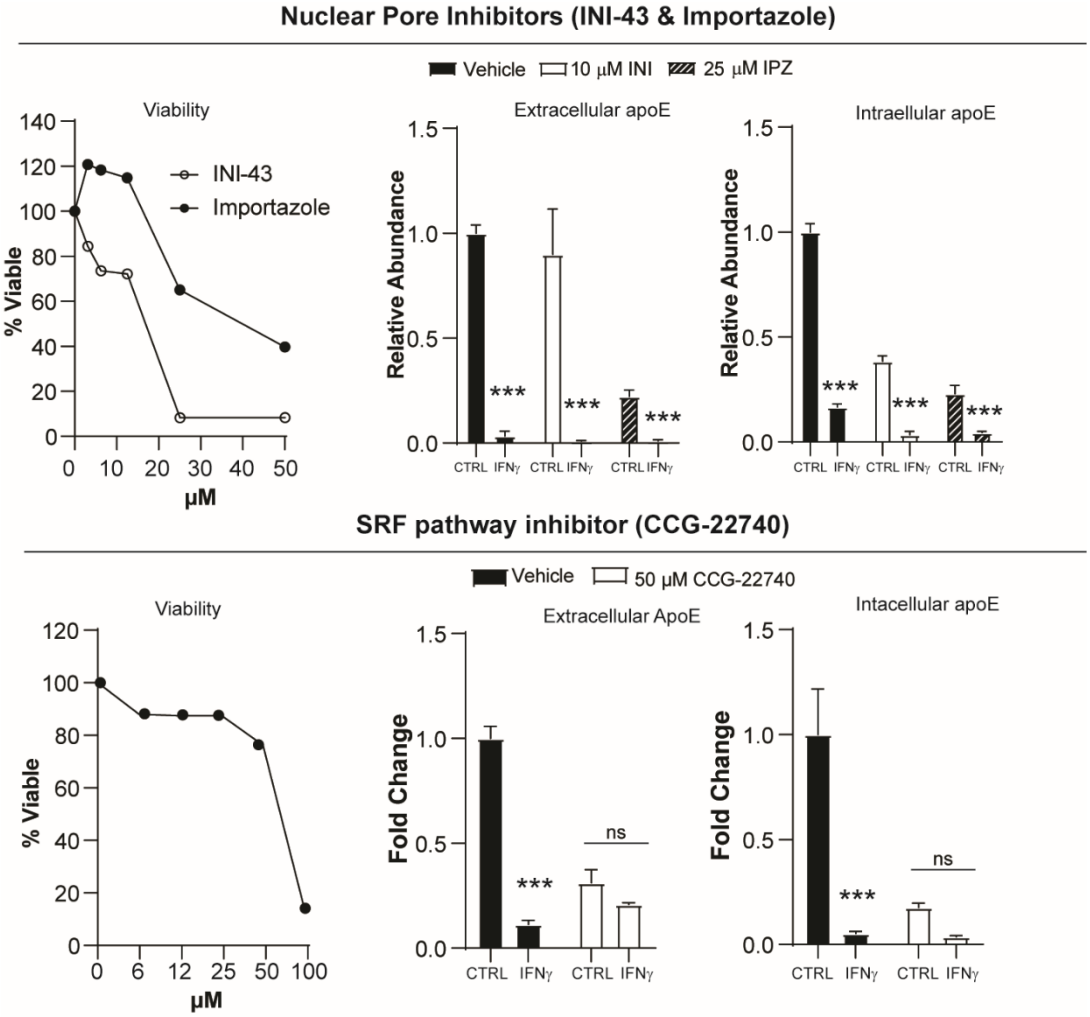

Figure 2.13 Inhibiting translocation of transcription factors by blocking nuclear pores using small molecule inhibitors. BMDMs were treated with increasing doses of the nuclear pore inhibitors INI-43 and Importazole (IPZ) or SRF inhibitor (CCG-22740. (Left) Cell viability was assessed after 24h of treatment measured by Calcein AM. BMDMs were pre-treated with or without INI-43 (10 μM), Importazole (25 μM), or CCG-22740 (50 μM) for 2h and treated with or without IFNγ for 24 h. Extracellular (middle) and intracellular (right) apoE levels were assessed. Results are mean ± SEM. ns ($p > 0.05$), * ($p \leq 0.05$), ** ($p \leq 0.01$), *** ($p \leq 0.001$), **** ($p \leq 0.0001$) (student's *t*-test) n=3

2.8 MAPK signaling pathway inhibition.

Small molecule inhibitors targeting PEBP1, p38, MEK1/2, and ERK1/2, components of the MAPK signaling pathway, were used to investigate the impact of these candidate proteins on the effects of IFNγ on apoE (**Figure 2.14**). To establish a dose that does not cause cell death, we initially assessed the viability of BMDMs treated with each compound. Subsequently, we examined the levels of extra- and intracellular apoE in IFNγ-treated BMDMs with and without the presence of these inhibitor compounds. Our findings demonstrated that these inhibitors (p38, MEK1/2, and ERK1/2), with the exception of PEBP1 inhibitor, alone decreased extracellular apoE in BMDMs, mimicking the effects of IFNγ. However, the MEK1/2 inhibitor restored the levels of intracellular apoE in the presence of IFNγ (**Figure 2.14**). This observation underscores the complexity involved in interpreting these results. Taken together, these findings may suggest a potential involvement of MEK1/2 in the downregulation of macrophage apoE secretion induced by IFNγ.

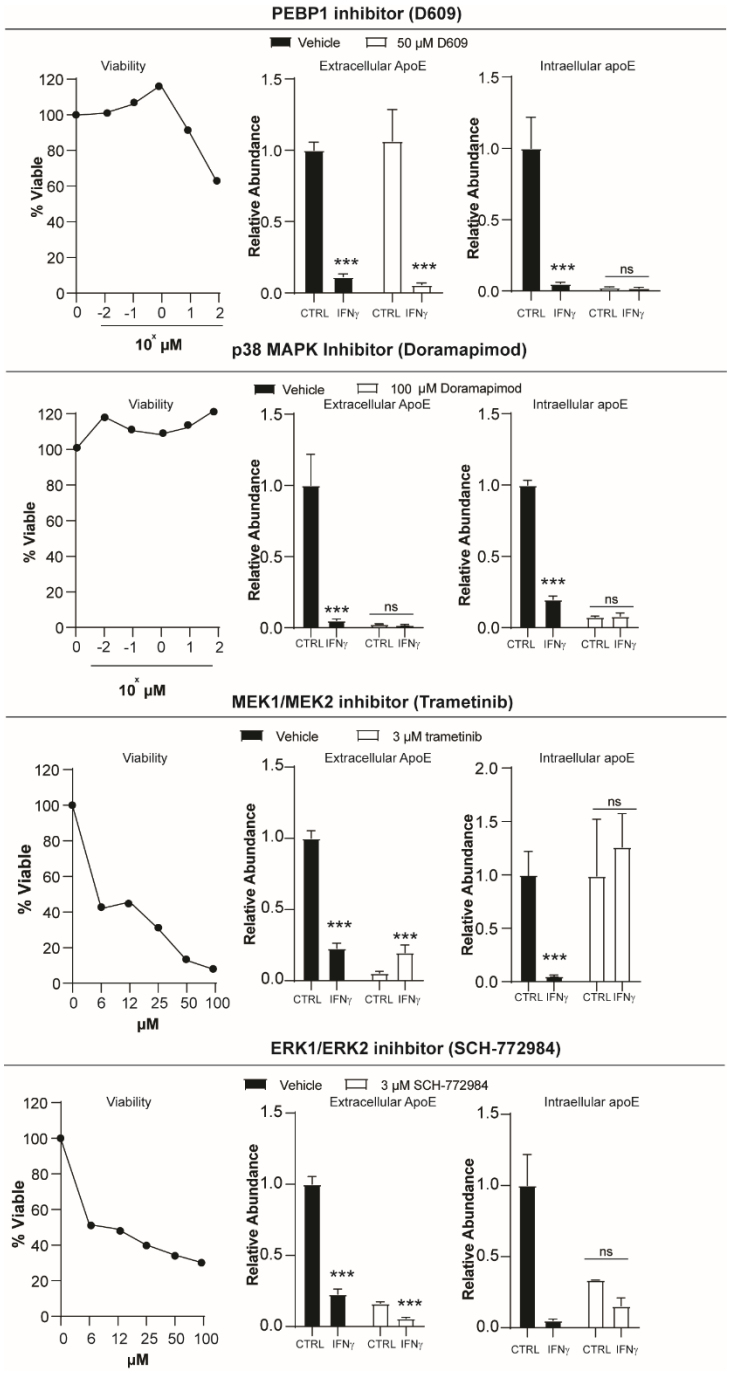

Figure 2.14 Targeting phosphoproteomic candidates in MAPK pathway using small molecule inhibitors. BMDMs were treated with increasing doses of inhibitors against PEBP1 (D609), p38 MAPK (Doramapimod), MEK1/2 (Trametinib), and ERK1/2 (SCH772984). Cell viability was assessed after 24h of treatment and measured by Calcein AM (left). BMDMs were pre-treated with or without inhibitors of proteins in the MAPK pathway for 2h and treated with or without IFNγ for 24 h. Extracellular (middle) and intracellular apoE levels were assessed. Results are mean ± SEM. ns ($p > 0.05$), * ($p \leq 0.05$), ** ($p \leq 0.01$), *** ($p \leq 0.001$), **** ($p \leq 0.0001$) (student's *t*-test) n=3

2.9 Vesicle transport machinery inhibition

Both cyclin G associated kinase (GAK) and vesicle associated membrane protein 3 (VAMP3) are reported to be play a role in vesicle trafficking and autophagy. We sought to use small molecule inhibitors to study their involvement. However, small molecule inhibitors were only commercially available for clyclin G associated kinase (GAK) and not for VAMP3. Given this, we pursued our studies on GAK alone (Kovackova et al., 2015). GAK is widely expressed and shares 43% homology with auxilin, a neuronal-specific protein involved in uncoating clathrin vesicles. GAK has been shown to play a key role in regulating clathrin-mediated trafficking in the endocytic and secretory pathways (He et al., 2020; Kanaoka et al., 1997; Kovackova et al., 2015; Zhang et al., 2005). Furthermore, genome wide association studies (GWAS) have suggested apoE and GAK may be interacting in Alzheimer's disease, converging on the autophagy machinery. Given this circumstantial evidence we hypothesized that GAK may play a role in trafficking apoE for degradation in response to IFNγ. GAK inhibitors alone showed decrease of apoE on its own. In addition, co-treatment of IFNγ and GAK inhibitor showed no effect when compared to GAKi treated BMDMs (**Figure 2.15**). The interpretation of these results is challenging due to the unknown activation status of GAK in response to IFNγ. More experiments using genetic methods need to be done to uncover this. If IFNγ do indeed inhibit these proteins, then adding an additional inhibitor would not restore extracellular apoE. Instead, the inhibitors alone would phenocopy the effects of IFNγ on apoE, which is what we observe with GAK inhibitor.

Our analysis of small molecule inhibitors presents challenges in interpretation due to two important factors. Firstly, the impact of phosphorylation sites identified in our study on protein activation or inhibition remains unknown, as these sites have not been previously reported.

Secondly, the lack of specificity of these inhibitors introduces the possibility of off-target effects. However, these inhibitors did provide valuable insights, suggesting that macrophages play a role in post-translational regulation of apoE, IFNγ may lead to apoE degradation, and autophagy-lysosome processes may be involved.

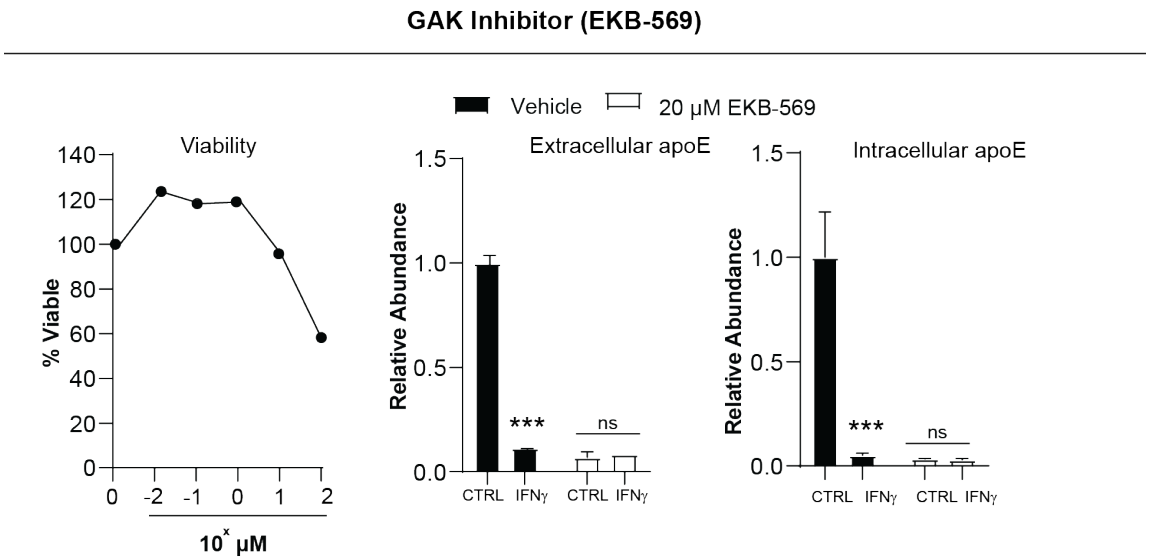

Figure 2.15 Targeting cyclin G associated kinase using small molecule inhibitors. BMDMs were treated with increasing doses of the GAK inhibitor EKB-569 and cell viability after 24h determined by Calcein AM (left). BMDMs were pre-treated with or without EKB-569 for 2h and treated with or without IFNγ for 24 h. Extracellular (middle) and intracellular (apoE) levels were assessed. Results are mean ± SEM. ns ($p > 0.05$), * ($p \leq 0.05$), ** ($p \leq 0.01$), *** ($p \leq 0.001$), **** ($p \leq 0.0001$) (student's *t*-test) n=3

2.10 Discussion and Future Directions

The studies outlined in this chapter showed *in vivo* evidence that the canonical IFNγ-STAT1-IRF1 signaling pathway does not play a role in atherogenesis in the context of obesity/IR. Pro-atherogenic m*Irf1-/-* BMT *Ldlr-/-* mice fed a WTD revealed no significant differences in metabolic parameters or atherosclerotic lesion size. Similarly, pro-atherogenic m*Stat1-/-* mice fed a WTD revealed no significant differences in metabolic parameters or atherosclerotic lesion size. Based on these findings, combined with previous in *vitro* data, we concluded that the canonical IFNγ-STAT1-IRF1 pathway does not play a role in exacerbating atherosclerosis in obesity/IR, pointing to a novel IFNγ pro-atherogenic signaling cascade.

To understand this novel mechanism, we pursued to understand the fate of macrophage apoE in response to IFNγ. We observed both extracellular and intracellular apoE was downregulated in response to IFNγ. The decrease in apoE occurred post-transcriptionally, as mRNA levels were unaffected. Furthermore, macrophages co-treated with IFNγ and chloroquine (autophagy & lysosome acidification inhibitor) or MG-132 (proteasome inhibitor) in restored intracellular apoE but not extracellular apoE. This suggests that preventing apoE degradation does not restore its secretion.

While MG-132 is purported to target the proteasome, macrophages treated with this compound exhibit high levels of LC3-II levels, comparable to chloroquine. The elevated LC3-II in both chloroquine and MG-132 suggests both compounds inhibit autophagy. Taken together, these data show that reducing autophagy restores intracellular apoE and the contribution of the proteasome cannot be assessed due to elevated LC3-II. Furthermore, lysosome disruption through TFEB ablation in macrophages similarly restored intracellular apoE. The data presented

in this study indicate that the downregulation of intracellular apoE, enabled by IFNγ, likely occurs through the autophagy-lysosome pathway. Furthermore, inhibiting the degradation process does not result in the recovery of extracellular apoE. These findings offer valuable insights into the dual pro-atherogenic mechanisms by which IFNγ regulates apoE levels in macrophages.

To unveil this novel pro-atherogenic and host-defense-independent cascade induced by IFNγ we pursued an unbiased phosphoproteomics approach to identify potential candidates. Through statistical analysis and literature mining we found several protein candidates that may be involved. To screen these candidates in IFNγ signaling, we probed for extra- and intracellular apoE levels using commercially available small molecule inhibitors on macrophages treated with or without IFNγ. Our rationale for using small molecule inhibitors assumed that IFNγ activates these candidate proteins. However, one of the challenges of our phosphoproteomics results is that we do not know if the phosphorylation of the protein activates or inhibits its action, as the phosphorylation sites we found have not been reported in the literature. The results obtained with the compound inhibitors were an excellent starting point; however, inhibitor results obtained in this chapter alone are not sufficient to make reasonable conclusions on the IFNγ effects on apoE. To validate our findings, it would be necessary to perform genetic interventions in parallel with the small molecule inhibitors. For example, if IFNγ inhibits a protein to modulate apoE, then it would be paramount to overexpress the protein and observe its effects on apoE in response to IFNγ. One of the challenges of overexpression systems in primary macrophages is that they readily degrade foreign genetic material, as they are surveillance cells of the immune system. Transducing them with foreign DNA leads to activation of the inflammatory response, adding to an additional variable to our system. Furthermore, generating a stable cell line overexpressing a

gene of interest is not feasible as these primary macrophages cannot be kept in culture indefinitely. To overcome this, we plan to deliver mRNA transcripts synthesized with non-natural nucleotides to evade the macrophage detection system and to overexpress these proteins (Moradian et al., 2020). Using this overexpression system, we could obtain strong evidence on which candidate proteins plays a role in regulating the extracellular expression of apoE in IFNγ treated macrophages.

Furthermore, to obtain even more conclusive evidence on our initial results, it is necessary to repeat the phosphoproteomics studies using targeted phosphoproteomics using *in vivo* lipid loaded peritoneal macrophages from obese/IR mice and compare these results to results obtained from BMDMs. This is based on our candidate list being from the autophagy/MAPK signaling cascade, which suggest the degradative machinery is implicated.

The compromised lysosome function observed in foam macrophages leads to a similar impairment in the degradative machinery responsible for autophagy (Marques et al., 2021)(van Eijk & Aerts, 2021)(Cox et al., 2007)(Jaishy & Abel, 2016). Considering our initial screening was conducted in bone marrow-derived macrophages (BMDMs), it becomes crucial to validate these candidate proteins in the context of lipid-loaded macrophages treated with IFNγ, rather than solely relying on BMDMs. Confirming the presence of the same candidate proteins in both models would then necessitate further verification of their involvement through genetic techniques such as silencing and overexpression, as described previously. Notably, our extensive findings using compound inhibitors indicate that these inhibitors alone reduce extracellular apoE levels. Interestingly, our studies suggest that canonical IFNγ signaling may not play a role in atherosclerosis in vivo. Instead, phosphoproteomics results point towards the involvement of the MAPK pathway and the autophagy system.

Our initial goal was to identify a signaling cascade triggered by IFNγ that is independent of host defense, with the aim of discovering potential therapeutic targets to mitigate atherosclerosis in high-risk patients, particularly those with obesity and type 2 diabetes (T2D). It is worth highlighting that MEK, one of our candidate proteins, inhibition has demonstrated the ability to diminish inflammation while preserving bactericidal activity (Long et al., 2017). If IFNγ achieves downregulation of apoE through MEK inhibition, this non-canonical pathway holds promise as an attractive target for intervention in treating atherosclerosis. Further studies would need to be performed to uncover this.

CHAPTER THREE: PREFERENTIALLY DELIVERING LXR AGONIST T090137 TO MURINE ATHEROSCLEROTIC LESIONS USING A DNA NANODEVICE

3.1 Introduction

Cholesterol is an important lipid involved in a variety of cellular functions, such as maintaining membrane integrity and mediating signaling. Dysregulation of cholesterol homeostasis contributes to atherosclerosis pathology. Foam macrophages, quintessential cells of atherosclerotic lesions, accumulate excess cholesterol through unregulated uptake of modified lipoproteins mediated via scavenger receptors (de Villiers & Smart, 1999; Yu et al., 2013) This aberrant state of excess lipid accumulation contributes to multiple aspects of atherosclerosis pathogenesis. RCT refers to the mechanism where cholesterol is removed from peripheral tissues and delivered to the liver for elimination (Rosenson et al., 2012). Stimulating RCT in foam macrophages could be an effective strategy to attenuate atherosclerosis.

The liver X receptors (LXRs) are oxysterol-activated nuclear hormone receptors that exist in two different isoforms, LXRα and LXRβ, and are widely expressed but play key roles in lipid homeostasis in the liver and macrophages. Furthermore, LXRs are key regulators of the RCT process and induce the expression of genes involved cholesterol efflux and other participants in RCT. These genes include the cholesterol transporters *Abca1*(Venkateswaran et al., 2000), and *Abcg1* (Venkateswaran et al., 2000), which efflux cholesterol out of macrophages on to apoA-I and high-density lipoprotein (HDL) particles, as well as proteins such as cholesteryl ester transfer protein (CETP), CPY7A1, ABCG5, and ABCG8, which facilitate cholesterol trafficking to the liver and ultimate excretion of effluxed cholesterol through feces (Tontonoz & Mangelsdorf, 2003).

In addition, LXRs have been shown to attenuate inflammation, regulating both innate and acquired immunity (Zelcer & Tontonoz, 2006). Due to their RCT and immunomodulatory effects, LXR agonists have robust anti-atherosclerotic activity in mice (Joseph et al., 2002; Kirchgessner et al., 2016; Peng et al., 2008) and rabbit models. Unfortunately, in animal models LXR agonists have been shown increase fatty acid and triglyceride (TG) synthesis through the induction of SREBP1c, FAS, SCD1, and other genes in the liver (Schultz et al., 2000), resulting in elevated VLDL secretion, hypertriglyceridemia, and hepatic steatosis. The inducible degrader of LDL receptor (IDOL), an E3 ubiquitin ligase that targets the LDL receptor for degradation (Zelcer et al., 2009), is also upregulated by LXR and thus has the potential to elevate LDL through reducing hepatic LDL receptors. In addition, increased production of VLDL, induction of CETP, and stimulation of peripheral cholesterol trafficking to the liver, thereby inhibiting hepatic SREBP2-dependent LDL receptor expression, could all contribute to elevated LDL. Thus, multiple LXR-regulated hepatic pathways have the potential to cause hepatic steatosis and dyslipidemia, and indeed LXR agonists including GW3965 and T0901317 have been shown to increase liver and plasma TG and LDL in mice and hamsters (Schultz et al., 2000; Tangirala et al., 2002). More limited experiments in primates have shown variable responses, depending on the agonist and study (Kirchgessner et al., 2015). Thus, the use of LXR agonists for atherosclerosis has been challenging to implement. However, one possible strategy to overcome the on-target effects of LXR activation in the liver would be to preferentially target macrophages in the atherosclerotic lesion with small molecule ligands of LXR while avoiding hepatocyte uptake.

DNA nanotechnology has emerged as a versatile tool for targeting organelles with high precision ((Q. Hu et al., 2019), making it ideal for clinical and research applications.

Furthermore, studies have shown that anionic DNA nanostructures can be efficiently internalized by cells through scavenger receptor mediated endocytosis (Cui et al., 2021; Umemura et al., 2021; Veetil et al., 2018)(Saha et al., 2015). Macrophages are professional phagocytes and as such they express very high levels of scavenger receptors. Our lab has leveraged this feature to selectively target tumor associated macrophages (TAMs). Tumors evade immune surveillance through inhibition of antigen presentation. To combat this, Dr. Kasturi Chakraborty attached a cysteine protease inhibitor to a DNA 38mer duplex nanodevice(Umemura et al., 2021; Veetil et al., 2017) and Chang Cui and colleagues showed that it can suppress tumor growth by enhancing the antigen presentation ability of tumor-associated macrophages (TAMs). This approach resulted in an increase in antigen presentation and led to the successful attenuation of tumor growth in mice (Cui et al., 2021).

The clinical use of DNA nanostructures to deliver small molecules to macrophages faces several challenges, such as their susceptibility to being trapped and degraded in lysosomes, which can hinder their therapeutic targeting of extra lysosomal targets such as the constitutively nuclear hormone receptor LXR. Previous attempts to modify the intracellular fate of DNA nanostructures by adding different materials have been expensive and resulted in low yields (J. Li & Fan, 2021; Martin et al., 2020). However, Cui & Chakraborty et al. demonstrated that the DNA 38mer nanodevice has an intrinsic ability to target lysosomes of macrophages, making them a promising and easily accessible strategy for modulating macrophage biology.

In this chapter, we propose to use this DNA nanotechnology that is proven to be preferentially taken up by macrophages in vivo and use it to deliver LXR agonists to aortic wall macrophages. The goal is to preferentially deliver them to macrophages in the aortic lesion, all while avoiding the negative effects on the liver. In this chapter we demonstrate that the DNA

nanodevice can deliver small molecules to non-lysosomal cellular proteins in macrophages to influence macrophage functions. Here we show using DNA nanodevice conjugated to fluorescent molecules that the DNA in the nanodevice can be degraded by macrophage lysosomes leading to the release of the conjugated molecule from the lysosome. We also show that DNA nanodevice conjugated to the LXR agonist T090137 (T0-DNA) targets LXR genes in macrophages indicating that the membrane permeable LXR agonist was able to leave the lysosome and interact with LXR in the cytosol and nucleus. Then we show that the fluorescently conjugated DNA nanodevice preferentially targets atherosclerotic lesions in vivo and that the T0-DNA nanodevice significantly reduces atherosclerotic lesions in an atherogenic mouse model without eliciting hypertriglyceridemia.

Impact. Our work achieves two important milestones. One, it adds to the versatility of DNA nanodevice repertoire by demonstrating that the nanodevice can be used to deliver membrane permeable drugs that act upon proteins in non-lysosomal sites in macrophage. Second, we show that LXR agonists could potentially be used as a therapy for atherosclerosis by avoiding liver uptake and being preferentially delivered to macrophages.

3.2 Methods

Regulatory. Animal studies were approved by the Institutional Animal Care and Use Committee (ACUP 72209) at the University of Chicago.

Mouse models. 6-7-week-old C57BL/6 (stock no. 000664), *Ldlr-/-* (stock no. stock no. 002207), were purchased from The Jackson Laboratory. For atherogenic studies, 8-week-old male *Ldlr-/-* mice were placed on a western-type diet (WTD) (TD96121, Harlan Teklad: 21% milk fat, 1.25% cholesterol) diet for up to 16 weeks. Mice were housed in the specific pathogen free animal facility at the Gordon Center for Integrative Science building at the University of Chicago.

Bone marrow-derived macrophage (BMDMs) isolation and activation. BMDMs were differentiated from bone marrow stem cells with L-cell conditioned media for six days as previously described (Reardon et al., 2018).

Thioglycolate-elicited peritoneal macrophage (pMACs) isolation. pMACs were isolated as previously described (Reardon et al. 2018). Briefly, peritoneal macrophages were collected by lavaging the peritoneal cavity with PBS containing 2% endotoxin-free BSA (Sigma) 5 days after 4% thioglycolate injection (3 mL/mouse).

Macrophage Cholesterol Loading

BMDMs were incubated for 24 hr. in serum-free medium supplemented with 2% serum from control wild type C57BL/6 mice or hyperlipidemic serum from *Ldlr*−/− mice fed a WTD for 12-16 weeks. Cholesterol loading was confirmed via Oil Red O staining and imaged using a Nikon Eclipse Ti2 microscope.

Primary Hepatocyte Isolation: Mice were anaesthetized with tribromoethanol. Following anesthesia, the inferior vena cava was cannulated to establish a retrograde perfusion system. The liver was then perfused with a calcium chelating solution using a peristaltic pump (ThermoFisher) to eliminate blood and dissociate extracellular matrix. Following the chelation step, mice was perfused with Liberase Collagenase solution. The liver was carefully dissected to obtain the desired hepatocytes for further purification. Hepatocytes were isolated by serial low-speed centrifugation at 50g to separate them from other cell types.

Western blot analyses. Cells were lysed with 1% SDS containing protease and phosphatase inhibitors (Sigma), and protein was quantified with the BCA Protein Assay Kit (Pierce). Proteins (10-20mg) were resolved on 10%, 12.5%, or 15% SDS-PAGE gels depending on the target protein, transferred to PVDF membranes (Millipore), blocked with 5% BSA (Sigma) in 0.1% TBS/Tween-20 at RT for 2h, stained with primary and secondary antibodies, and visualized using the ECL detection kit (Biorad) and a LI-COR Odyssey Imagining system. Antibodies include: Lamp1 (abcam), GRP75 (proteintech), cal-reticulin (abcam), cathepsinB (abcam), and DNAse II (Invitrogen).

Measurement of gene expression by qRT-PCR. RNA was isolated using QIAGEN Midi-Prep Kits and RT with Quantiscript (QIAGEN) using random hexamers (Invitrogen). mRNA levels were measured with specific primers (IDT) using SYBR green on a One Step Plus system (Applied Biosystems). Relative levels of each target gene were calculated using the ΔΔCt formula and 18S RNA as a control.

Primer sequences are:

18s forward:	GCCGCTAGAGGTGAAATTCTT
18s reverse:	CGTCTTCGAACCTCCGACT
Abca1 forward:	CATCGTGTCTCGCCTGTTCT
Abca1 reverse:	CTTGATCTGCCGTAACATTCTC
Apoe forward:	CTGACAGGATGCCTAGCCG
Apoe reverse:	CGCAGGTAATCCCAGAAGC
Abcg1 forward:	GTGGATGAGGTTGAGACAGACC
Abcg1 reverse:	AACTCAACTGTGAAATGCCACC
Il1b forward:	CATCAGGACAGCCCAGGTC
Il1b reverse:	CCTCGGGTACAGAGTAGGAAAG
Nkb2 forward:	CTACAGACACAGCGCACACT
Nfkb2 reverse:	GGCCGGAAGACCTATCCTACT
Il6 forward:	TACTCGGCAAACCTAGTGCG
Il6 reverse:	GTGTCCCAACATTCATATTGTCAGT

Compound-DNA 38-mer nanodevice synthesis

All DNA nanodevices were engineered and generated by Dr. Kasturi Chakraborty (Chakraborty et al., 2021; Cui et al., 2021; Saha et al., 2015). DBCO labeled 38-mer DNA, nondegradable 38-mer DNA, fluorophore labeled DNA strands, and unlabeled DNA strands were obtained from IDT. After duplex formation T0901317 or fluorescent probes were conjugated to DBCO labeled DNA duplex via copper free click chemistry. The conjugate reaction mixture contained 10 equivalents excess T0 or 5 equivalents excess other compounds. To remove excess compound, and other reagents, the DNA conjugate reaction mixture was passed through a 3kDa cut-off

centrifugal filter (Amicon, Millipore) and washing multiple times. Conjugation was confirmed using gel mobility shift assays. Compound-DNA conjugated were stored at -20°C till further use.

Treatment of BMDMs with TO-DNA. BMDMs seeded at 250,000 cells/well in 24 well plate (Corning) and differentiated using L-cell medium as described above. On day 6 BMDMs were treated with or without DMSO (vehicle), 10 mM T0901317, 5 mM T0-DNA (10 mM T0901317), or 5 mM DNA for 24h. RNA was isolated for quantitative real-time qPCR.

Fluorescent-DNA uptake. To observe DNA uptake by macrophages via fluorescence imaging, BMDMs (60,000 cells/well) or pMACS (120,000 cells/well) were plated in 8 well dishes. Cells were then treated with Alexa 647-DNA (F-DNA; 500 nM) for 30min at 37^0C, washed with PBS, and then imaged using a Leica SP5 confocal microscope. Images were analyzed using ImageJ/Fiji 1.51.

DNA trafficking to lysosome in vitro. To visualize lysosomal trafficking of DNA, BMDMs (50,000 cells/well) and pMACs (120,000 cells/well) were plated in 8 well dishes. Cells were then treated with A647-DNA (F-DNA; 500 nM) for 30 min at 37^0C, washed with PBS, and then stained with LysoTracker Green DND-26 (50 nM, ThermoFisher Scientific) in complete medium for 30 mins and then imaged directly using a Leica SP5 confocal microscope. Images were analyzed using ImageJ/Fiji 1.5.

DNA degradation by macrophages in vitro. To observe DNA degradation by macrophages via fluorescence imaging, BMDMs (50,000 cells/well) were plated in 8 well dishes. Cells were then treated with FRET-DNA or ndFRET-DNA (500 nM) for 30 min at 37˚C, and chased for varying times. Cells were then washed with PBS, stained with Hoescht and then imaged using a Leica SP5 confocal microscope. Images were analyzed using ImageJ/Fiji 1.51.

In vivo DNA uptake – atherosclerotic lesions. To observe DNA uptake in atherosclerotic lesions, 4Alexa 647-DNA (4F-DNA; 125mg) was injected intravenously (i.v.) by the retro-orbital route into WTD fed (16 weeks) *Ldlr-/-* mice. After 1 hour, anesthetized mice were perfused with PBS. The heart and upper vasculature were excised, cleaned of adventitia, and imbedded in optimal cutting temperature (OCT), and serial 10-μm sections in the aortic root were collected. Sections, beginning at the appearance of the coronary artery and aortic valve leaflets, were stained for immunofluorescence labeling. Slides were washed and stained with Alexa 488 labeled anti- rat MAC2 (CedarLane) antibody overnight at 4°C in the dark, counterstained with DAPI (ThermoFisher), and imaged on imaged using a Leica SP5 confocal microscope equipped with 63×, 1.4 NA, oil immersion objective. Alexa 488 was excited using an Argon ion laser for 488 nm excitation, DAPI using near UV laser at 405 nm excitation, Alexa 647 using He-Ne laser for 633 excitations. Images were analyzed using ImageJ/Fiji 1.51.

In vivo DNA uptake – livers. To observe DNA uptake in livers, 4Alexa-647-DNA (4F-DNA; 125mg) was injected intravenously (i.v.) by the retro-orbital route into WTD fed (16 weeks) *Ldlr-/-* mice. After 1-hour, anesthetized mice were perfused with PBS. A small portion of the liver lobe was excised and embedded optimal cutting temperature (OCT) medium, and serial 5-

μm sections were collected. Slides were fixed for 15 mins with 4% microscopy grade PFA (washed and stained with Alexa-488 labeled anti- rat MAC2 (CedarLane) antibody overnight at 4°C in the dark, counterstained with DAPI (ThermoFisher), and imaged on imaged using a Leica SP5 confocal microscope equipped with 63×, 1.4 NA, oil immersion objective. Alexa 488 was excited using an Argon ion laser for 488 nm excitation, DAPI using near UV laser at 405nm excitation, Alexa 647 using He-Ne laser for 633 excitations. Images were analyzed using ImageJ/Fiji 1.51.

DNase II digestion of FRET-DNA. DNA degradation was performed using varying units of DNase II (from bovine pancreas, Sigma Aldrich) incubated in 25 mL of lysosomal elution buffer (150 mM NaCl, 20 mM HEPES, 10 mM KCl, 1.5 mM $MgCl_2$, 1 mM EDTA, 1 mM EGTA; pH 7.4, Protease inhibitors and 16% CHAPS) for 15 minutes. At t=0 75mL of 500nM of FRET-DNA or nondegradable FRET-DNA (ndFRET-DNA) in 50 mM sodium acetate buffer pH 4.8 was added to the DNase II solution. DNA degradation was measured using plate reader and native polyacrylamide gel electrophoresis. FRET signal in plate reader format was measured using the Syntex HTX 96-well reader in kinetics mode (15 min increments) using a pre-set automated reader at 37˚ C by using an excitation filter: 530/20 and emission filter: 680/30. Results were normalized from initial signal (I/I0). For native PAGE, 10 pmoles of DNA from each reaction was run and imaged by staining with 1 ug/mL ethidium bromide and visualizing fluorophores (Alexa-546 and Alexa-647).

Fluorescence labeling of magnetic beads and time course of localization to lysosomes. Amine (-NH3) conjugatable sites on 500 nm Abramag magnetic beads were utilized for conjugation with

Alexa647 in a 1:1 ratio **by Dr. Chakraborty**. Conjugation reaction was performed in PBS and stirred overnight at room temperature. To remove any unbound Alexa647, the magnetic beads were subjected to multiple washes, and the supernatant was separated using a magnetic rack.

Lysosome isolations. For lysosomal isolation experiments, BMDMs were plated on 15 cm^2 dishes. Cells were pulsed with 100 mg/mL of 0.5 mm magnetic beads (Abramag amine magnetic beads) for one hour at 37º C followed by an overnight chase (12 hours) for maximal lysosomal labeling. Cells were harvested with a cell scraper using 20 mL ice cold PBS with 2 mM EDTA and pelleted with a 500 x g 5 minute spin. Cells were then resuspended in 1 mL of ice-cold PBS and subjected to magnetic rack-based separation of unbound (nonmagnetic) cells. The cells were then lysed with a dounce homogenizer (15 strokes in 250 mM sucrose, 20 mM HEPES pH 7.4, 10 mM KCl, 1.5 mM $MgCl_2$, 1 mM EDTA, 1 mM EGTA and Protease inhibitors). The cells were then subjected to multiple rounds of magnetic separation to collect Flow Through; Washes 1-5; elution (elution buffer: 150 mM NaCl, 20 mM HEPES pH 7.4, 10 mM KCl, 1.5 mM $MgCl_2$, 1 mM EDTA, 1 mM EGTA, Protease inhibitors and 16% CHAPS). Protein levels in each of these aliquots were quantified using BCA. To confirm purity, the samples were used for western blots. The eluted lysosomal samples (0.5 mg) were used for DNA degradation assays (gel electrophoresis and fluorescence plate reader).

Treatment of *Ldlr-/-* mice with T0-DNA. Six-week-old male *Ldlr-/-* mice were fed a WTD for six weeks. Subsequently, the mice were administered DNA or T0-DNA intravenously at a dosage of 0.066 mg/kg, five days a week for four weeks, while still on the WTD.

Cross sectional quantification of atherosclerosis. Tribromoethanol anesthetized mice were perfused with PBS for 5 min, followed by 4% paraformaldehyde with 5% sucrose in PBS for 10 mins. The heart and upper vasculature were excised and cleaned of adventitia. For cross-sectional analysis the top third of the heart and the upper vasculature were imbedded in optimal cutting temperature (OCT). Serial 10-µm sections of the innominate artery and the aortic root were collected using the Leica Cryocut 1800 cryostat as previously described (Reardon et al. 2018). Atherosclerosis in the innominate artery was assessed by averaging the lesion area in four sections between 150-450 mm above the junction of the innominate artery with the greater curvature of the aortic arch. Atherosclerosis in the aortic root was assessed by averaging lesion area in three sections beginning at the appearance of the coronary artery and aortic valve leaflets. All sections were 100 mm apart. Sections were co-stained with Oil Red O (ORO), Fast Green, and hematoxylin and digital images were captured using a Nikon Eclipse Ti2 widefield microscope using 20x magnification for the innominate artery and 2x magnification for the aortic root using brightfield. Atherosclerosis lesion area was quantified using ImageJ/Fiji 1.51 and expressed as mm^2.

En face quantification of atherosclerosis. For *en face* analysis, aorta in the upper vasculature through the thoracic aorta were removed, cleaned of adventitia, opened longitudinally, and stained with ORO. The aortas were imaged using a MD500A ultra-compact 5MP USB digital microscope camera attached to a Leica dissecting microscope. Images were captured as RGB TIFF files using AM software for Mac (2015). ORO-stained lesion area was analyzed using ImageJ/Fiji 1.51 and expressed as the percentage of the total aortic surface area covered by lesions.

Plasma lipid levels. Total plasma cholesterol and triglyceride levels in fasted blood were determined using Infinity Cholesterol and Wako Triglyceride assay kits according to manufactures Instructions.

3.3 Results

3.4 BMDMs and pMACs internalize DNA nanodevice.

We began our investigation by confirming that the double stranded DNA nanodevice (DNA), consisting of 38 base pair double stranded DNA, could be effectively taken up by non-tumor-associated macrophages. To do this, we used fluorescence microscopy to examine the uptake of the DNA by peritoneal (pMACs) and bone-marrow derived macrophages (BMDMs), which are commonly used as surrogates for aortic macrophages (Becker, 2010). To visualize the uptake of DNA, Dr. Kasturi Chakraborty chemically linked excess fluorophore Alexa-647 to the 5¢ end of strand 2 of the DNA nanodevice (F-DNA) using click chemistry (**Figure 3.1a**), and excess fluorophores were eliminated using serial washes on a 3 kDa Centricon. Native polyacrylamide gel electrophoresis (PAGE) of F-DNA and DNA showed differences in electrostatic mobility, suggesting that the fluorophore was successfully attached to the DNA via click chemistry. Furthermore, using excess Alexa-647 and DNA as the limiting factor we ensured that the reaction was close to 100% (van Steenis et al., 2005).

Microscopy analysis showed pMACs and BMDMs internalized F-DNA (**Figure 3.1b**), similar with our previous studies in TAMs. Furthermore, we noticed that BMDMs took up more F-DNA than pMACs, consistent with previous reports of BMDMs being more phagocytic than pMACs(Zajd et al., 2020). Next wanted to confirm that the F-DNA uptake was localized to lysosomes using confocal microscopy. F-DNA treated macrophages were co-stained with Lysotracker Green DND-26 to visualize the lysosome. To assess co-localization, we employed Pearson's Correlation Coefficient (PCC). PCC calculates the covariance of signal levels between two images at the pixel level. By subtracting the mean intensity of each pixel, PCC becomes independent of signal levels and background offset, enabling accurate analysis of co-localization

in two-color images without prior preprocessing. To ensure rigor, we incorporated a 15-pixel frameshift (+shift) in the PCC measurements, providing confidence in the PCC value for colocalization. A PCC value of 1 indicates complete co-localization, while a value of 0 or negative indicates no correlation between the signals. Our results showed F-DNA reached the lysosomes in both peritoneal macrophages and bone-marrow derived macrophages with most if not all the F-DNA signal localized to the lysosomes at 30 min pulse (**Figure 3.1c**). These data suggests that the nanodevice is taken up by both pMACs and BMDMs, and it reaches the lysosome.

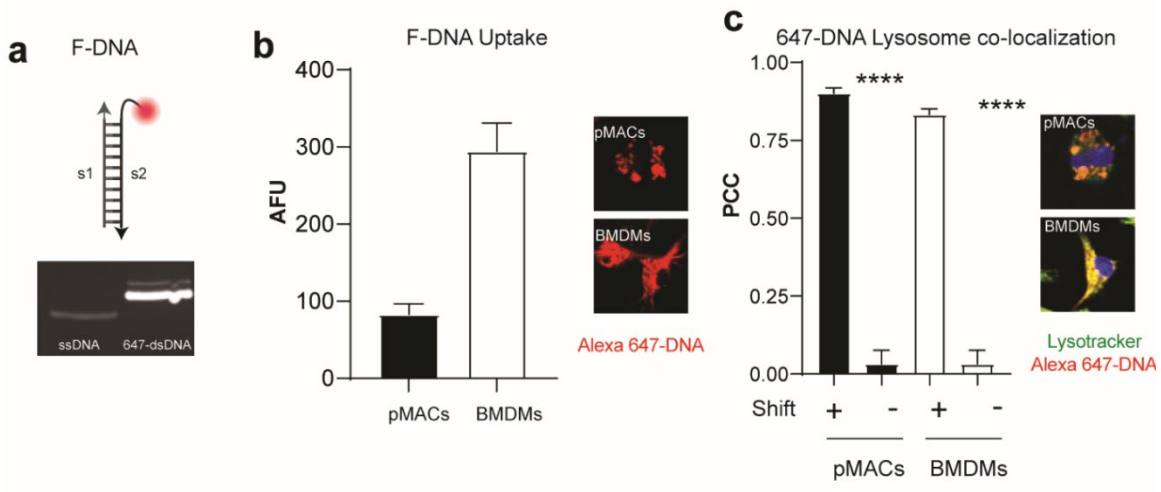

Figure 3.1 647-DNA is delivered to the lysosomes of BMDMs and pMACs. (a) Schematic of dsDNA nanodevice conjugated to one Alexa-647 moiety (top). 647-DNA purity was assessed by comparing to single stranded DNA (ssDNA) using native polyacrylamide gel (bottom). (b) Uptake of 500 nM 647-DNA nanodevice by pMACs and BMDMs, intensity of fluorophore depicted by integrated fluorescence units (n=30). (c) Co-localization analysis of 64-DNA and lysosome using 50 nM Lysotracker Green-DND-26. Co-localization was analyzed using Pearson's Correlation Coefficient (PCC) with and without frameshift of 10 pixels (n=30). Results are mean ± SEM. n.s. = no significance. *$p < 0.05$, **$p<0.001$, ***$p<0.0001$ (student's *t*-test).

3.5 Macrophage lysosomes degrade DNA nanodevice.

In the Becker Lab's previous research using E64-DNA, successful delivery of small molecule inhibitors of cysteine proteases to tumor-associated macrophage lysosomes using DNA nanodevices were exquisitely shown to attenuate tumor growth. However, it is important to note that LXR, a constitutively nuclear protein, is non-lysosomal. Targeting such proteins using the DNA nanodevice would require the molecule to exit the lysosome. This would necessitate either the migration of the molecule-DNA device out of the lysosome or the degradation of the DNA nanodevice to enable the molecule to exit the lysosome, both of which would require membrane permeability of the small molecule.

We hypothesize that the lysosome degrades the DNA nanodevice via the lysosomal DNA degradation enzyme, DNAseII. And that degradation of the DNA nanodevice is required to liberate the attached compound. To address our hypothesis, we faced two distinct challenges: first, we needed to develop a technique to monitor the degradation of DNA nanodevices by lysosomes in an *in vitro* system, and second, we needed to evaluate degradation by live cells in the lysosome in an *in celulo* system. To overcome these challenges, we utilized Forster Resonance Energy Transfer (FRET) principles. FRET involves energy transfer between two light-sensitive molecules in proximity (in the order of Angstroms), where the donor fluorophore, in an excited state, transfers energy to an acceptor fluorophore. When the fluorophores are not in proximity, the energy transfer does not occur. The readout for this assay is the acceptor fluorophore emission on confocal microscopy or plate reader. To implement this technique on the scale of DNA nanodevices, we attached fluorophore Alexa 546 to the 5' end of strand 1 and Alexa 647 at the 3' end of strand 2 of the DNA nanodevice (FRET-DNA). When Alexa 546 is excited, its emission spectra excite Alexa 647. However, this energy transfer requires a minimum of 74 Angstroms. If the distance is larger than that the energy transfer does not occur. What this

means is that when the DNA is intact, we can measure FRET; however, when the DNA is degraded or the strands are separated, we see a decrease in FRET. As a control we also attached the two Alexa fluorophores to non-degradable DNA nanodevice (FRET-ndDNA) (**Figure 3.2a**). In the FRET system, non-degradable DNA is utilized as a control for degradation. This non-degradable DNA differs from regular DNA in that it possesses a sulfur backbone instead of an oxygen backbone. This feature prevents recognition and degradation by the lysosomal DNA degradation enzyme, DNAseII.

DNase II is the primary acidic endonuclease in lysosomes. It is active at acidic pH (~4.8) without the requirement of divalent cations, and it hydrolyzes the phosphodiester backbone of DNA. We hypothesized that the nanodevice is degraded by DNAseII to liberate the attached compound. Next, we wanted to establish that digestion of the DNA nanodevice by DNase II would result in the loss of FRET signal. For this, we performed a 120-minute kinetic fluorometric assay using 100 nanomoles of FRET-DNA with increasing units (0-1 units) of purified DNase II under lysosome-like conditions (pH 4.8 and 37˚ C). As time and units of DNase II increased, we observed a progressive decline in the FRET signal (**Figure 3.2b**). We validated that the decrease in FRET signal observed in the plate assay was attributed to DNA degradation by performing a parallel kinetic experiment using FRET-DNA and FRET-ndDNA incubated with 1U of DNase II and examined the integrity of the DNA molecules on non-denaturing polyacrylamide gels looking at both ethidium bromide staining of DNA and fluorescence of the FRET signal and the individual fluorescent molecules along with the plate assay measuring FRET signal. The declining FRET signal in FRET-DNA corresponded to the degradation and the loss of FRET signal and appearance of the individual fluorescent markers observed by native polyacrylamide gel electrophoresis (PAGE) analysis (**Figure 3.2c**).

The signal corresponding to the intact ds FRET-DNA is moderately decreased in both the native gel and the plate assay at 10 minutes, significantly degraded by 20 minutes and undetectable by 30 minutes. The 'bands' detected after 30 mins in the fluorescence channels corresponds to degraded DNA, as the ethidium bromide shows absence of DNA. In contrast, there was no evidence of degradation (in native PAGE) or loss of the FRET signal with the non-degradable FRET-ndDNA. These findings confirm that the FRET system on DNA can be a reliable indicator of DNA degradation.

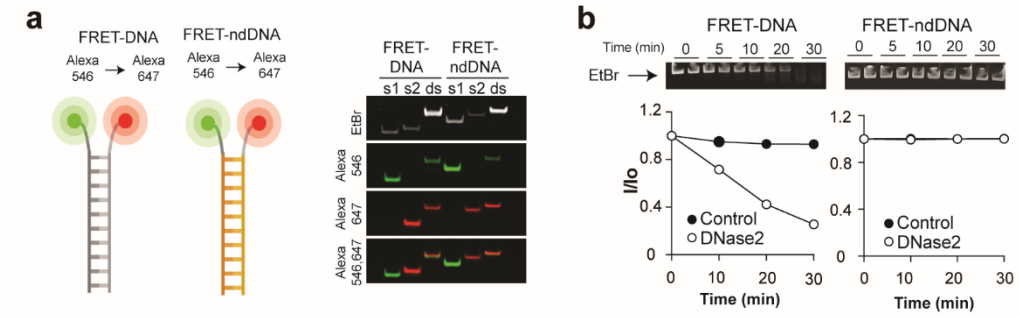

Figure 3.2 Loss of FRET signal as a reporter of degradation of DNA nanodevice. (a) Schematic of FRET-dsDNA (FRET-DNA) nanodevice conjugated to one Alexa546 on s1 and one Alexa-647 moiety on s2 (right). Schematic of FRET non-degradable dsDNA (FRET-ndDNA) nanodevice conjugated to one Alexa546 on s1 and one Alexa-647 moiety on s2 (left). FRET-DNA and FRET-ndDNA purity was assessed by comparing to single stranded DNA (ssDNA) using native polyacrylamide gel. (b) Kinetic assay using 1 unit of DNaseII and 100 nM FRET-DNA and ndFRET-DNA, validation of DNA degradation was visualized by native PAGE stained with ethidium bromide and loss of FRET was assessed using a fluorimeter.

3.6 Macrophages degrade DNA nanodevice releasing fluorophores attached on DNA.

Having established that *in vitro* FRET-DNA nanodevice can be degraded by DNase II our next goals were to determine whether lysosomes from macrophages could degrade the DNA nanodevice and if the liberated attached molecule can leave the lysosomes **(Figure 3.3a**). Using FRET as a monitor for DNA degradation and fluorophores as substitutes for small molecules we could answer our two most pressing questions. First, we wanted to determine if lysosomes from macrophages could degrade the nanodevice in an *in vitro* system and second we wanted to know if intact macrophages degrade the DNA nanodevice in an *in cellulo* system (**Figure 3.3b**).

To answer the first point, we needed to isolate lysosomes from macrophages. Our strategy was to take advantage of the fact that macrophages are phagocytic to deliver magnetic nanobeads (0.5 um diameter) to lysosomes so that we could use magnets to isolate the lysosomes from the cell lysate which and prepare a lysosomal extract (LE) (**Figure 3.3c**). We first needed to determine the time course of delivery of the magnetic beads to the macrophage lysosomes. By attaching the fluorophore Alexa 647 to the bead and staining with Lysotracker, we were able to track its progress of the beads to the lysosome through the endocytic system in a pulse-chase experiment (**Figure 3.3d**). Confocal microscopy revealed that it took a minimum of four hours for the beads to reach the lysosome after phagocytosis and traveling through the endocytic pathway and we used this information to perform our assays. To isolate lysosomal extracts, we mechanically lysed the BMDMs loaded with magnetic beads, isolated lysosomes using a magnetic rack, washed the beads extensively before lysing the lysosomes with buffer containing CHAPS. As shown in **Figure 3.3e** ~10% of the protein in the cell homogenate was eluted from the magnetic beads. The eluate was enriched in lysosomal proteins LAMP1 and cathepsin B and contained DNase II and were deficient or had low levels of proteins that are markers of

mitochondria (TOM20), cytoplasm (glucose regulated protein 75, GRP75) and endoplasmic reticulum (calreticulin) as assessed by western blotting (**Figure 3.3e**).

Having validated that we have generated a lysosomal extract enriched in lysosomal proteins, we next wanted to confirm that the lysosomal extracts are capable of degrading the DNA nanodevice. Using FRET-DNA we compared degradation by 0.1 unit of DNase II to the degradation by 0.25 ug of lysosomal extract. In this study we used lower amount of DNase II than used in **figure 3.2** since we reasoned based in part on the western blot **in figure 3.3d** that DNase II would represent only a small percentage of the protein in the lysosomal extract. The lysosomal extract reduced the FRET signal and degraded the FRET-DNA comparable to DNase II but had no impact on FRET-ndDNA (**Figure 3.3f**). This confirmed that lysosomes from macrophages can degrade the nanodevice in an *in vitro* system.

To investigate whether lysosomes in macrophages could degrade the nanodevice, we conducted microscopy experiments using FRET-DNA and FRET-ndDNA. After pulsing BMDMs with the FRET and ndFRET nanodevices for 30 minutes, the cells were imaged by confocal microscopy at end of the pulse period and at various times during the chase period and fluorescent intensity of the FRET signal, acceptor signal and donor signal measured. The peak of all 3 signals peaked at 1 hour in cells incubated with FRET-DNA and progressively decreased over time until little signal was observed in the cells (**Figure 3.3g**). On the other hand, the ndFRET signal remained unchanged after 1 hour, indicating that it was not degraded in the lysosome to release the fluorophore. The lack of decrease in fluorescence signaling ndFRET nanodevice also indicates that the fluorescence signals are not decreased over time in the acid environment of the lysosome. These findings suggest that the fluorophores readily exit the

lysosome after degradation, supporting the hypothesis that T0 liberation from the lysosome requires degradation of the nanodevice.

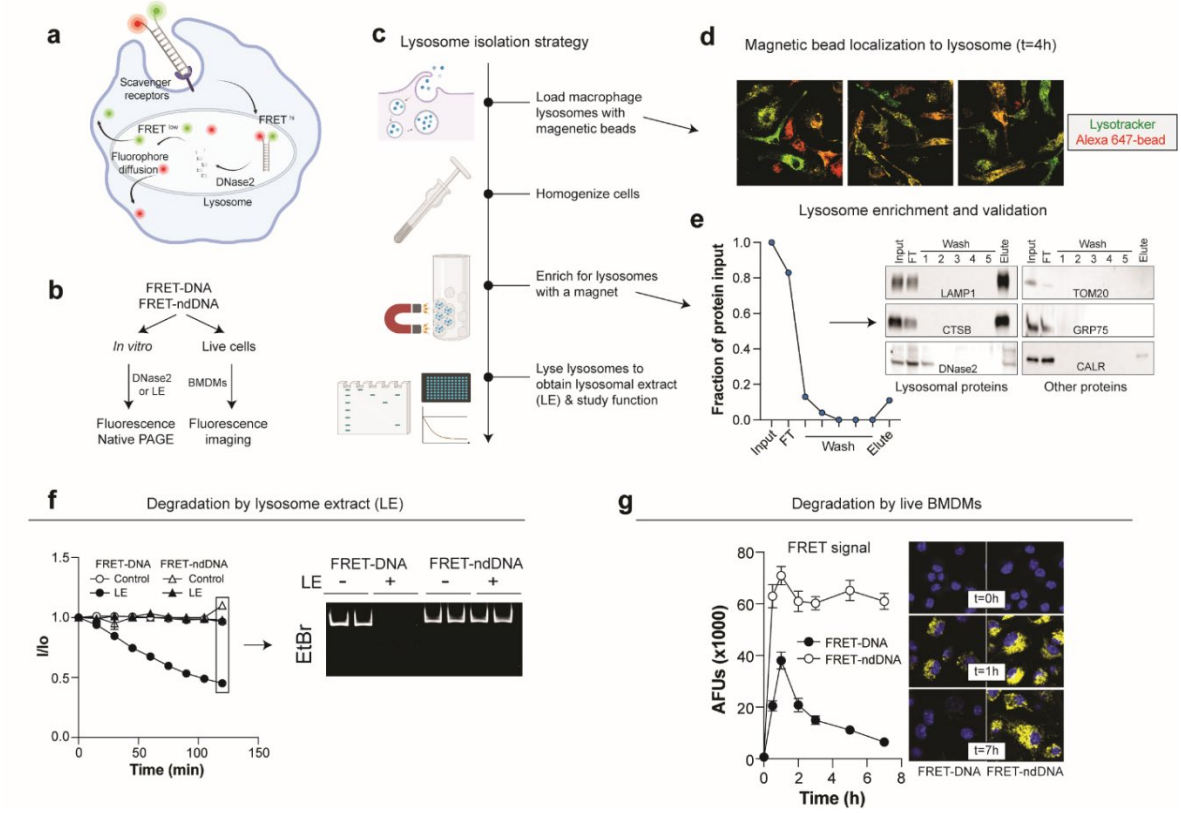

Figure 3.3 Degradation of DNA nanodevice is necessary for fluorophore release. (a) Schematic of FRET-DNA uptake by macrophages where high FRET signal indicates intact DNA and loss of FRET signal indicates DNA degradation and fluorophore diffusion. (b) Experimental plan using *in vitro* and *in cellulo* methods to detect DNA degradation (c) Lysosome isolation strategy using magnetic nanobeads. (d) Co-localization images using magnetic beads conjugated to Alexa-647 and 50 nM lysotracker green. (e) Protein concentration of fractions obtained from lysosome isolation procedure. (f) *in vitro* Kinetic assay measuring FRET-DNA and FRET-ndDNA degradation by lysosomal extracts (LE) and corresponding end-point products visualized by native PAGE. (g) *in cellulo* detection of loss of FRET signal in degradable DNA, and signal retainment in lysosomes by FRET-nDNA. Results are mean ± SEM. n.s. = no significance. *$p < 0.05$, **$p<0.001$, ***$p<0.0001$ (student's *t*-test).

3.7 T0-DNA activates LXR target genes *in vitro*.

Our next objective was to determine whether attaching an LXR agonist to the DNA nanodevice could activate the expression of LXR target genes in macrophages. We reasoned that the DNA would be degraded in the lysosome, liberating the cell-permeable agonist and lead to activation of target genes. The gene for the cholesterol transporter protein ABCA1 contains an LXR binding site in its promoter and activation of LXR by agonists has been shown to induce *Abca1* expression several fold (Kirchgessner et al., 2016; Levin et al., 2005). Using induction of *Abca1* expression as readout, we screened two of the most widely available LXR agonists GW3965 and T0901317 for their relative ability to activate LXR. Both agonists are membrane permeable and activate LXRa and LXRb. Quantitative real-time PCR of in vitro treated pMACs and BMDMs with increasing concentrations of GW3965 or T0901317 revealed T0901317 was more effective at activating LXR (**Figure 3.4a**).

We subsequently attached T0901317 to the DNA nanodevice (T0-DNA). To reduce the amount of DNA being delivered to the cells, Dr. Chakraborty used click chemistry to attach two molecules of T0901317 to the nanodevice, one at each of the 5' end of the DNA strands (**Figure 3.4b**). Free T0901317 was removed by sequential filtrations using 3kDa Amicon Centricon filter. Dr. Chakraborty used mass spectrometry, gel electrophoresis, and functional analysis of the final filtration to demonstrate the lack of free molecule in the final T0-DNA product (**Figure 3.4b** and data not shown). It should be noted that the attachment of the DNA nanodevice rendered the hydrophobic T0901317 soluble in aqueous buffers.

To establish that the T0-DNA targets LXR in macrophages, we compared the ability of free T0 and T0-DNA at equal T0 concentrations (10 uM) to induce expression of *Abca1* in

BMDMs (**Figure 3.4c**). The T0-DNA was almost as potent as free T0 in inducing *Abca1* expression. Macrophages can detect foreign nucleic acids that are seen as foreign or indicators of cellular stress, leading to the activation of signal transduction pathways and inflammatory responses. One receptor involved in this process is cyclic GMP-AMP synthase (cGAS), which recognizes cytoplasmic double-stranded DNA (dsDNA) associated with viral or bacterial infections, as well as the misplacement of nuclear or mitochondrial DNA (Burdette & Vance, 2013; Chen et al., 2016; Hopfner & Hornung, 2020). When cGAS binds to dsDNA, it synthesizes a cyclic dinucleotide called cyclic GMP-AMP (cGAMP), serving as a second messenger. This molecule then interacts with the adapter protein STING on the endoplasmic reticulum membrane, initiating a cascade of signal transduction events that activate the transcription factor IRF3 and stimulate cytokine production (Chen et al., 2016; Hopfner & Hornung, 2020). We wanted to know if the DNA nanodevice induces cytokines dsDNA can activate the stimulator of interferon gene (STING) pathway, as inflammation can accelerate atherosclerosis. Real-time quantitative PCR showed that the nanodevice does not elicit expression of inflammatory cytokines *Il-1b*, *IL-6*, and *Nf-kb*, suggesting that our nanodevice does not induce this and is suitable for delivery of LXR agonists **(Figure 3.4d**).

Macrophages in aortic lesions are enriched in cholesterol due to the uptake of apoB containing lipoproteins. Some of the free cholesterol in the lipid-loaded macrophage can be enzymatically oxidized and generate oxysterols that activate LXR. Indeed, LXR target genes (e.g. *Apoe, Abca1, Abcg1*) are increased in macrophage foam cells (Levin et al., 2005). Given this, we wanted to investigate whether the nanodevice could be taken up by foam cell macrophages and whether T0-DNA is able to induce expression of LXR target gene *Abca1*. To generate foam cells BMDMs were incubated with 2% atherogenic serum from WTD fed *Ldlr-/-*

mice or from wild type C57BL/6 mice (Ctrl) for 24 hours to lipid load the cells prior to incubation with F-DNA. To confirm lipid loading, cells were stained with Oil Red O, which stains neutral lipids (**Figure 3.4e**). Confocal microscopy analysis revealed that lipid loaded macrophages took up the nanodevice as efficiently as non-lipid loaded macrophages (**Figure 3.4e**). Lipid loaded BMDMs treated with T0 alone or T0-DNA and their controls (**Figure 3.4f**) revealed that LXR activation by T0-DNA in foam cell macrophages was comparable to that observed in non-lipid loaded BMDMs. This finding suggests that T0-DNA is suitable for an atherosclerotic model in mice. Overall, these results suggest that the DNA nanodevice has promising potential as a therapeutic agent for targeting aortic macrophage function in aortic lesions.

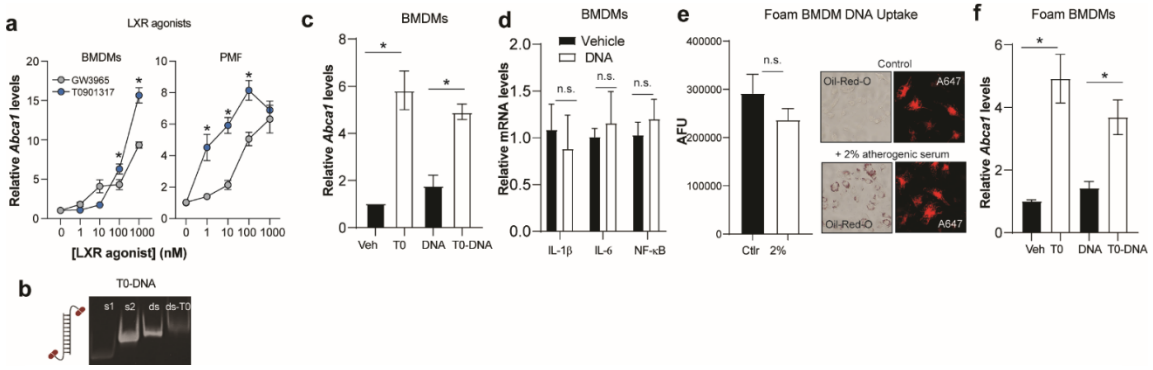

Figure 3.4 T0-DNA targets LXR in control and lipid loaded macrophages. (a) Gene expression of *Abca1*, target gene of LXR in response to BMDMs or pMACs treated with increasing doses of GW3965 or T0-901317. (b) Depiction of T0 conjugated to DNA nanodevice. Purity was assessed by comparing to single stranded DNA (ssDNA; s1, s2) to double stranded DNA conjugated to T0 (T0-DNA) using native polyacrylamide gel. (c) T0-DNA efficiency in activating *Abca1* compared to T0 alone in BMDMs. (d) Gene expression of IL-1B, IL-6, and NF-kB in response BMDMs treated with DNA or vehicle (PBS). (e) Representative images of ORO-stained foam BMDMs treated with 500 nM 647-DNA and quantification (n=30). (f) T0-DNA efficiency in activating *Abca1* compared to T0 alone in BMDMs. Results are mean ± SEM. n.s. = no significance. *$p < 0.05$, **$p<0.001$, ***$p<0.0001$ (student's *t*-test).

3.8 Detecting DNA nanodevice in atherosclerotic lesions and livers *in vivo*.

Next, we aimed to investigate the targeting ability and localization of the DNA nanodevice to the atherosclerotic lesion and liver. The Alexa F-DNA we used in the above *in vitro* studies contained a single fluorophore attached to only one end of one strand of the DNA. Sections of atherosclerotic lesions and livers contain higher levels of autofluorescence compared to *in vitro* imaging, to overcome this challenge and to enhance the signal for detecting DNA uptake *in vivo*, Dr. Chakraborty synthesized DNA containing 4-fluorophores, with one attached to the 5' and 3' ends of both strands of DNA (4F-DNA) (**Figure 3.5a**). 4F-DNA (125 ug DNA) was intravenously injected into *Ldlr-/-* mice fed WTD for 16 weeks (**Figure 3.5b**). Animals were sacrificed 1h post 4F-DNA injection. This time frame was chosen to allow the 4F-DNA to gain access to the artery wall but short enough that all the fluorophores would not have left the lysosomes. The heart/upper vasculature and livers were embedded in OCT and 5 μm sections were obtained for aortic root and livers. The sections were stained with anti-Mac2 antibody to identify macrophages and DAPI to identify nuclei. Representative images of the aortic root are shown in **Figure 3.6a.** As expected, there is autofluorescence in the Alexa 647 channel in the lesions of the PBS injected mice, however, increased signal is observed in mice injected with 4F-DNA (**Figure 3.6a**). In contrast, we did not observe differences in Alexa-647 signal between PBS and 4F-DNA injected, suggesting the DNA was not detectable in the liver despite the autofluorescence observed in these sections (**Figure 3.6b**). Overall, these findings demonstrate the preferential targeting of the DNA nanodevice to atherosclerotic lesions while showing limited or no targeting n in the liver.

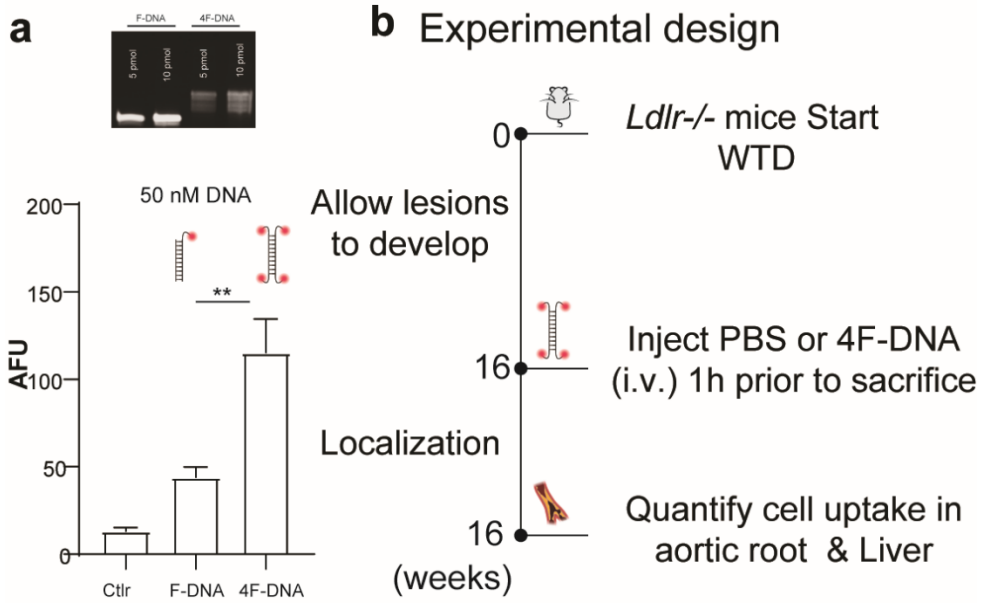

Figure 3.5 4F-DNA as a probe to track localization *in vivo*. (a) F-DNA (one fluorophore-DNA conjugate) or 4F-DNA (four fluorophore-DNA conjugate) purity was assessed with native polyacrylamide gel (top) Uptake of 50 nM F-DNA or 4F-DNA in BMDMs (bottom). (b) Experimental design for detecting 4F-DNA localization *in vivo*. Results are mean ± SEM. n.s. = no significance. *$p < 0.05$, **$p<0.001$, ***$p<0.0001$ (student's *t*-test).

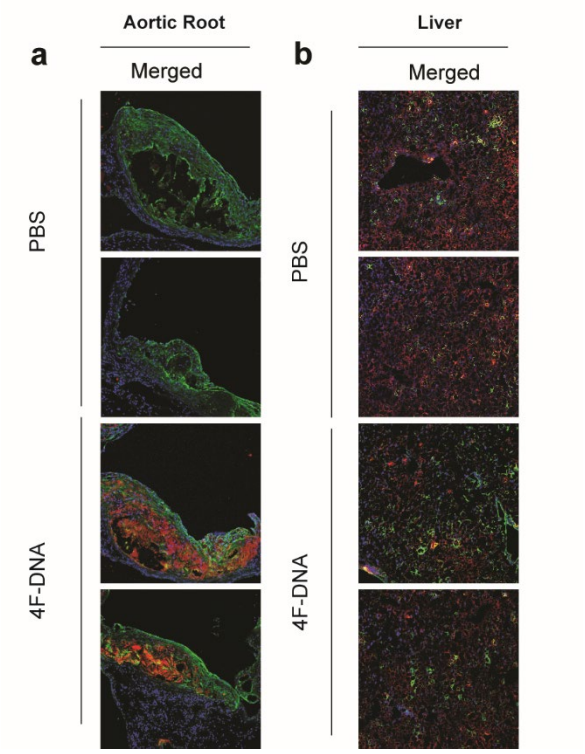

Figure 3.6 DNA nanodevice targets atherosclerotic lesions but not livers *in vivo.* (a) Representative images of aortic lesions from *Ldlr-/-* mice injected with 50 ug 4F-DNA or PBS. 5 um aortic root sections were co-stained with Mac2. (b) Representative images of liver sections from *Ldlr-/-* mice injected with 50 ug 4F-DNA or PBS. 5 um liver sections were co-stained with Mac2 and DAPI.

3.9 T0-DNA decreases atherosclerotic lesion size without inducing hypertriglyceridemia.

To assess the impact of conjugated T0-DNA on atherosclerosis and plasma triglyceride levels, we conducted two independent studies focusing on different modalities of atherosclerotic lesion interrogations. The first study involved cross-sectional analysis to evaluate atherosclerosis in the innominate artery and aortic root, providing insights into lesion thickness and complexity. The second study utilized *en face* analysis to assess atherosclerosis in the upper vasculature, providing information about the extent of aortic lesions. For the experiments, eight-week-old

male *Ldlr-/-* mice were placed on a WTD for six weeks. Following the diet period, the mice were intravenously injected with 0.066 mg/kg of T0901317 conjugated to DNA (0.033 mg/kg) or an equivalent amount of DNA (0.033 mg/kg) five days a week for four weeks while still on the WTD (**Figure 3.7**). In both independent experiments, body and spleen weights were not significantly different between DNA and T0-DNA treated mice, suggesting that the nanodevice does not elicit whole body inflammation as indicated by spleen weight, and does not affect body weight.

The cross-sectional analyses demonstrated that T0-DNA treatment significantly reduced lesion size in both the innominate artery and the aortic root, compared to mice treated with DNA alone (**Figure 3.8**). Additionally, *en face* analysis revealed a significant reduction in the surface area of atherosclerotic lesions in the upper vasculature + thoracic. Two lesion quantification approaches were used for the *en face* results. The first one was total lesion area of the total vasculature to obtain the extent of the lesions, and the second one the thoracic + upper vasculature (lesions on aortic arch and above, dotted line), including the aortic arch, innominate artery, and carotid, to take into account the areas where most of the lesions develop and most *en face* experts suggest (**Figure 3.8b**). Importantly, plasma triglyceride levels were assessed in both studies and consistently showed no significant differences between T0-DNA-treated mice and those treated with DNA alone (**Figure 3.9a** and **Figure 3.9b**). In contrast, a comparison of mice treated with T0 alone, vehicle, DNA, or T0-DNA show that in the order of days T0 alone significantly induces plasma triglycerides when compared to T0-DNA (**Figure 3.9c**). These results align with- and corroborate our previous findings indicating that nanodevice does not target the liver (4F-DNA localization). In support of these findings, we also observe that primary hepatocytes do not take up F-DNA when compared to peritoneal macrophages (**Figure 3.9d**).

Together these data suggest that the DNA nanodevice targets macrophages and not livers. Collectively, these findings suggest that conjugated T0-DNA has the potential to serve as a therapeutic agent for atherosclerosis without causing hypertriglyceridemia, the main side effect that has hindered the use of LXR agonists as a therapeutic agent for atherosclerosis.

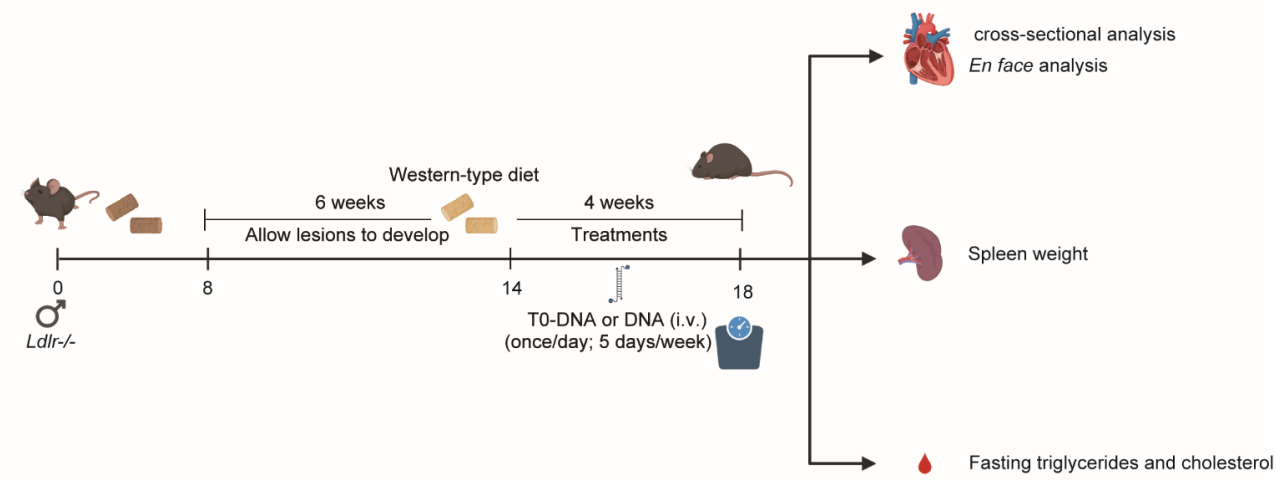

Figure 3.7 Strategy for testing T0-DNA efficacy in atherosclerotic *Ldlr-/-* mice. (a) 6-week-old C57Bl6/J *Ldlr-/-* male mice were placed on a western-type diet (WTD; 21% milk fat, 1.25% cholesterol) for 6 weeks to allow for lesions to develop. After 6 weeks on WTD, mice were treated with T0-DNA or DNA 5/days week i.v. at 0.0666 mg/kg. Prior to sacrifice mice were weighed and fasted for at least 3h to collect blood for plasma cholesterol and triglyceride levels. At sacrifice the heart and upper vasculature were collected for cross sectional analyses or whole aortas were collected for lesion area analysis. Spleen weight was observed as a proxy for inflammation.

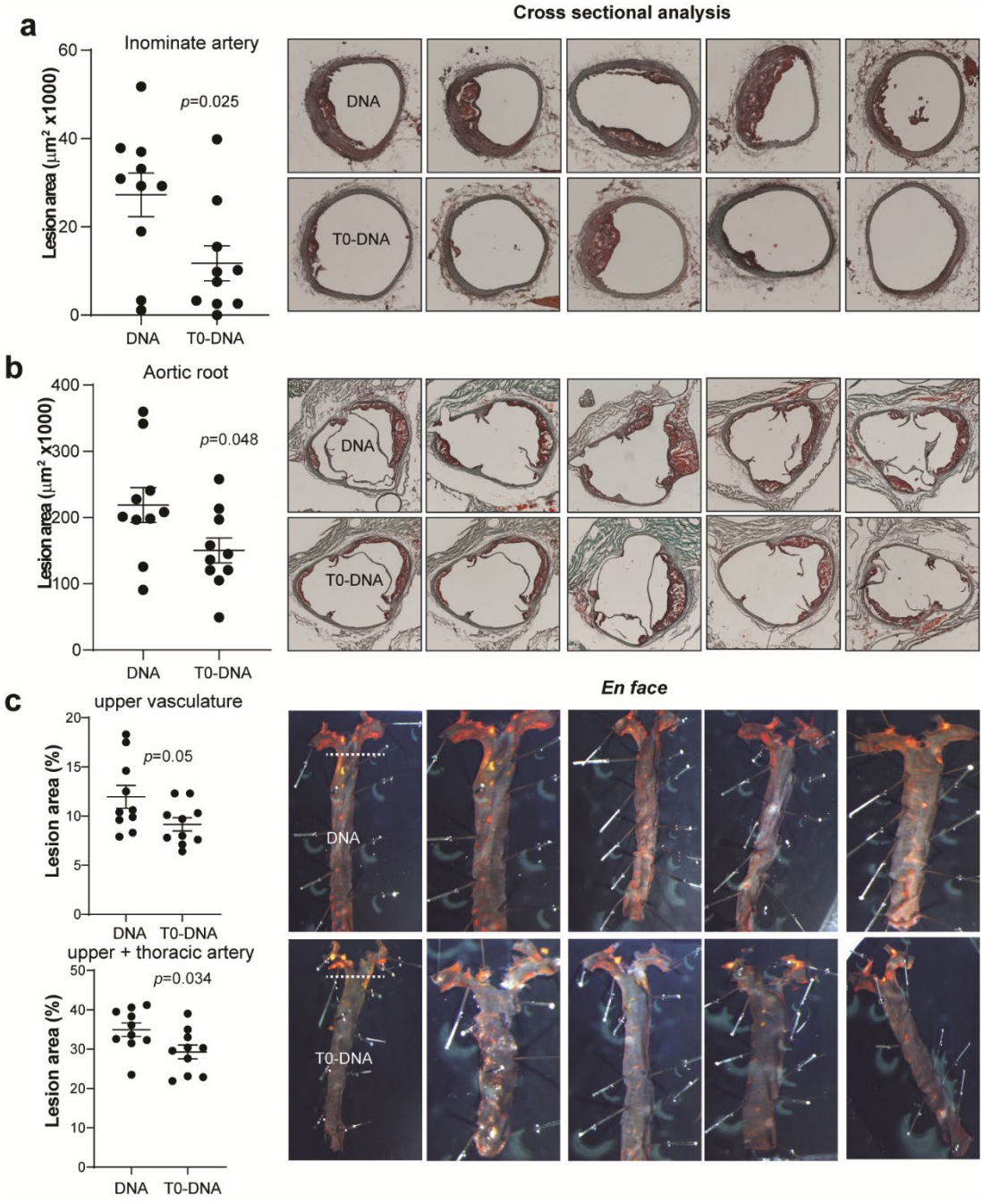

Figure 3.8 T0-DNA significantly reduces atherosclerotic lesion size in *Ldlr-/-* mice fed a WTD in two independent experiments After 4 weeks of T0-DNA treatment atherosclerosis was measured in (a) the innominate artery and aortic root by cross sectional analysis (expressed as mm^2) in the first experiment and (b) upper vasculature (dotted line) and upper plus thoracic artery by *en face* analysis (expressed as % lesion of total area and % lesion of the upper vasculature or total area) in the second experiment. Results are mean ± SEM. n.s. = no significance. *$p < 0.05$ (student's *t*-test); *n*=10/group (DNA/T0-DNA)

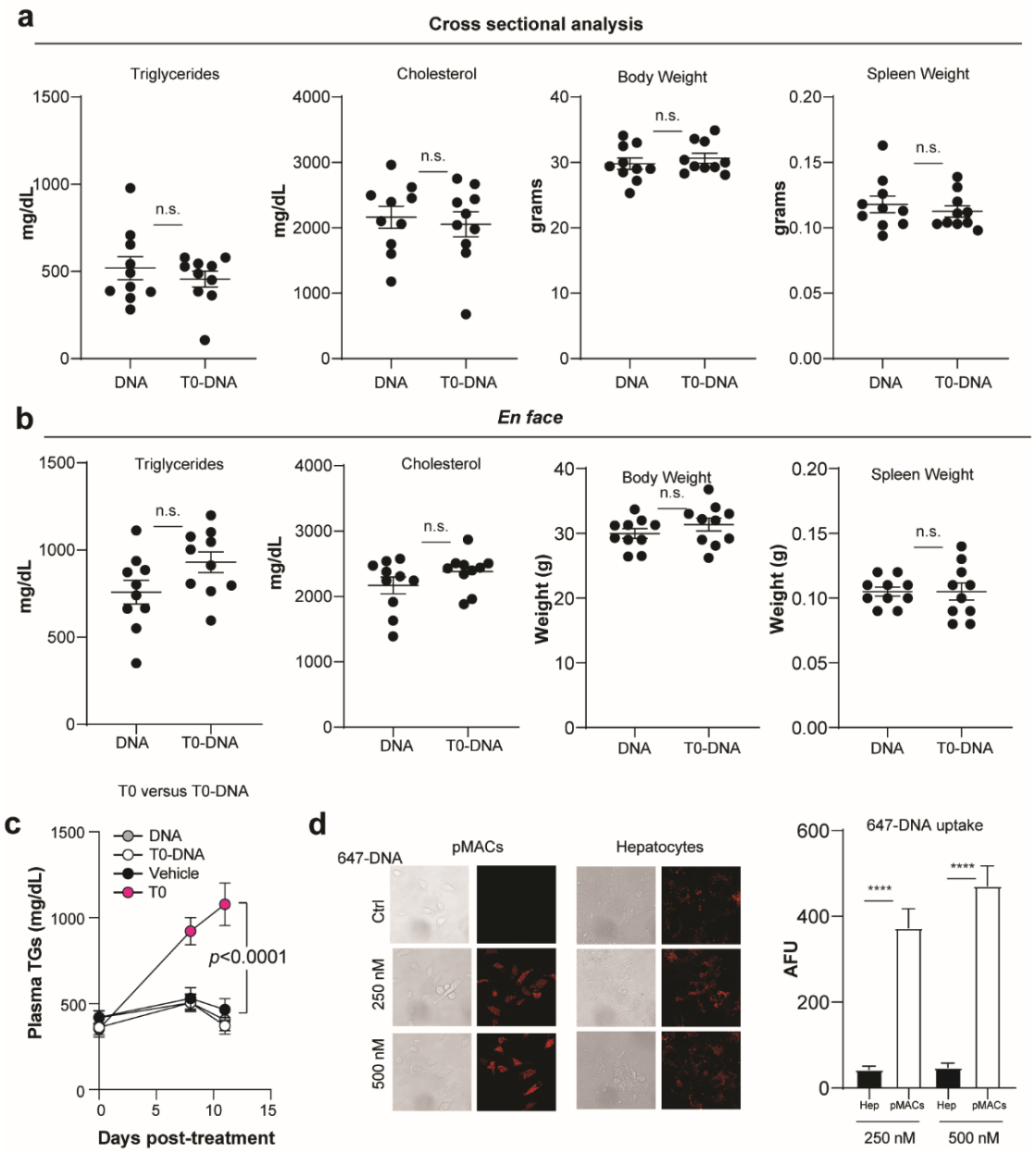

Figure 3.9 T0-DNA does not induce hypertriglyceridemia. Metabolic parameters from DNA or T0-DNA treated mice from two independent experiments. (a) Metabolic paratemers include plasma cholesterol, plasma triglycerides, and body weight from cross sectional and *in vivo* studies. (b) Metabolic parameters including plasma cholesterol, plasma triglycerides, and body weight *en face* analysis. (c) plasma triglycerides from *Ldlr-/-* mice fed a WTD for 6 weeks and treated with T0 alone, vehicle, DNA, or T0-DNA. (d) Representative images and quantification of F-DNA uptake in peritoneal macrophages and primary hepatocytes. Results are mean ± SEM. n.s. = no significance. Results are mean ± SEM. n.s. = no significance. *$p < 0.05$, **$p<0.001$, ***$p<0.0001$ (student's *t*-test); *n*=12/group

3.10 Discussion & Future Directions

LXR agonists have the potential to be used as a therapeutic to decrease atherosclerotic lesion size by acting on macrophages of the atherosclerotic lesion to upregulate the cholesterol efflux machinery and attenuate inflammation. Countless studies have shown significant reduction in atherosclerotic lesion size in rats, mice, and monkeys following LXR agonist treatment. While LXR activation in macrophages of the aortic root is beneficial, LXR activation in the liver has adverse effects, namely upregulation of triglyceride synthesis resulting in blood hypertriglyceridemia. These adverse on-target effects on the liver have hindered the therapeutic application for LXR agonists in atherosclerosis. Previous work has attempted to use nanodevices such liposomes and PEGylated devices and to selectively deliver LXR agonist to aortic lesions; however, these nanodevices can elicit the immune response as most of these are not biodegradable. In this chapter we show a biodegradable DNA nanodevice to be used as an LXR small molecule agonist carrier to preferentially target atherosclerotic lesions. We showed the internalization of the nanodevice, degradation of the nanodevice by the lysosome, and release of the compound attached to the nanodevice in macrophages. Furthermore, we observed that this carrier is preferential to the lesion and not the liver.

This nanodevice was previously used to successfully deliver a lysosomal cysteine protease small molecule inhibitor (E64) to TAMs and showed tumor reduction *in vivo* efficacy. To adapt this technology to the atherosclerotic system, we started our investigation by confirming that the DNA nanodevice was internalized up by non-TAMs, including BMDMs and pMACs, and localized to lysosomes. LXR is a constitutively nuclear protein and to employ this nanodevice for successful LXR agonist delivery it would require compound liberation from the lysosome and reach the nucleus. To explore the nanodevice metabolism and compound liberation we used FRET-DNA as a tool to extrapolate nanodevice degradation in the lysosome. A non-

degradable FRET-DNA used as a control. FRET-DNA is internalized in macrophages and the FRET signal decays over time, this decay in FRET signal occurs at a faster rate than the decay in donor signal, suggesting that the DNA is degraded, and the fluorophores are liberated. Attaching the membrane permeable LXR agonist T0 to the nanodevice (T0-DNA) effectively targeted LXR and induced gene expression in macrophages, like free T0 agonist.

Using 4F-DNA to enhance detection we showed the targeting ability of the DNA to atherosclerotic lesions and livers in vivo. The results showed significant signal in the lesion areas of mice injected with the modified DNA, indicating preferential targeting to atherosclerotic lesions. However, there was no significant signal observed in the livers, suggesting limited dissemination to that organ. Another study found that treatment with the modified DNA reduced the size of atherosclerotic lesions without causing hypertriglyceridemia. These findings suggest that the modified DNA nanodevice could be a potential therapeutic agent for atherosclerosis without adverse effects.

As mentioned previously, other researchers have attempted to deliver LXR agonists to macrophages in various ways, including nanodevice delivery or modifying the chemical structure of LXR ligands to target LXR isoform mostly expressed in macrophages. However, these methods can still have off-target effects on the liver. Other methods, such as antibody drug conjugates and nanoparticles, have been used but have shown deleterious effects. In our study, we are adding to this repertoire by using DNA nanodevices, which have the potential to attenuate atherosclerosis, as it preferentially targets the atherosclerotic lesion without inducing hypertriglyceridemia. This DNA nanodevice is a useful tool to modulate macrophage behavior to attenuate disease. Future studies include expanding on ligands of lipid metabolism and inflammation targets, for example, as compounds that activate PPAR gamma, as activation of

PPAR in macrophages has been shown to decrease atherosclerotic lesion size (Chawla, 2010; Miao et al., 2023).

Other critical experiments include evaluating the efficacy and safety of the DNA nanodevice in larger mammals and the maximal foreign DNA a larger organism can tolerate, such as non-human primates, and evaluate its toxicity and safety. Taken together these studies make an impact on broadening the usefulness of DNA nanotechnology in the atherosclerosis field.

CHAPTER FOUR GENERAL DISCUSSION

Atherosclerosis is a chronic immunometabolic disorder where inappropriate inflammation and lipid metabolism in macrophages drive atherosclerotic lesion formation(Libby, 2021b). Atherosclerosis is the most common underlying cause of CVD, which is the leading cause of global deaths (*Heart Disease Facts | cdc.gov*, n.d.). In my doctoral dissertation, I focused on exploring the intricate relationship between inflammation and lipid metabolism within atherosclerotic macrophages. Through my research, I aimed to gain a deeper understanding of this interplay and utilized this knowledge to apply innovative therapeutic intervention models. In chapter two, my research centered around the identification of the pro-atherogenic effects of the inflammatory cytokine IFNγ. Our lab has previously found that metabolic inflammation, through IFNγ, induced by obesity and insulin resistance (IR) enhances atherosclerosis lesion size. Reardon et al. found that IFNγ enhances macrophage cholesterol loading. I continued this story by attempting to delineate the underlying mechanism of enhanced macrophage lipid loading. In chapter three, we integrated DNA nanotechnology developed by Dr. Kasturi Chakraborty, who has previously demonstrated successful delivery of therapeutics to tumor-associated macrophages. Leveraging this innovative technology, our study aimed to selectively deliver LXR agonists to atherosclerotic lesions. The objective was to reduce the size of atherosclerotic lesions by enhancing cholesterol efflux, while also avoiding any adverse effects on the liver that could arise from on-target interactions.

4.1 Pro-atherogenic non-canonical IFNγ signaling in macrophages.

Obese and insulin resistance patients have an increased risk to develop atherosclerosis, even in the face of controlled traditional risk factors. Our lab identified the host defense cytokine IFNγ to influence this significant risk through disruption in the macrophage sterol responsive network (MSRN) leading to macrophage cholesterol loading. Therapies against IFNγ can be useful to attenuate atherosclerosis. However, antagonizing IFNγ directly as a therapeutic avenue is challenging, as this cytokine is critical in bacterial killing and host defense. Congenital IFNγ deficient patients are observed to be severely immunocompromised (McLaren & Ramji, 2009), providing evidence against antagonizing IFNγ for atherosclerosis. Reardon et al's studies allude to the effects of IFNγ being independent of the host defense response, providing a possible therapeutic target, but the mechanisms remain to be elucidated. Furthermore, the research outlined by Reardon et al. suggests that IFNγ exacerbates atherosclerosis by increasing cholesterol loading in macrophages, and this IFNγ is induced by obesity and insulin resistance. The effects of IFNγ on macrophage cholesterol loading, and therefore its pro-atherogenic effects, may occur through a signaling cascade independent of the STAT1-IRF. This is not contradicting ample evidence that STAT1 plays a role lesion development, as it certainly does, particularly by converging the inflammatory signals induced by IFNγ, TLR4, and IL-6 (Sikorski et al., 2011). Instead, our investigations are centered on the effects of IFNγ and obesity/IR induced atherosclerotic lesion increase, and this may be independent of macrophage STAT1 and IRF1 signaling.

In chapter two we further explore this concept and show that the downstream effectors of IFNγ signaling IRF1 and STAT1 in atheroprone (*Ldlr-/-*) obese and insulin resistant male mice. Our results show that neither IRF1 or STAT1 exacerbate atherosclerosis *in vivo,* within the context of obesity and insulin resistance.

One limitation of our *in vivo* studies is the use of bone marrow transplantation (BMT) to study the effects of macrophage IRF1 in the context of obesity and insulin resistance. Indeed, BMT has been shown to replace blood-borne monocytes; however, other leukocytes such as lymphocytes (T and B cells), dendritic cells, neutrophils, eosinophils, and basophils to name a few, are also replaced (Duran-Struuck & Dysko, 2009; Sreeramkumar & Hidalgo, 2015). These leukocytes have been shown to play a role in atherogenesis, and the extension of the roles of IRF1 derived from these cells or monocytes cannot be evaluated using the BMT model (Gisterå & Hansson, 2017). Recently, Du & colleagues showed atheroprotective effects of global IRF1 knockout mice in a *Apoe-/-* mice (Du et al., 2019). While these results are compelling, the contributions of leukocyte, more specifically macrophage, derived IRF1 in the context of obesity and insulin resistance cannot be assessed in Du's studies and is not suitable to compare to our BMT IRF1 investigations for two reasons. One, the genetic models used in this study does not account for the contribution of leukocytes, and the response of other cells may play a role in the atheroprotective effects observed. Two, the atherogenic *Apoe-/-* mouse is not insulin resistance (Kawashima et al., 2009), therefore the contributions of IFNγ to obesity/insulin resistance enhancement of atherosclerosis cannot be discerned. Our approach places our studies in the context of macrophages and obesity/IR. This difference in experimental design highlights the importance of considering specific disease contexts and genetic backgrounds when studying the role of signaling pathways in atherosclerosis. Further experimentation would be required to evaluate the role of macrophage IRF1 in response to obesity/IR- IFNγ, this would require the use of a conditional mutagenesis of the lysMCre in *Ldlr-/-* mice to extrapolate the contributions of macrophages. If the results in these studies do not show a difference in lesion size in the context of obesity/IR then IRF1 may not play a role in enhancing atherosclerosis. Other limitations of

our studies in chapter two is the sole use of male mice in the results. While we attempted to use female mice in our studies however, we could not discern conclusions since the *Ldlr-/-* female mice were not obese or insulin resistant after 16 weeks on diet, consistent with reports from the literature. Future studies must include identifying a suitable female mouse model to study pre-clinical atherosclerosis in the context of obesity and insulin resistance.

In addition, our mechanistic investigations have unveiled a potential pro-atherogenic signaling cascade triggered by IFNγ, which leads to the downregulation of apoE—a crucial node required for cholesterol efflux (Becker et al. 2010). We provided evidence supporting the post-transcriptional downregulation of apoE by IFNγ in macrophages, consistent with previous findings reported in the literature (Brand et al., 1993). apoE has been shown to be regulated and shuttled for degradation in a post-golgi and autophagy mediated method in hepatocytes and astorcytes (Fote et al., 2022). Our mechanistic studies have also suggested the involvement of autophagy-lysosome pathways in the degradation of apoE. However, it is important to acknowledge the limitations of our study. We did not pursue experiments to investigate the secretion of apoE, which would require tracking a labeled population of apoE. Traditionally, radiolabeling has been used for this purpose, but alternative techniques that do not involve radioactivity have emerged. For instance, labeling apoE with L-azido-methionine (suitable for click chemistry) would allow us to specifically monitor the fate of apoE and draw conclusions regarding its degradation in response to IFNγ without use of radioactivity. Furthermore, conducting such a labeling experiment with apoE would enable us to not only detect changes in its population in response to IFNγ but also determine its subcellular localization. This discovery adds to the ever-growing understanding of the intricate regulatory mechanisms contributing to the development of atherosclerosis. The utilization of phosphoproteomics and small molecule

inhibitor assays offered a comprehensive approach to identify potential candidate proteins and pathways involved in IFNγ signaling and apoE regulation. While the inhibitor assays alone presented challenges in interpretation as it has off target effects, they however provided valuable starting points for further investigations. We acknowledge the need for genetic interventions, such as overexpression or silencing, to validate the effects of candidate proteins on apoE regulation and have proposed a method to overexpress proteins in macrophages, including using synthetic mRNA delivery to evade the STING and inflammatory pathways (Moradian et al., 2020; D. J. Williams et al., 2010).

The significance of these findings lies in their potential implications for therapeutic strategies aimed at mitigating atherosclerosis in high-risk patient populations, particularly those with obesity and type 2 diabetes. By identifying a non-canonical pathway involving the MAPK pathway and autophagy system, this study offers new targets for intervention that may have a beneficial impact on atherosclerosis progression.

In summary, the studies conducted in this chapter have advanced the field's understanding of the IFNγ -STAT1-IRF1 signaling pathway, its role in atherosclerosis, and the novel pro-atherogenic cascade involving apoE regulation. These findings provide valuable insights into the intricate interplay between immunity and metabolism and highlight the challenges in untangling these pathways for therapeutic approaches. The study contributes to the broader body of knowledge in atherosclerosis research and offer potential avenues for future investigations and therapeutic interventions.

4.2 Preferential delivery of LXR agonist T0901317 to murine aortic macrophages using a DNA nanodevice.

In chapter three, we used a DNA nanodevice to preferentially deliver LXR agonist T0901317 to the atherosclerotic lesions. This allowed us to widen the therapeutic window for LXR agonists. LXR agonists first emerged as a promising therapeutic a few decades ago and were shown to decrease lesion size in murine and rabbit models (Levin et al., 2005). However, the activation of LXR in the liver resulted in hypertriglyceridemia which has hindered its application for therapeutic use (Kirchgessner et al., 2016).

One way to overcome this would be by the application of nanodevices to deliver therapeutics with precision to a specific cell or tissue (Liu et al., 2022; Bhaladhare and Bhattacharjee, 2023). Recently, nanotherapeutic research has gained momentum, particularly in the field of cancer therapy, with approximately 250 different nanotherapeutic drugs being explored in preclinical or clinical studies since the approval of adriamycin liposomes in 1995 (Zhang et al., 2015; Xu et al., 2023). Notably, there is a growing body of nanotherapeutic investigations focusing on atherosclerosis treatment (Soumya and Raghu, 2023). As nanotechnology continues to advance, nanocarriers can effectively target macrophages within atherosclerotic plaques, enhancing therapeutic efficacy while minimizing the side effects of loaded drugs. Delivering LXR agonist using this approach facilitates intracellular cholesterol efflux without inducing fatty liver, offering promising prospects for atherosclerosis treatment with LXR agonists.

Here, we present an addition to the repertoire of targeted carriers: a biologic DNA nanodevice designed to specifically target macrophages through their heavily expressed scavenger receptors. *In vitro* experiments comparing LXR agonist alone (T0) to LXR-agonist-DNA (T0-DNA) demonstrates remarkable efficacy measured by expression of LXR target gene

Abca1. The efficiency at this concentration does not elicit cytokines that are part of the STING pathway. We hypothesize the STING pathway is not activated by our DNA nanodevice, as it is internalized through the endocytic pathway and is readily degraded by the lysosome.

Localization studies using confocal microscopy with 4F-DNA *in vivo*, showed that the nanodevice is preferentially delivered to the atherosclerotic lesion and not the liver. Further investigations in pre-clinical cancer models show that F-DNA can enter Kupffer cells (resident liver macrophages) but not hepatocytes *in vivo* by flow cytometry (data not shown). These data suggest that F-DNA can enter the liver through Kupffer cells but not hepatocytes. To validate these findings, further investigations need to be performed in atherosclerotic models.

Furthermore, by delivering T0-DNA *in vivo,* we effectively reduced atherosclerotic lesions in atheroprone mice fed a WTD while circumventing any adverse effects on the liver, mainly hypertriglyceridemia, which are typically associated with on-target delivery of LXR agonists. The dose in which this was achieved (0.066 mg/kg) was significantly lower than that previously used (2 mg/kg) (Peng et al., 2009). Though the route of administration is different (i.v. vs oral), the effective oral dose promotes a decreased lesion size in the innominate artery more so than the aortic root, a result that is consistent with our studies (Peng et al., 2009).

Mechanistically, we showed the internalization, degradation, and release of the compound attached to the nanodevice by purified DNAseII and macrophage lysosomal extract *in vitro* and macrophages *in cellulo*. Based on these findings, we propose a mechanism in which DNA nanodevices are metabolized by internalization of macrophages, localization to lysosomes, degraded by lysosomal enzyme DNAseII, and attached therapeutic compounds released. While these studies were successful at attenuating murine atherosclerosis without any observable side effects, more studies are needed to be performed in larger mammals, specifically non-human

primates. Exogenous DNA has been shown to be highly immunogenic (Surana et al., 2015), and while our *in vitro* studies of DNA treated BMDMs show no significant expression of inflammatory cytokines, and our in vivo studies do not show observable inflammation as measured by spleen weights these studies need to be repeated in higher organisms.

DNA nanotechnology at this stage requires I.V. administration for multiple days per week, for multiple weeks. This is unfeasible and may not be plausible to implement. Other specific delivery methods would need to be implemented for this to be plausible. Furthermore, studies performed in both stories delineated in this dissertation were performed in male mice, and it is critical to recapitulate these findings in female mice as well.

4.3 Impact of atherosclerotic research to benefit populations that desperately need it.

Atherosclerosis is a chronic immunometabolic disorder where inappropriate inflammation and lipid metabolism in macrophages drive atherosclerotic lesions. While patients with obesity and insulin resistance are more likely to experience cardiac events compared to lean and insulin sensitive individuals, other impacts on atherosclerosis do exist. For example, social economic status, perceived ethnicity, and gender (as mentioned above) play a significant role.

The impact of socioeconomic status (SES) on atherosclerosis, is now starting to be appreciated. Studies have consistently shown that lower SES is associated with higher rates of atherosclerosis prevalence and incidence (Vart et al., 2017)(Lynch et al., 1995). Several factors contribute to this relationship. For one, limited access to healthcare services is a significant factor. Individuals with lower income and education levels often face challenges in accessing healthcare, including preventive care and timely treatment for cardiovascular risk factors (Mannoh et al., 2021)(Zegeye et al., 2021). This limited access may result in delays in diagnosis,

inadequate management of risk factors, and suboptimal treatment for atherosclerosis-related conditions.

Moreover, socioeconomic disparities contribute to differences in the prevalence of traditional cardiovascular risk factors associated with atherosclerosis. Individuals from lower SES backgrounds are more likely to engage in unhealthy behaviors, including smoking, poor dietary habits, and physical inactivity (Gregório et al., 2017)(Yang et al., 2020). They also have higher rates of obesity and are more susceptible to hypertension, diabetes, and dyslipidemia, all of which increase the risk of developing atherosclerosis.

Additionally, individuals with higher SES generally experience better disease management and outcomes related to atherosclerosis (Christine et al., 2017). They have increased access to healthcare resources, early interventions, and advanced medical treatments. Moreover, they are more likely to engage in lifestyle modifications such as adopting healthier diets and being physically active. In contrast, individuals with lower SES may face delays in seeking medical care, exhibit poorer adherence to medications, and experience higher rates of complications and adverse cardiovascular events. To address socioeconomic disparities in atherosclerosis, comprehensive strategies are necessary. Improving access to healthcare services, especially for preventive care and early intervention, is crucial. Efforts should focus on ensuring affordable healthcare coverage, increasing the availability of primary care providers, and implementing community-based interventions that target at-risk populations. Promoting health equity is another essential aspect. Addressing social determinants of health, such as poverty and limited education, can positively influence atherosclerosis outcomes. Providing education and resources to empower individuals from disadvantaged backgrounds to adopt healthier lifestyles is also important.

SES plays a significant role in the development and progression of atherosclerosis. Lower SES is associated with higher prevalence and incidence of atherosclerosis, driven by limited access to healthcare, higher exposure to risk factors, and poorer disease management. Addressing socioeconomic disparities in atherosclerosis requires a multifaceted approach that encompasses improving access to healthcare, promoting health equity, and addressing social determinants of health. Providing effective targets for atherosclerosis is paramount, as it is the leading cause of death. However, detangling the intricate relationship between inflammation and lipid metabolism is challenging. My dissertation work has provided a novel delivery method for targeting macrophages in the atherosclerotic lesion. New technologies are needed to make this approach cost-effective and equitable to be delivered to patients who need it most.

BIBLIOGRAPHY

Afonso, M. da S., Castilho, G., Lavrador, M. S. F., Passarelli, M., Nakandakare, E. R., Lottenberg, S. A., & Lottenberg, A. M. (2014). The impact of dietary fatty acids on macrophage cholesterol homeostasis. *The Journal of Nutritional Biochemistry*, *25*(2), 95–103. https://doi.org/10.1016/j.jnutbio.2013.10.001

Ait-Oufella, H., Taleb, S., Mallat, Z., & Tedgui, A. (2011). Recent advances on the role of cytokines in atherosclerosis. *Arteriosclerosis, Thrombosis, and Vascular Biology*, *31*(5), 969–979. https://doi.org/10.1161/ATVBAHA.110.207415

Ajayi-Smith, A., van der Watt, P., Mkwanazi, N., Carden, S., Trent, J. O., & Leaner, V. D. (2021). Novel small molecule inhibitor of Kpnβ1 induces cell cycle arrest and apoptosis in cancer cells. *Experimental Cell Research*, *404*(2), 112637. https://doi.org/10.1016/j.yexcr.2021.112637

Andraws, R., Berger, J. S., & Brown, D. L. (2005). Effects of antibiotic therapy on outcomes of patients with coronary artery disease: a meta-analysis of randomized controlled trials. *The Journal of the American Medical Association*, *293*(21), 2641–2647. https://doi.org/10.1001/jama.293.21.2641

Bäck, M., & Hansson, G. K. (2015). Anti-inflammatory therapies for atherosclerosis. *Nature Reviews. Cardiology*, *12*(4), 199–211. https://doi.org/10.1038/nrcardio.2015.5

Bajno, L., Peng, X. R., Schreiber, A. D., Moore, H. P., Trimble, W. S., & Grinstein, S. (2000). Focal exocytosis of VAMP3-containing vesicles at sites of phagosome formation. *The Journal of Cell Biology*, *149*(3), 697–706. https://doi.org/10.1083/jcb.149.3.697

Barvitenko, N., Ashrafuzzaman, M., Lawen, A., Skverchinskaya, E., Saldanha, C., Manca, A., Uras, G., Aslam, M., & Pantaleo, A. (2022). Endothelial Cell Plasma Membrane Biomechanics Mediates Effects of Pro-Inflammatory Factors on Endothelial Mechanosensors: Vicious Circle Formation in Atherogenic Inflammation. *Membranes*, *12*(2). https://doi.org/10.3390/membranes12020205

Bazmandegan, G., Abbasifard, M., Nadimi, A. E., Alinejad, H., & Kamiab, Z. (2023). Cardiovascular risk factors in diabetic patients with and without metabolic syndrome: a study based on the Rafsanjan cohort study. *Scientific Reports*, *13*(1), 559. https://doi.org/10.1038/s41598-022-27208-5

Becker, K. G., Hosack, D. A., Dennis, G., Lempicki, R. A., Bright, T. J., Cheadle, C., & Engel, J. (2003). PubMatrix: a tool for multiplex literature mining. *BMC Bioinformatics*, *4*, 61. https://doi.org/10.1186/1471-2105-4-61

Becker, L., Gharib, S. A., Irwin, A. D., Wijsman, E., Vaisar, T., Oram, J. F., & Heinecke, J. W. (2010). A macrophage sterol-responsive network linked to atherogenesis. *Cell Metabolism*, *11*(2), 125–135. https://doi.org/10.1016/j.cmet.2010.01.003

Beckman, J. A., Creager, M. A., & Libby, P. (2002). Diabetes and atherosclerosis: epidemiology, pathophysiology, and management. *The Journal of the American Medical Association*, *287*(19), 2570–2581. https://doi.org/10.1001/jama.287.19.2570

Beers, C., Honey, K., Fink, S., Forbush, K., & Rudensky, A. (2003). Differential regulation of cathepsin S and cathepsin L in interferon gamma-treated macrophages. *The Journal of Experimental Medicine*, *197*(2), 169–179. https://doi.org/10.1084/jem.20020978

Bentzon, J. F., Otsuka, F., Virmani, R., & Falk, E. (2014). Mechanisms of plaque formation and rupture. *Circulation Research*, *114*(12), 1852–1866. https://doi.org/10.1161/CIRCRESAHA.114.302721

Bevilacqua, M. P., Pober, J. S., Mendrick, D. L., Cotran, R. S., & Gimbrone, M. A. (1987). Identification of an inducible endothelial-leukocyte adhesion molecule. *Proceedings of the National Academy of Sciences of the United States of America*, *84*(24), 9238–9242. https://doi.org/10.1073/pnas.84.24.9238

Blagov, A. V., Markin, A. M., Bogatyreva, A. I., Tolstik, T. V., Sukhorukov, V. N., & Orekhov, A. N. (2023). The role of macrophages in the pathogenesis of atherosclerosis. *Cells*, *12*(4). https://doi.org/10.3390/cells12040522

Borén, J., Taskinen, M.-R., Björnson, E., & Packard, C. J. (2022). Metabolism of triglyceride-rich lipoproteins in health and dyslipidaemia. *Nature Reviews. Cardiology*, *19*(9), 577–592. https://doi.org/10.1038/s41569-022-00676-y

Brand, K., Mackman, N., & Curtiss, L. K. (1993). Interferon-gamma inhibits macrophage apolipoprotein E production by posttranslational mechanisms. *The Journal of Clinical Investigation*, *91*(5), 2031–2039. https://doi.org/10.1172/JCI116425

Braun, M., Pietsch, P., Felix, S. B., & Baumann, G. (1995). Modulation of intercellular adhesion molecule-1 and vascular cell adhesion molecule-1 on human coronary smooth muscle cells by cytokines. *Journal of Molecular and Cellular Cardiology*, *27*(12), 2571–2579. https://doi.org/10.1006/jmcc.1995.0044

Brown, J. M., & Yu, L. (2009). Opposing Gatekeepers of Apical Sterol Transport: Niemann-Pick C1-Like 1 (NPC1L1) and ATP-Binding Cassette Transporters G5 and G8 (ABCG5/ABCG8). *Immunology, Endocrine & Metabolic Agents in Medicinal Chemistry*, *9*(1), 18–29. https://doi.org/10.2174/187152209788009797

Buck, M. D., O'Sullivan, D., & Pearce, E. L. (2015). T cell metabolism drives immunity. *The Journal of Experimental Medicine*, *212*(9), 1345–1360. https://doi.org/10.1084/jem.20151159

Burdette, D. L., & Vance, R. E. (2013). STING and the innate immune response to nucleic acids in the cytosol. *Nature Immunology*, *14*(1), 19–26. https://doi.org/10.1038/ni.2491

Burke, A. P., Farb, A., Malcom, G. T., Liang, Y., Smialek, J. E., & Virmani, R. (1999). Plaque rupture and sudden death related to exertion in men with coronary artery disease. *The Journal of the American Medical Association*, *281*(10), 921–926. https://doi.org/10.1001/jama.281.10.921

Caligiuri, G., Rottenberg, M., Nicoletti, A., Wigzell, H., & Hansson, G. K. (2001). Chlamydia pneumoniae infection does not induce or modify atherosclerosis in mice. *Circulation*, *103*(23), 2834–2838. https://doi.org/10.1161/01.cir.103.23.2834

Calkin, A. C., & Tontonoz, P. (2010). Liver x receptor signaling pathways and atherosclerosis. *Arteriosclerosis, Thrombosis, and Vascular Biology*, *30*(8), 1513–1518. https://doi.org/10.1161/ATVBAHA.109.191197

Campos-Vazquez, R. M., & Gonzalez, E. (2020). Obesity and hiring discrimination. *Economics and Human Biology*, *37*, 100850. https://doi.org/10.1016/j.ehb.2020.100850

Cellular and molecular pathobiology of cardiovascular disease. (2014). Elsevier. https://doi.org/10.1016/C2012-0-02409-X

Chakraborty, K., Anees, P., Surana, S., Martin, S., Aburas, J., Moutel, S., Perez, F., Koushika, S. P., Kratsios, P., & Krishnan, Y. (2021). Tissue-specific targeting of DNA nanodevices in a multicellular living organism. *ELife*, *10*. https://doi.org/10.7554/eLife.67830

Chardin, P., & McCormick, F. (1999). Brefeldin A. *Cell*, *97*(2), 153–155. https://doi.org/10.1016/S0092-8674(00)80724-2

Chatel-Chaix, L., & Bartenschlager, R. (2014). Dengue virus- and hepatitis C virus-induced replication and assembly compartments: the enemy inside--caught in the web. *Journal of Virology*, *88*(11), 5907–5911. https://doi.org/10.1128/JVI.03404-13

Chawla, A. (2010). Control of macrophage activation and function by PPARs. *Circulation Research*, *106*(10), 1559–1569. https://doi.org/10.1161/CIRCRESAHA.110.216523

Cha, J.-Y., & Repa, J. J. (2007). The liver X receptor (LXR) and hepatic lipogenesis. The carbohydrate-response element-binding protein is a target gene of LXR. *The Journal of Biological Chemistry*, *282*(1), 743–751. https://doi.org/10.1074/jbc.M605023200

Chen, Q., Sun, L., & Chen, Z. J. (2016). Regulation and function of the cGAS-STING pathway of cytosolic DNA sensing. *Nature Immunology*, *17*(10), 1142–1149. https://doi.org/10.1038/ni.3558

Chistiakov, D. A., Bobryshev, Y. V., & Orekhov, A. N. (2016). Macrophage-mediated cholesterol handling in atherosclerosis. *Journal of Cellular and Molecular Medicine*, *20*(1), 17–28. https://doi.org/10.1111/jcmm.12689

Chistiakov, D. A., Melnichenko, A. A., Myasoedova, V. A., Grechko, A. V., & Orekhov, A. N. (2017). Mechanisms of foam cell formation in atherosclerosis. *Journal of Molecular Medicine*, *95*(11), 1153–1165. https://doi.org/10.1007/s00109-017-1575-8

Christine, P. J., Young, R., Adar, S. D., Bertoni, A. G., Heisler, M., Carnethon, M. R., Hayward, R. A., & Diez Roux, A. V. (2017). Individual- and area-level SES in diabetes risk prediction: The Multi-Ethnic Study of Atherosclerosis. *American Journal of Preventive Medicine*, *53*(2), 201–209. https://doi.org/10.1016/j.amepre.2017.04.019

Cochain, C., Vafadarnejad, E., Arampatzi, P., Pelisek, J., Winkels, H., Ley, K., Wolf, D., Saliba, A.-E., & Zernecke, A. (2018). Single-Cell RNA-Seq Reveals the Transcriptional Landscape and Heterogeneity of Aortic Macrophages in Murine Atherosclerosis. *Circulation Research*, *122*(12), 1661–1674. https://doi.org/10.1161/CIRCRESAHA.117.312509

Collins, R. G., Velji, R., Guevara, N. V., Hicks, M. J., Chan, L., & Beaudet, A. L. (2000). P-Selectin or intercellular adhesion molecule (ICAM)-1 deficiency substantially protects against atherosclerosis in apolipoprotein E-deficient mice. *The Journal of Experimental Medicine*, *191*(1), 189–194. https://doi.org/10.1084/jem.191.1.189

Cox, B. E., Griffin, E. E., Ullery, J. C., & Jerome, W. G. (2007). Effects of cellular cholesterol loading on macrophage foam cell lysosome acidification. *Journal of Lipid Research*, *48*(5), 1012–1021. https://doi.org/10.1194/jlr.M600390-JLR200

Cui, C., Chakraborty, K., Tang, X. A., Schoenfelt, K. Q., Hoffman, A., Blank, A., McBeth, B., Pulliam, N., Reardon, C. A., Kulkarni, S. A., Vaisar, T., Ballabio, A., Krishnan, Y., & Becker, L. (2021). A lysosome-targeted DNA nanodevice selectively targets macrophages to attenuate tumours. *Nature Nanotechnology*, *16*(12), 1394–1402. https://doi.org/10.1038/s41565-021-00988-z

Curtiss, L. K. (2000). ApoE in Atherosclerosis. *Arteriosclerosis, Thrombosis, and Vascular Biology*, *20*(8), 1852–1853. https://doi.org/10.1161/01.ATV.20.8.1852

Cybulsky, M. I., & Gimbrone, M. A. (1991). Endothelial expression of a mononuclear leukocyte adhesion molecule during atherogenesis. *Science*, *251*(4995), 788–791. https://doi.org/10.1126/science.1990440

da Luz, P. L., Chagas, A. C. P., Dourado, P. M. M., & Laurindo, F. R. M. (2018). Endothelium in atherosclerosis: plaque formation and its complications. In *Endothelium and cardiovascular diseases* (pp. 493–512). Elsevier. https://doi.org/10.1016/B978-0-12-812348-5.00033-7

de Villiers, W. J., & Smart, E. J. (1999). Macrophage scavenger receptors and foam cell formation. *Journal of Leukocyte Biology*, *66*(5), 740–746. https://doi.org/10.1002/jlb.66.5.740

Duan, L.-P., Wang, H. H., Ohashi, A., & Wang, D. Q.-H. (2006). Role of intestinal sterol transporters Abcg5, Abcg8, and Npc1l1 in cholesterol absorption in mice: gender and age

effects. *American Journal of Physiology. Gastrointestinal and Liver Physiology*, *290*(2), G269-76. https://doi.org/10.1152/ajpgi.00172.2005

Duran-Struuck, R., & Dysko, R. C. (2009). Principles of bone marrow transplantation (BMT): providing optimal veterinary and husbandry care to irradiated mice in BMT studies. *Journal of the American Association for Laboratory Animal Science : JAALAS*, *48*(1), 11–22.

Du, M., Wang, X., Mao, X., Yang, L., Huang, K., Zhang, F., Wang, Y., Luo, X., Wang, C., Peng, J., Liang, M., Huang, D., & Huang, K. (2019). Absence of Interferon Regulatory Factor 1 Protects Against Atherosclerosis in Apolipoprotein E-Deficient Mice. *Theranostics*, *9*(16), 4688–4703. https://doi.org/10.7150/thno.36862

Fote, G. M., Geller, N. R., Efstathiou, N. E., Hendricks, N., Vavvas, D. G., Reidling, J. C., Thompson, L. M., & Steffan, J. S. (2022). Isoform-dependent lysosomal degradation and internalization of apolipoprotein E requires autophagy proteins. *Journal of Cell Science*, *135*(2). https://doi.org/10.1242/jcs.258687

Gargalovic, P. S., Imura, M., Zhang, B., Gharavi, N. M., Clark, M. J., Pagnon, J., Yang, W.-P., He, A., Truong, A., Patel, S., Nelson, S. F., Horvath, S., Berliner, J. A., Kirchgessner, T. G., & Lusis, A. J. (2006). Identification of inflammatory gene modules based on variations of human endothelial cell responses to oxidized lipids. *Proceedings of the National Academy of Sciences of the United States of America*, *103*(34), 12741–12746. https://doi.org/10.1073/pnas.0605457103

GBD 2015 Obesity Collaborators, Afshin, A., Forouzanfar, M. H., Reitsma, M. B., Sur, P., Estep, K., Lee, A., Marczak, L., Mokdad, A. H., Moradi-Lakeh, M., Naghavi, M., Salama, J.

S., Vos, T., Abate, K. H., Abbafati, C., Ahmed, M. B., Al-Aly, Z., Alkerwi, A., Al-Raddadi, R., … Murray, C. J. L. (2017). Health Effects of Overweight and Obesity in 195 Countries over 25 Years. *The New England Journal of Medicine*, *377*(1), 13–27. https://doi.org/10.1056/NEJMoa1614362

Gehre, L., Gorgette, O., Perrinet, S., Prevost, M.-C., Ducatez, M., Giebel, A. M., Nelson, D. E., Ball, S. G., & Subtil, A. (2016). Sequestration of host metabolism by an intracellular pathogen. *ELife*, *5*, e12552. https://doi.org/10.7554/eLife.12552

Getz, G. S., & Reardon, C. A. (2012). Animal models of atherosclerosis. *Arteriosclerosis, Thrombosis, and Vascular Biology*, *32*(5), 1104–1115. https://doi.org/10.1161/ATVBAHA.111.237693

Getz, G. S., & Reardon, C. A. (2016). ApoE knockout and knockin mice: the history of their contribution to the understanding of atherogenesis. *Journal of Lipid Research*, *57*(5), 758–766. https://doi.org/10.1194/jlr.R067249

Getz, G. S., & Reardon, C. A. (2018). Apoprotein E and reverse cholesterol transport. *International Journal of Molecular Sciences*, *19*(11). https://doi.org/10.3390/ijms19113479

Ginhoux, F., & Jung, S. (2014). Monocytes and macrophages: developmental pathways and tissue homeostasis. *Nature Reviews. Immunology*, *14*(6), 392–404. https://doi.org/10.1038/nri3671

Gisterå, A., & Hansson, G. K. (2017). The immunology of atherosclerosis. *Nature Reviews. Nephrology*, *13*(6), 368–380. https://doi.org/10.1038/nrneph.2017.51

Gore, M. O., McGuire, D. K., Lingvay, I., & Rosenstock, J. (2015). Predicting cardiovascular risk in type 2 diabetes: the heterogeneity challenges. *Current Cardiology Reports*, *17*(7), 607. https://doi.org/10.1007/s11886-015-0607-7

Gosling, J., Slaymaker, S., Gu, L., Tseng, S., Zlot, C. H., Young, S. G., Rollins, B. J., & Charo, I. F. (1999). MCP-1 deficiency reduces susceptibility to atherosclerosis in mice that overexpress human apolipoprotein B. *The Journal of Clinical Investigation*, *103*(6), 773–778. https://doi.org/10.1172/JCI5624

Gregório, M. J., Rodrigues, A. M., Eusébio, M., Sousa, R. D., Dias, S., André, B., Grønning, K., Coelho, P. S., Mendes, J. M., Graça, P., Espnes, G. A., Branco, J. C., & Canhão, H. (2017). Dietary Patterns Characterized by High Meat Consumption Are Associated with Other Unhealthy Life Styles and Depression Symptoms. *Frontiers in Nutrition*, *4*, 25. https://doi.org/10.3389/fnut.2017.00025

Gupta, S., Pablo, A. M., Jiang, X. c, Wang, N., Tall, A. R., & Schindler, C. (1997). IFN-gamma potentiates atherosclerosis in ApoE knock-out mice. *The Journal of Clinical Investigation*, *99*(11), 2752–2761. https://doi.org/10.1172/JCI119465

Hardy, P.-O., Diallo, T. O., Matte, C., & Descoteaux, A. (2009). Roles of phosphatidylinositol 3-kinase and p38 mitogen-activated protein kinase in the regulation of protein kinase C-alpha activation in interferon-gamma-stimulated macrophages. *Immunology*, *128*(1 Suppl), e652-60. https://doi.org/10.1111/j.1365-2567.2009.03055.x

Hashimoto, D., Chow, A., Noizat, C., Teo, P., Beasley, M. B., Leboeuf, M., Becker, C. D., See, P., Price, J., Lucas, D., Greter, M., Mortha, A., Boyer, S. W., Forsberg, E. C., Tanaka, M., van

Rooijen, N., García-Sastre, A., Stanley, E. R., Ginhoux, F., … Merad, M. (2013). Tissue-resident macrophages self-maintain locally throughout adult life with minimal contribution from circulating monocytes. *Immunity*, *38*(4), 792–804. https://doi.org/10.1016/j.immuni.2013.04.004

Heart Disease Facts | cdc.gov. (n.d.). Retrieved May 18, 2023, from https://www.cdc.gov/heartdisease/facts.htm

Heinecke, N. L., Pratt, B. S., Vaisar, T., & Becker, L. (2010). PepC: proteomics software for identifying differentially expressed proteins based on spectral counting. *Bioinformatics*, *26*(12), 1574–1575. https://doi.org/10.1093/bioinformatics/btq171

He, K., Song, E., Upadhyayula, S., Dang, S., Gaudin, R., Skillern, W., Bu, K., Capraro, B. R., Rapoport, I., Kusters, I., Ma, M., & Kirchhausen, T. (2020). Dynamics of Auxilin 1 and GAK in clathrin-mediated traffic. *The Journal of Cell Biology*, *219*(3). https://doi.org/10.1083/jcb.201908142

Hoeffel, G., Wang, Y., Greter, M., See, P., Teo, P., Malleret, B., Leboeuf, M., Low, D., Oller, G., Almeida, F., Choy, S. H. Y., Grisotto, M., Renia, L., Conway, S. J., Stanley, E. R., Chan, J. K. Y., Ng, L. G., Samokhvalov, I. M., Merad, M., & Ginhoux, F. (2012). Adult Langerhans cells derive predominantly from embryonic fetal liver monocytes with a minor contribution of yolk sac-derived macrophages. *The Journal of Experimental Medicine*, *209*(6), 1167–1181. https://doi.org/10.1084/jem.20120340

Hong, C., & Tontonoz, P. (2014). Liver X receptors in lipid metabolism: opportunities for drug discovery. *Nature Reviews. Drug Discovery*, *13*(6), 433–444. https://doi.org/10.1038/nrd4280

Hopfner, K.-P., & Hornung, V. (2020). Molecular mechanisms and cellular functions of cGAS-STING signalling. *Nature Reviews. Molecular Cell Biology*, *21*(9), 501–521. https://doi.org/10.1038/s41580-020-0244-x

Hu, C., Hardee, D., & Minnear, F. (2007). Membrane fusion by VAMP3 and plasma membrane t-SNAREs. *Experimental Cell Research*, *313*(15), 3198–3209. https://doi.org/10.1016/j.yexcr.2007.06.008

Hu, Q., Li, H., Wang, L., Gu, H., & Fan, C. (2019). DNA Nanotechnology-Enabled Drug Delivery Systems. *Chemical Reviews*, *119*(10), 6459–6506. https://doi.org/10.1021/acs.chemrev.7b00663

Im, S.-S., & Osborne, T. F. (2011). Liver x receptors in atherosclerosis and inflammation. *Circulation Research*, *108*(8), 996–1001. https://doi.org/10.1161/CIRCRESAHA.110.226878

Inaba, T., Ishibashi, S., Harada, K., Osuga, J., Yagyu, H., Ohashi, K., Yazaki, Y., & Yamada, N. (1996). Synergistic effects of transforming growth factor-beta on the expression of c-fms, macrophage colony-stimulating factor receptor gene, in vascular smooth muscle cells. *FEBS Letters*, *399*(3), 207–210. https://doi.org/10.1016/s0014-5793(96)01322-1

Ishibashi, S., Herz, J., Maeda, N., Goldstein, J. L., & Brown, M. S. (1994). The two-receptor model of lipoprotein clearance: tests of the hypothesis in “knockout” mice lacking the low density lipoprotein receptor, apolipoprotein E, or both proteins. *Proceedings of the National Academy of Sciences of the United States of America*, *91*(10), 4431–4435. https://doi.org/10.1073/pnas.91.10.4431

Jaishy, B., & Abel, E. D. (2016). Lipids, lysosomes, and autophagy. *Journal of Lipid Research*, *57*(9), 1619–1635. https://doi.org/10.1194/jlr.R067520

Jeong, S. J., Lee, M. N., & Oh, G. T. (2017). The role of macrophage lipophagy in reverse cholesterol transport. *Endocrinology and Metabolism (Seoul, Korea)*, *32*(1), 41–46. https://doi.org/10.3803/EnM.2017.32.1.41

Joseph, S. B., Laffitte, B. A., Patel, P. H., Watson, M. A., Matsukuma, K. E., Walczak, R., Collins, J. L., Osborne, T. F., & Tontonoz, P. (2002). Direct and indirect mechanisms for regulation of fatty acid synthase gene expression by liver X receptors. *The Journal of Biological Chemistry*, *277*(13), 11019–11025. https://doi.org/10.1074/jbc.M111041200

Jović, M., Kean, M. J., Dubankova, A., Boura, E., Gingras, A.-C., Brill, J. A., & Balla, T. (2014). Endosomal sorting of VAMP3 is regulated by PI4K2A. *Journal of Cell Science*, *127*(Pt 17), 3745–3756. https://doi.org/10.1242/jcs.148809

Kanaoka, Y., Kimura, S. H., Okazaki, I., Ikeda, M., & Nojima, H. (1997). GAK: a cyclin G associated kinase contains a tensin/auxilin-like domain[1]. *FEBS Letters*, *402*(1), 73–80. https://doi.org/10.1016/S0014-5793(96)01484-6

Kawashima, Y., Chen, J., Sun, H., Lann, D., Hajjar, R. J., Yakar, S., & Leroith, D. (2009). Apolipoprotein E deficiency abrogates insulin resistance in a mouse model of type 2 diabetes mellitus. *Diabetologia*, *52*(7), 1434–1441. https://doi.org/10.1007/s00125-009-1378-8

Kirchgessner, T. G., Martin, R., Sleph, P., Grimm, D., Liu, X., Lupisella, J., Smalley, J., Narayanan, R., Xie, Y., Ostrowski, J., Cantor, G. H., Mohan, R., & Kick, E. (2015).

Pharmacological characterization of a novel liver X receptor agonist with partial LXRα activity and a favorable window in nonhuman primates. *The Journal of Pharmacology and Experimental Therapeutics*, *352*(2), 305–314. https://doi.org/10.1124/jpet.114.219923

Kirchgessner, T. G., Sleph, P., Ostrowski, J., Lupisella, J., Ryan, C. S., Liu, X., Fernando, G., Grimm, D., Shipkova, P., Zhang, R., Garcia, R., Zhu, J., He, A., Malone, H., Martin, R., Behnia, K., Wang, Z., Barrett, Y. C., Garmise, R. J., … Frost, R. J. A. (2016). Beneficial and adverse effects of an LXR agonist on human lipid and lipoprotein metabolism and circulating neutrophils. *Cell Metabolism*, *24*(2), 223–233. https://doi.org/10.1016/j.cmet.2016.07.016

Kivimäki, M., Kuosma, E., Ferrie, J. E., Luukkonen, R., Nyberg, S. T., Alfredsson, L., Batty, G. D., Brunner, E. J., Fransson, E., Goldberg, M., Knutsson, A., Koskenvuo, M., Nordin, M., Oksanen, T., Pentti, J., Rugulies, R., Shipley, M. J., Singh-Manoux, A., Steptoe, A., … Jokela, M. (2017). Overweight, obesity, and risk of cardiometabolic multimorbidity: pooled analysis of individual-level data for 120 813 adults from 16 cohort studies from the USA and Europe. *The Lancet. Public Health*, *2*(6), e277–e285. https://doi.org/10.1016/S2468-2667(17)30074-9

Klionsky, D. J., Abdelmohsen, K., Abe, A., Abedin, M. J., Abeliovich, H., Acevedo Arozena, A., Adachi, H., Adams, C. M., Adams, P. D., Adeli, K., Adhihetty, P. J., Adler, S. G., Agam, G., Agarwal, R., Aghi, M. K., Agnello, M., Agostinis, P., Aguilar, P. V., Aguirre-Ghiso, J., … et al. (2016). Guidelines for the use and interpretation of assays for monitoring autophagy (3rd edition). *Autophagy*, *12*(1), 1–222. https://doi.org/10.1080/15548627.2015.1100356

Koelwyn, G. J., Corr, E. M., Erbay, E., & Moore, K. J. (2018). Regulation of macrophage immunometabolism in atherosclerosis. *Nature Immunology*, *19*(6), 526–537. https://doi.org/10.1038/s41590-018-0113-3

Koenig, W., & Khuseyinova, N. (2007). Biomarkers of atherosclerotic plaque instability and rupture. *Arteriosclerosis, Thrombosis, and Vascular Biology*, *27*(1), 15–26. https://doi.org/10.1161/01.ATV.0000251503.35795.4f

Kong, P., Cui, Z.-Y., Huang, X.-F., Zhang, D.-D., Guo, R.-J., & Han, M. (2022). Inflammation and atherosclerosis: signaling pathways and therapeutic intervention. *Signal Transduction and Targeted Therapy*, *7*(1), 131. https://doi.org/10.1038/s41392-022-00955-7

Konstantinov, I. E., Mejevoi, N., & Anichkov, N. M. (2006). Nikolai N. Anichkov and his theory of atherosclerosis. *Texas Heart Institute Journal*, *33*(4), 417–423.

Korolchuk, V. I., & Banting, G. (2002). CK2 and GAK/auxilin2 are major protein kinases in clathrin-coated vesicles. *Traffic*, *3*(6), 428–439. https://doi.org/10.1034/j.1600-0854.2002.30606.x

Kovackova, S., Chang, L., Bekerman, E., Neveu, G., Barouch-Bentov, R., Chaikuad, A., Heroven, C., Šála, M., De Jonghe, S., Knapp, S., Einav, S., & Herdewijn, P. (2015). Selective Inhibitors of Cyclin G Associated Kinase (GAK) as Anti-Hepatitis C Agents. *Journal of Medicinal Chemistry*, *58*(8), 3393–3410. https://doi.org/10.1021/jm501759m

Kypreos, K. E., Morani, P., van Dijk, K. W., Havekes, L. M., & Zannis, V. I. (2001). The amino-terminal 1-185 domain of apoE promotes the clearance of lipoprotein remnants in vivo. The

carboxy-terminal domain is required for induction of hyperlipidemia in normal and apoE-deficient mice. *Biochemistry*, *40*(20), 6027–6035. https://doi.org/10.1021/bi002414a

Lah, T. T., Hawley, M., Rock, K. L., & Goldberg, A. L. (1995). Gamma-interferon causes a selective induction of the lysosomal proteases, cathepsins B and L, in macrophages. *FEBS Letters*, *363*(1–2), 85–89. https://doi.org/10.1016/0014-5793(95)00287-j

Lee, M.-S., & Bensinger, S. J. (2022). Reprogramming cholesterol metabolism in macrophages and its role in host defense against cholesterol-dependent cytolysins. *Cellular & Molecular Immunology*, *19*(3), 327–336. https://doi.org/10.1038/s41423-021-00827-0

Levin, N., Bischoff, E. D., Daige, C. L., Thomas, D., Vu, C. T., Heyman, R. A., Tangirala, R. K., & Schulman, I. G. (2005). Macrophage liver X receptor is required for antiatherogenic activity of LXR agonists. *Arteriosclerosis, Thrombosis, and Vascular Biology*, *25*(1), 135–142. https://doi.org/10.1161/01.ATV.0000150044.84012.68

Libby, P., Ridker, P. M., & Maseri, A. (2002). Inflammation and atherosclerosis. *Circulation*, *105*(9), 1135–1143. https://doi.org/10.1161/hc0902.104353

Libby, P. (2012). Inflammation in atherosclerosis. *Arteriosclerosis, Thrombosis, and Vascular Biology*, *32*(9), 2045–2051. https://doi.org/10.1161/ATVBAHA.108.179705

Libby, P. (2021a). Inflammation in Atherosclerosis-No Longer a Theory. *Clinical Chemistry*, *67*(1), 131–142. https://doi.org/10.1093/clinchem/hvaa275

Libby, P. (2021b). The changing landscape of atherosclerosis. *Nature*, *592*(7855), 524–533. https://doi.org/10.1038/s41586-021-03392-8

Lichtman, A. H., Binder, C. J., Tsimikas, S., & Witztum, J. L. (2013). Adaptive immunity in atherogenesis: new insights and therapeutic approaches. *The Journal of Clinical Investigation*, *123*(1), 27–36. https://doi.org/10.1172/JCI63108

Linton, M. F., Atkinson, J. B., & Fazio, S. (1995). Prevention of atherosclerosis in apolipoprotein E-deficient mice by bone marrow transplantation. *Science*, *267*(5200), 1034–1037. https://doi.org/10.1126/science.7863332

Li, H., Cybulsky, M. I., Gimbrone, M. A., & Libby, P. (1993). An atherogenic diet rapidly induces VCAM-1, a cytokine-regulatable mononuclear leukocyte adhesion molecule, in rabbit aortic endothelium. *Arteriosclerosis and Thrombosis : A Journal of Vascular Biology / American Heart Association*, *13*(2), 197–204. https://doi.org/10.1161/01.atv.13.2.197

Li, H., Freeman, M. W., & Libby, P. (1995). Regulation of smooth muscle cell scavenger receptor expression in vivo by atherogenic diets and in vitro by cytokines. *The Journal of Clinical Investigation*, *95*(1), 122–133. https://doi.org/10.1172/JCI117628

Li, J., & Fan, C. (2021). A DNA nanodevice boosts tumour immunity. *Nature Nanotechnology*, *16*(12), 1306–1307. https://doi.org/10.1038/s41565-021-01002-2

Li, Q., & Bever, C. T. (1997). Interferon-γ induced increases in intracellular cathepsin B activity in THP-1 cells are dependent on RNA transcription. *Journal of Neuroimmunology*, *74*(1–2), 77–84. https://doi.org/10.1016/S0165-5728(96)00208-1

Long, M. E., Gong, K.-Q., Eddy, W. E., Liles, W. C., & Manicone, A. M. (2017). Pharmacologic inhibition of MEK1/2 reduces lung inflammation without impairing bacterial clearance in

experimental Pseudomonas aeruginosa pneumonia. *Pneumonia (Nathan Qld.)*, *9*, 13. https://doi.org/10.1186/s41479-017-0037-y

Loppnow, H., & Libby, P. (1990). Proliferating or interleukin 1-activated human vascular smooth muscle cells secrete copious interleukin 6. *The Journal of Clinical Investigation*, *85*(3), 731–738. https://doi.org/10.1172/JCI114498

Lund-Katz, S., & Phillips, M. C. (2010). High density lipoprotein structure-function and role in reverse cholesterol transport. *Sub-Cellular Biochemistry*, *51*, 183–227. https://doi.org/10.1007/978-90-481-8622-8_7

Luo, J., Yang, H., & Song, B.-L. (2020). Mechanisms and regulation of cholesterol homeostasis. *Nature Reviews. Molecular Cell Biology*, *21*(4), 225–245. https://doi.org/10.1038/s41580-019-0190-7

Lynch, J., Kaplan, G. A., Salonen, R., Cohen, R. D., & Salonen, J. T. (1995). Socioeconomic status and carotid atherosclerosis. *Circulation*, *92*(7), 1786–1792. https://doi.org/10.1161/01.cir.92.7.1786

Mach, F., Sauty, A., Iarossi, A. S., Sukhova, G. K., Neote, K., Libby, P., & Luster, A. D. (1999). Differential expression of three T lymphocyte-activating CXC chemokines by human atheroma-associated cells. *The Journal of Clinical Investigation*, *104*(8), 1041–1050. https://doi.org/10.1172/JCI6993

Mahley, R. W., & Rall, S. C. (2000). Apolipoprotein E: far more than a lipid transport protein. *Annual Review of Genomics and Human Genetics*, *1*, 507–537. https://doi.org/10.1146/annurev.genom.1.1.507

Mannoh, I., Hussien, M., Commodore-Mensah, Y., & Michos, E. D. (2021). Impact of social determinants of health on cardiovascular disease prevention. *Current Opinion in Cardiology*, *36*(5), 572–579. https://doi.org/10.1097/HCO.0000000000000893

Marques, A. R. A., Ramos, C., Machado-Oliveira, G., & Vieira, O. V. (2021). Lysosome (Dys)function in Atherosclerosis-A Big Weight on the Shoulders of a Small Organelle. *Frontiers in Cell and Developmental Biology*, *9*, 658995. https://doi.org/10.3389/fcell.2021.658995

Martín-Timón, I., Sevillano-Collantes, C., Segura-Galindo, A., & Del Cañizo-Gómez, F. J. (2014). Type 2 diabetes and cardiovascular disease: Have all risk factors the same strength? *World Journal of Diabetes*, *5*(4), 444–470. https://doi.org/10.4239/wjd.v5.i4.444

Martin, J. D., Cabral, H., Stylianopoulos, T., & Jain, R. K. (2020). Improving cancer immunotherapy using nanomedicines: progress, opportunities and challenges. *Nature Reviews. Clinical Oncology*, *17*(4), 251–266. https://doi.org/10.1038/s41571-019-0308-z

Matsuzawa, T., Fujiwara, E., & Washi, Y. (2014). Autophagy activation by interferon-γ via the p38 mitogen-activated protein kinase signalling pathway is involved in macrophage bactericidal activity. *Immunology*, *141*(1), 61–69. https://doi.org/10.1111/imm.12168

Mauthe, M., Orhon, I., Rocchi, C., Zhou, X., Luhr, M., Hijlkema, K.-J., Coppes, R. P., Engedal, N., Mari, M., & Reggiori, F. (2018). Chloroquine inhibits autophagic flux by decreasing autophagosome-lysosome fusion. *Autophagy*, *14*(8), 1435–1455. https://doi.org/10.1080/15548627.2018.1474314

McLaren, J. E., & Ramji, D. P. (2009). Interferon gamma: a master regulator of atherosclerosis. *Cytokine & Growth Factor Reviews*, *20*(2), 125–135. https://doi.org/10.1016/j.cytogfr.2008.11.003

McMichael, J. (1979). Fats and atheroma: an inquest. *British Medical Journal*, *1*(6157), 173–175. https://doi.org/10.1136/bmj.1.6157.173

Mc Namara, K., Alzubaidi, H., & Jackson, J. K. (2019). Cardiovascular disease as a leading cause of death: how are pharmacists getting involved? *Integrated Pharmacy Research & Practice*, *8*, 1–11. https://doi.org/10.2147/IPRP.S133088

Miao, M., Wang, X., Liu, T., Li, Y.-J., Yu, W.-Q., Yang, T.-M., & Guo, S.-D. (2023). Targeting PPARs for therapy of atherosclerosis: A review. *International Journal of Biological Macromolecules*, 125008. https://doi.org/10.1016/j.ijbiomac.2023.125008

Miyazaki, M., Hiramoto, M., Takano, N., Kokuba, H., Takemura, J., Tokuhisa, M., Hino, H., Kazama, H., & Miyazawa, K. (2021). Targeted disruption of GAK stagnates autophagic flux by disturbing lysosomal dynamics. *International Journal of Molecular Medicine*, *48*(4). https://doi.org/10.3892/ijmm.2021.5028

Moazed, T. C., Kuo, C., Grayston, J. T., & Campbell, L. A. (1997). Murine models of Chlamydia pneumoniae infection and atherosclerosis. *The Journal of Infectious Diseases*, *175*(4), 883–890. https://doi.org/10.1086/513986

Moore, K. J., Sheedy, F. J., & Fisher, E. A. (2013). Macrophages in atherosclerosis: a dynamic balance. *Nature Reviews. Immunology*, *13*(10), 709–721. https://doi.org/10.1038/nri3520

Moore, K. J., & Tabas, I. (2011). Macrophages in the pathogenesis of atherosclerosis. *Cell*, *145*(3), 341–355. https://doi.org/10.1016/j.cell.2011.04.005

Moradian, H., Roch, T., Lendlein, A., & Gossen, M. (2020). mRNA Transfection-Induced Activation of Primary Human Monocytes and Macrophages: Dependence on Carrier System and Nucleotide Modification. *Scientific Reports*, *10*(1), 4181. https://doi.org/10.1038/s41598-020-60506-4

Morgan, A. C., LaBerge, N., Larremore, D. B., Galesic, M., Brand, J. E., & Clauset, A. (2022). Socioeconomic roots of academic faculty. *Nature Human Behaviour*, *6*(12), 1625–1633. https://doi.org/10.1038/s41562-022-01425-4

Mosammaparast, N., & Pemberton, L. F. (2004). Karyopherins: from nuclear-transport mediators to nuclear-function regulators. *Trends in Cell Biology*, *14*(10), 547–556. https://doi.org/10.1016/j.tcb.2004.09.004

Moss, J. W., & Ramji, D. P. (2015). Interferon-γ: Promising therapeutic target in atherosclerosis. *World Journal of Experimental Medicine*, *5*(3), 154–159. https://doi.org/10.5493/wjem.v5.i3.154

Mroczkiewicz, M., Winkler, K., Nowis, D., Placha, G., Golab, J., & Ostaszewski, R. (2010). Studies of the synthesis of all stereoisomers of MG-132 proteasome inhibitors in the tumor targeting approach. *Journal of Medicinal Chemistry*, *53*(4), 1509–1518. https://doi.org/10.1021/jm901619n

Mullick, A. E., Soldau, K., Kiosses, W. B., Bell, T. A., Tobias, P. S., & Curtiss, L. K. (2008). Increased endothelial expression of Toll-like receptor 2 at sites of disturbed blood flow exacerbates early atherogenic events. *The Journal of Experimental Medicine*, *205*(2), 373–383. https://doi.org/10.1084/jem.20071096

Nakashima, Y., Plump, A. S., Raines, E. W., Breslow, J. L., & Ross, R. (1994). ApoE-deficient mice develop lesions of all phases of atherosclerosis throughout the arterial tree. *Arteriosclerosis and Thrombosis : A Journal of Vascular Biology / American Heart Association*, *14*(1), 133–140. https://doi.org/10.1161/01.ATV.14.1.133

Nandi, S., Ma, L., Denis, M., Karwatsky, J., Li, Z., Jiang, X.-C., & Zha, X. (2009). ABCA1-mediated cholesterol efflux generates microparticles in addition to HDL through processes governed by membrane rigidity. *Journal of Lipid Research*, *50*(3), 456–466. https://doi.org/10.1194/jlr.M800345-JLR200

Napolitano, G., & Ballabio, A. (2016). TFEB at a glance. *Journal of Cell Science*, *129*(13), 2475–2481. https://doi.org/10.1242/jcs.146365

Netter MD, F. H. (2018). *Atlas of Human Anatomy (Netter Basic Science)* (7th ed., p. 640). Elsevier.

Nilsson, J. (1993). Cytokines and smooth muscle cells in atherosclerosis. *Cardiovascular Research*, *27*(7), 1184–1190. https://doi.org/10.1093/cvr/27.7.1184

Noh, H. S., Hah, Y.-S., Zada, S., Ha, J. H., Sim, G., Hwang, J. S., Lai, T. H., Nguyen, H. Q., Park, J.-Y., Kim, H. J., Byun, J.-H., Hahm, J. R., Kang, K. R., & Kim, D. R. (2016). PEBP1, a RAF kinase inhibitory protein, negatively regulates starvation-induced autophagy by direct interaction with LC3. *Autophagy*, *12*(11), 2183–2196. https://doi.org/10.1080/15548627.2016.1219013

Olive, A. J., & Sassetti, C. M. (2016). Metabolic crosstalk between host and pathogen: sensing, adapting and competing. *Nature Reviews. Microbiology*, *14*(4), 221–234. https://doi.org/10.1038/nrmicro.2016.12

Parthasarathy, S., & Rankin, S. M. (1992). Role of oxidized low density lipoprotein in atherogenesis. *Progress in Lipid Research*, *31*(2), 127–143. https://doi.org/10.1016/0163-7827(92)90006-5

Paulo, J. A., Gaun, A., & Gygi, S. P. (2015). Global Analysis of Protein Expression and Phosphorylation Levels in Nicotine-Treated Pancreatic Stellate Cells. *Journal of Proteome Research*, *14*(10), 4246–4256. https://doi.org/10.1021/acs.jproteome.5b00398

Peng, D., Hiipakka, R. A., Dai, Q., Guo, J., Reardon, C. A., Getz, G. S., & Liao, S. (2008). Antiatherosclerotic effects of a novel synthetic tissue-selective steroidal liver X receptor agonist in low-density lipoprotein receptor-deficient mice. *The Journal of Pharmacology and Experimental Therapeutics*, *327*(2), 332–342. https://doi.org/10.1124/jpet.108.142687

Peng, D., Hiipakka, R. A., Reardon, C. A., Getz, G. S., & Liao, S. (2009). Differential anti-atherosclerotic effects in the innominate artery and aortic sinus by the liver X receptor agonist T0901317. *Atherosclerosis*, *203*(1), 59–66. https://doi.org/10.1016/j.atherosclerosis.2008.05.058

Peters, J. P., & Van Slyke, D. D. (1947). Quantitative clinical chemistry. interpretations. *The American Journal of the Medical Sciences*, *213*(6), 757. https://doi.org/10.1097/00000441-194706000-00017

Poole, J. C., & Florey, H. W. (1958). Changes in the endothelium of the aorta and the behaviour of macrophages in experimental atheroma of rabbits. *The Journal of Pathology and Bacteriology*, *75*(2), 245–251. https://doi.org/10.1002/path.1700750202

Possemato, A. P., Paulo, J. A., Mulhern, D., Guo, A., Gygi, S. P., & Beausoleil, S. A. (2017). Multiplexed phosphoproteomic profiling using titanium dioxide and immunoaffinity enrichments reveals complementary phosphorylation events. *Journal of Proteome Research*, *16*(4), 1506–1514. https://doi.org/10.1021/acs.jproteome.6b00905

Powell-Wiley, T. M., Poirier, P., Burke, L. E., Després, J.-P., Gordon-Larsen, P., Lavie, C. J., Lear, S. A., Ndumele, C. E., Neeland, I. J., Sanders, P., St-Onge, M.-P., & American Heart Association Council on Lifestyle and Cardiometabolic Health; Council on Cardiovascular and Stroke Nursing; Council on Clinical Cardiology; Council on Epidemiology and Prevention; and Stroke Council. (2021). Obesity and cardiovascular disease: A scientific statement from the american heart association. *Circulation*, *143*(21), e984–e1010. https://doi.org/10.1161/CIR.0000000000000973

Puhl, R., & Suh, Y. (2015). Health Consequences of Weight Stigma: Implications for Obesity Prevention and Treatment. *Current Obesity Reports*, *4*(2), 182–190. https://doi.org/10.1007/s13679-015-0153-z

Rader, D. J., & Puré, E. (2005). Lipoproteins, macrophage function, and atherosclerosis: beyond the foam cell? *Cell Metabolism*, *1*(4), 223–230. https://doi.org/10.1016/j.cmet.2005.03.005

Raffaï, R. L., Hasty, A. H., Wang, Y., Mettler, S. E., Sanan, D. A., Linton, M. F., Fazio, S., & Weisgraber, K. H. (2003). Hepatocyte-derived ApoE is more effective than non-hepatocyte-derived ApoE in remnant lipoprotein clearance. *The Journal of Biological Chemistry*, *278*(13), 11670–11675. https://doi.org/10.1074/jbc.M212873200

Rakhra, V., Galappaththy, S. L., Bulchandani, S., & Cabandugama, P. K. (2020). Obesity and the western diet: how we got here. *Missouri Medicine*, *117*(6), 536–538.

Ramana, C. V., Gil, M. P., Schreiber, R. D., & Stark, G. R. (2002). Stat1-dependent and -independent pathways in IFN-γ-dependent signaling. *Trends in Immunology*, *23*(2), 96–101. https://doi.org/10.1016/S1471-4906(01)02118-4

Randall, G. (2018). Lipid Droplet Metabolism during Dengue Virus Infection. *Trends in Microbiology*, *26*(8), 640–642. https://doi.org/10.1016/j.tim.2018.05.010

Rasheed, A., & Rayner, K. J. (2021). Macrophage responses to environmental stimuli during homeostasis and disease. *Endocrine Reviews*, *42*(4), 407–435. https://doi.org/10.1210/endrev/bnab004

Reardon, C. A., Lingaraju, A., Schoenfelt, K. Q., Zhou, G., Cui, C., Jacobs-El, H., Babenko, I., Hoofnagle, A., Czyz, D., Shuman, H., Vaisar, T., & Becker, L. (2018). Obesity and Insulin Resistance Promote Atherosclerosis through an IFNγ-Regulated Macrophage Protein Network. *Cell Reports*, *23*(10), 3021–3030. https://doi.org/10.1016/j.celrep.2018.05.010

Redford, Hoyer, J. K. M. (2017). First-GenerationandContinuing-GenerationCollegeStudents:AComparisonofHighSchoolandPostsecondary Experiences.StatsinBrief. *Library of Congress*, 1–18.

Reupert, A., Straussner, S. L., Weimand, B., & Maybery, D. (2022). It takes a village to raise a child: understanding and expanding the concept of the "village". *Frontiers in Public Health*, *10*, 756066. https://doi.org/10.3389/fpubh.2022.756066

Rifkind, B. M. (1984). Lipid Research Clinics Coronary Primary Prevention Trial: results and implications. *The American Journal of Cardiology*, *54*(5), 30C-34C. https://doi.org/10.1016/0002-9149(84)90854-3

Rigamonti, E., Chinetti-Gbaguidi, G., & Staels, B. (2008). Regulation of macrophage functions by PPAR-alpha, PPAR-gamma, and LXRs in mice and men. *Arteriosclerosis, Thrombosis, and Vascular Biology*, *28*(6), 1050–1059. https://doi.org/10.1161/ATVBAHA.107.158998

Rocha, V. Z., & Libby, P. (2009). Obesity, inflammation, and atherosclerosis. *Nature Reviews. Cardiology*, *6*(6), 399–409. https://doi.org/10.1038/nrcardio.2009.55

Rosenson, R. S., Brewer, H. B., Davidson, W. S., Fayad, Z. A., Fuster, V., Goldstein, J., Hellerstein, M., Jiang, X.-C., Phillips, M. C., Rader, D. J., Remaley, A. T., Rothblat, G. H.,

Tall, A. R., & Yvan-Charvet, L. (2012). Cholesterol efflux and atheroprotection: advancing the concept of reverse cholesterol transport. *Circulation*, *125*(15), 1905–1919. https://doi.org/10.1161/CIRCULATIONAHA.111.066589

Runwal, G., Stamatakou, E., Siddiqi, F. H., Puri, C., Zhu, Y., & Rubinsztein, D. C. (2019). LC3-positive structures are prominent in autophagy-deficient cells. *Scientific Reports*, *9*(1), 10147. https://doi.org/10.1038/s41598-019-46657-z

Saha, S., Prakash, V., Halder, S., Chakraborty, K., & Krishnan, Y. (2015). A pH-independent DNA nanodevice for quantifying chloride transport in organelles of living cells. *Nature Nanotechnology*, *10*(7), 645–651. https://doi.org/10.1038/nnano.2015.130

Saikku, P., Leinonen, M., Mattila, K., Ekman, M. R., Nieminen, M. S., Mäkelä, P. H., Huttunen, J. K., & Valtonen, V. (1988). Serological evidence of an association of a novel Chlamydia, TWAR, with chronic coronary heart disease and acute myocardial infarction. *The Lancet*, *2*(8618), 983–986. https://doi.org/10.1016/s0140-6736(88)90741-6

Schenkel, A. R., Mamdouh, Z., & Muller, W. A. (2004). Locomotion of monocytes on endothelium is a critical step during extravasation. *Nature Immunology*, *5*(4), 393–400. https://doi.org/10.1038/ni1051

Schipper, H. S., Prakken, B., Kalkhoven, E., & Boes, M. (2012). Adipose tissue-resident immune cells: key players in immunometabolism. *Trends in Endocrinology and Metabolism*, *23*(8), 407–415. https://doi.org/10.1016/j.tem.2012.05.011

Schultz, J. R., Tu, H., Luk, A., Repa, J. J., Medina, J. C., Li, L., Schwendner, S., Wang, S., Thoolen, M., Mangelsdorf, D. J., Lustig, K. D., & Shan, B. (2000). Role of LXRs in control of lipogenesis. *Genes & Development*, *14*(22), 2831–2838. https://doi.org/10.1101/gad.850400

Schulz, C., Gomez Perdiguero, E., Chorro, L., Szabo-Rogers, H., Cagnard, N., Kierdorf, K., Prinz, M., Wu, B., Jacobsen, S. E. W., Pollard, J. W., Frampton, J., Liu, K. J., & Geissmann, F. (2012). A lineage of myeloid cells independent of Myb and hematopoietic stem cells. *Science*, *336*(6077), 86–90. https://doi.org/10.1126/science.1219179

Shah, P. K. (2014). Biomarkers of plaque instability. *Current Cardiology Reports*, *16*(12), 547. https://doi.org/10.1007/s11886-014-0547-7

Shaulian, E., & Karin, M. (2002). AP-1 as a regulator of cell life and death. *Nature Cell Biology*, *4*(5), E131-6. https://doi.org/10.1038/ncb0502-e131

Shi, C., & Pamer, E. G. (2011). Monocyte recruitment during infection and inflammation. *Nature Reviews. Immunology*, *11*(11), 762–774. https://doi.org/10.1038/nri3070

Sikorski, K., Czerwoniec, A., Bujnicki, J. M., Wesoly, J., & Bluyssen, H. A. R. (2011). STAT1 as a novel therapeutical target in pro-atherogenic signal integration of IFNγ, TLR4 and IL-6 in vascular disease. *Cytokine & Growth Factor Reviews*, *22*(4), 211–219. https://doi.org/10.1016/j.cytogfr.2011.06.003

Skov, M., Tønnesen, C. K., Hansen, G. H., & Danielsen, E. M. (2011). Dietary cholesterol induces trafficking of intestinal Niemann-Pick Type C1 Like 1 from the brush border to

endosomes. *American Journal of Physiology. Gastrointestinal and Liver Physiology*, *300*(1), G33-40. https://doi.org/10.1152/ajpgi.00344.2010

Sreeramkumar, V., & Hidalgo, A. (2015). Bone marrow transplantation in mice to study the role of hematopoietic cells in atherosclerosis. *Methods in Molecular Biology*, *1339*, 323–332. https://doi.org/10.1007/978-1-4939-2929-0_22

Stary, H. C., Chandler, A. B., Glagov, S., Guyton, J. R., Insull, W., Rosenfeld, M. E., Schaffer, S. A., Schwartz, C. J., Wagner, W. D., & Wissler, R. W. (1994). A definition of initial, fatty streak, and intermediate lesions of atherosclerosis. A report from the Committee on Vascular Lesions of the Council on Arteriosclerosis, American Heart Association. *Circulation*, *89*(5), 2462–2478. https://doi.org/10.1161/01.cir.89.5.2462

Steffensen, L. B., Mortensen, M. B., Kjolby, M., Hagensen, M. K., Oxvig, C., & Bentzon, J. F. (2015). Disturbed laminar blood flow vastly augments lipoprotein retention in the artery wall: A key mechanism distinguishing susceptible from resistant sites. *Arteriosclerosis, Thrombosis, and Vascular Biology*, *35*(9), 1928–1935. https://doi.org/10.1161/ATVBAHA.115.305874

Steinberg, D. (2004). Thematic review series: the pathogenesis of atherosclerosis. An interpretive history of the cholesterol controversy: part I. *Journal of Lipid Research*, *45*(9), 1583–1593. https://doi.org/10.1194/jlr.R400003-JLR200

Surana, S., Shenoy, A. R., & Krishnan, Y. (2015). Designing DNA nanodevices for compatibility with the immune system of higher organisms. *Nature Nanotechnology*, *10*(9), 741–747. https://doi.org/10.1038/nnano.2015.180

Sviridov, D., & Bukrinsky, M. (2014). Interaction of pathogens with host cholesterol metabolism. *Current Opinion in Lipidology*, *25*(5), 333–338. https://doi.org/10.1097/MOL.0000000000000106

Tabas, I., & Bornfeldt, K. E. (2016). Macrophage phenotype and function in different stages of atherosclerosis. *Circulation Research*, *118*(4), 653–667. https://doi.org/10.1161/CIRCRESAHA.115.306256

Takahashi, Y., & Smith, J. D. (1999). Cholesterol efflux to apolipoprotein AI involves endocytosis and resecretion in a calcium-dependent pathway. *Proceedings of the National Academy of Sciences of the United States of America*, *96*(20), 11358–11363. https://doi.org/10.1073/pnas.96.20.11358

Tangirala, R. K., Bischoff, E. D., Joseph, S. B., Wagner, B. L., Walczak, R., Laffitte, B. A., Daige, C. L., Thomas, D., Heyman, R. A., Mangelsdorf, D. J., Wang, X., Lusis, A. J., Tontonoz, P., & Schulman, I. G. (2002). Identification of macrophage liver X receptors as inhibitors of atherosclerosis. *Proceedings of the National Academy of Sciences of the United States of America*, *99*(18), 11896–11901. https://doi.org/10.1073/pnas.182199799

Thim, T., Hagensen, M. K., Bentzon, J. F., & Falk, E. (2008). From vulnerable plaque to atherothrombosis. *Journal of Internal Medicine*, *263*(5), 506–516. https://doi.org/10.1111/j.1365-2796.2008.01947.x

Thorp, E., & Tabas, I. (2009). Mechanisms and consequences of efferocytosis in advanced atherosclerosis. *Journal of Leukocyte Biology*, *86*(5), 1089–1095. https://doi.org/10.1189/jlb.0209115

Tomiyama, A. J., Carr, D., Granberg, E. M., Major, B., Robinson, E., Sutin, A. R., & Brewis, A. (2018). How and why weight stigma drives the obesity "epidemic" and harms health. *BMC Medicine*, *16*(1), 123. https://doi.org/10.1186/s12916-018-1116-5

Tontonoz, P., & Mangelsdorf, D. J. (2003). Liver X receptor signaling pathways in cardiovascular disease. *Molecular Endocrinology*, *17*(6), 985–993. https://doi.org/10.1210/me.2003-0061

Trapani, L., Segatto, M., & Pallottini, V. (2012). Regulation and deregulation of cholesterol homeostasis: The liver as a metabolic "power station". *World Journal of Hepatology*, *4*(6), 184–190. https://doi.org/10.4254/wjh.v4.i6.184

Tsubuki, S., Saito, Y., Tomioka, M., Ito, H., & Kawashima, S. (1996). Differential inhibition of calpain and proteasome activities by peptidyl aldehydes of di-leucine and tri-leucine. *Journal of Biochemistry*, *119*(3), 572–576.

Umemura, K., Ohtsuki, S., Nagaoka, M., Kusamori, K., Inoue, T., Takahashi, Y., Takakura, Y., & Nishikawa, M. (2021). Critical contribution of macrophage scavenger receptor 1 to the uptake of nanostructured DNA by immune cells. *Nanomedicine : Nanotechnology, Biology, and Medicine*, *34*, 102386. https://doi.org/10.1016/j.nano.2021.102386

Valenzuela, P. L., Carrera-Bastos, P., Castillo-García, A., Lieberman, D. E., Santos-Lozano, A., & Lucia, A. (2023). Obesity and the risk of cardiometabolic diseases. *Nature Reviews. Cardiology*. https://doi.org/10.1038/s41569-023-00847-5

Vance, J. E., & Vance, D. E. (2008). *Biochemistry of Lipids, Lipoproteins and Membranes (New Comprehensive Biochemistry)* (5th ed., p. 624). Elsevier Science.

van der Wal, A. C., Becker, A. E., van der Loos, C. M., & Das, P. K. (1994). Site of intimal rupture or erosion of thrombosed coronary atherosclerotic plaques is characterized by an inflammatory process irrespective of the dominant plaque morphology. *Circulation*, *89*(1), 36–44. https://doi.org/10.1161/01.cir.89.1.36

van Eijk, M., & Aerts, J. M. F. G. (2021). The Unique Phenotype of Lipid-Laden Macrophages. *International Journal of Molecular Sciences*, *22*(8). https://doi.org/10.3390/ijms22084039

van Steenis, D. J. V. C., David, O. R. P., van Strijdonck, G. P. F., van Maarseveen, J. H., & Reek, J. N. H. (2005). Click-chemistry as an efficient synthetic tool for the preparation of novel conjugated polymers. *Chemical Communications*, *34*, 4333–4335. https://doi.org/10.1039/b507776a

Vart, P., Coresh, J., Kwak, L., Ballew, S. H., Heiss, G., & Matsushita, K. (2017). Socioeconomic Status and Incidence of Hospitalization With Lower-Extremity Peripheral Artery Disease: Atherosclerosis Risk in Communities Study. *Journal of the American Heart Association*, *6*(8). https://doi.org/10.1161/JAHA.116.004995

Vascular medicine: A companion to braunwald's heart disease. (2013). Elsevier. https://doi.org/10.1016/C2009-0-63388-2

Veetil, A. T., Chakraborty, K., Xiao, K., Minter, M. R., Sisodia, S. S., & Krishnan, Y. (2017). Cell-targetable DNA nanocapsules for spatiotemporal release of caged bioactive small

molecules. *Nature Nanotechnology*, *12*(12), 1183–1189. https://doi.org/10.1038/nnano.2017.159

Veetil, A. T., Jani, M. S., & Krishnan, Y. (2018). Chemical control over membrane-initiated steroid signaling with a DNA nanocapsule. *Proceedings of the National Academy of Sciences of the United States of America*, *115*(38), 9432–9437. https://doi.org/10.1073/pnas.1712792115

Venkateswaran, A., Laffitte, B. A., Joseph, S. B., Mak, P. A., Wilpitz, D. C., Edwards, P. A., & Tontonoz, P. (2000). Control of cellular cholesterol efflux by the nuclear oxysterol receptor LXR alpha. *Proceedings of the National Academy of Sciences of the United States of America*, *97*(22), 12097–12102. https://doi.org/10.1073/pnas.200367697

Viola, A., Munari, F., Sánchez-Rodríguez, R., Scolaro, T., & Castegna, A. (2019). The metabolic signature of macrophage responses. *Frontiers in Immunology*, *10*, 1462. https://doi.org/10.3389/fimmu.2019.01462

Virani, S. S., Alonso, A., Benjamin, E. J., Bittencourt, M. S., Callaway, C. W., Carson, A. P., Chamberlain, A. M., Chang, A. R., Cheng, S., Delling, F. N., Djousse, L., Elkind, M. S. V., Ferguson, J. F., Fornage, M., Khan, S. S., Kissela, B. M., Knutson, K. L., Kwan, T. W., Lackland, D. T., … American Heart Association Council on Epidemiology and Prevention Statistics Committee and Stroke Statistics Subcommittee. (2020). Heart Disease and Stroke Statistics-2020 Update: A Report From the American Heart Association. *Circulation*, *141*(9), e139–e596. https://doi.org/10.1161/CIR.0000000000000757

Vue, R. (2021). From First to First: Black, Indigenous, and People of Color First-Generation Faculty and Administrator Narratives of Intersectional Marginality and Mattering as Communal Praxis. *Education Sciences*, *11*(12), 773. https://doi.org/10.3390/educsci11120773

Wagner, E. F., & Nebreda, A. R. (2009). Signal integration by JNK and p38 MAPK pathways in cancer development. *Nature Reviews. Cancer*, *9*(8), 537–549. https://doi.org/10.1038/nrc2694

Wang, J., Tang, B., Liu, X., Wu, X., Wang, H., Xu, D., & Guo, Y. (2015). Increased monomeric CRP levels in acute myocardial infarction: a possible new and specific biomarker for diagnosis and severity assessment of disease. *Atherosclerosis*, *239*(2), 343–349. https://doi.org/10.1016/j.atherosclerosis.2015.01.024

Were The African Proverbs Mentioned At The DNC Really African Proverbs? : Goats and Soda : NPR. (n.d.). Retrieved July 20, 2023, from https://www.npr.org/sections/goatsandsoda/2016/07/30/487925796/it-takes-a-village-to-determine-the-origins-of-an-african-proverb

Williams, D. J., Puhl, H. L., & Ikeda, S. R. (2010). A Simple, Highly Efficient Method for Heterologous Expression in Mammalian Primary Neurons Using Cationic Lipid-mediated mRNA Transfection. *Frontiers in Neuroscience*, *4*, 181. https://doi.org/10.3389/fnins.2010.00181

Williams, N. C., & O'Neill, L. A. J. (2018). A role for the krebs cycle intermediate citrate in metabolic reprogramming in innate immunity and inflammation. *Frontiers in Immunology*, *9*, 141. https://doi.org/10.3389/fimmu.2018.00141

Wong, N. D., & Sattar, N. (2023). Cardiovascular risk in diabetes mellitus: epidemiology, assessment and prevention. *Nature Reviews. Cardiology*. https://doi.org/10.1038/s41569-023-00877-z

Wynn, T. A., Chawla, A., & Pollard, J. W. (2013). Macrophage biology in development, homeostasis and disease. *Nature*, *496*(7446), 445–455. https://doi.org/10.1038/nature12034

Xu, H., Jiang, J., Chen, W., Li, W., & Chen, Z. (2019). Vascular macrophages in atherosclerosis. *Journal of Immunology Research*, *2019*, 4354786. https://doi.org/10.1155/2019/4354786

Xu, J., Wagoner, G., Douglas, J. C., & Drew, P. D. (2009). Liver X receptor agonist regulation of Th17 lymphocyte function in autoimmunity. *Journal of Leukocyte Biology*, *86*(2), 401–409. https://doi.org/10.1189/jlb.1008600

Xu, Q., Bernardo, A., Walker, D., Kanegawa, T., Mahley, R. W., & Huang, Y. (2006). Profile and regulation of apolipoprotein E (ApoE) expression in the CNS in mice with targeting of green fluorescent protein gene to the ApoE locus. *The Journal of Neuroscience*, *26*(19), 4985–4994. https://doi.org/10.1523/JNEUROSCI.5476-05.2006

Xu, X., So, J.-S., Park, J.-G., & Lee, A.-H. (2013). Transcriptional control of hepatic lipid metabolism by SREBP and ChREBP. *Seminars in Liver Disease*, *33*(4), 301–311. https://doi.org/10.1055/s-0033-1358523

Yang, Y., Wang, S., Chen, L., Luo, M., Xue, L., Cui, D., & Mao, Z. (2020). Socioeconomic status, social capital, health risk behaviors, and health-related quality of life among Chinese

older adults. *Health and Quality of Life Outcomes*, *18*(1), 291. https://doi.org/10.1186/s12955-020-01540-8

Yorimitsu, T., & Klionsky, D. J. (2005). Autophagy: molecular machinery for self-eating. *Cell Death and Differentiation*, *12 Suppl 2*(Suppl 2), 1542–1552. https://doi.org/10.1038/sj.cdd.4401765

Yunna, C., Mengru, H., Lei, W., & Weidong, C. (2020). Macrophage M1/M2 polarization. *European Journal of Pharmacology*, *877*, 173090. https://doi.org/10.1016/j.ejphar.2020.173090

Yu, X.-H., Fu, Y.-C., Zhang, D.-W., Yin, K., & Tang, C.-K. (2013). Foam cells in atherosclerosis. *Clinica Chimica Acta*, *424*, 245–252. https://doi.org/10.1016/j.cca.2013.06.006

Zajd, C. M., Ziemba, A. M., Miralles, G. M., Nguyen, T., Feustel, P. J., Dunn, S. M., Gilbert, R. J., & Lennartz, M. R. (2020). Bone Marrow-Derived and Elicited Peritoneal Macrophages Are Not Created Equal: The Questions Asked Dictate the Cell Type Used. *Frontiers in Immunology*, *11*, 269. https://doi.org/10.3389/fimmu.2020.00269

Zegeye, B., El-Khatib, Z., Ameyaw, E. K., Seidu, A.-A., Ahinkorah, B. O., Keetile, M., & Yaya, S. (2021). Breaking Barriers to Healthcare Access: A Multilevel Analysis of Individual- and Community-Level Factors Affecting Women's Access to Healthcare Services in Benin. *International Journal of Environmental Research and Public Health*, *18*(2). https://doi.org/10.3390/ijerph18020750

Zelcer, N., Hong, C., Boyadjian, R., & Tontonoz, P. (2009). LXR regulates cholesterol uptake through Idol-dependent ubiquitination of the LDL receptor. *Science*, *325*(5936), 100–104. https://doi.org/10.1126/science.1168974

Zelcer, N., & Tontonoz, P. (2006). Liver X receptors as integrators of metabolic and inflammatory signaling. *The Journal of Clinical Investigation*, *116*(3), 607–614. https://doi.org/10.1172/JCI27883

Zernecke, A., & Weber, C. (2014). Chemokines in atherosclerosis: proceedings resumed. *Arteriosclerosis, Thrombosis, and Vascular Biology*, *34*(4), 742–750. https://doi.org/10.1161/ATVBAHA.113.301655

Zhang, C. X., Engqvist-Goldstein, A. E. Y., Carreno, S., Owen, D. J., Smythe, E., & Drubin, D. G. (2005). Multiple roles for cyclin G-associated kinase in clathrin-mediated sorting events. *Traffic*, *6*(12), 1103–1113. https://doi.org/10.1111/j.1600-0854.2005.00346.x

Zipes MD, D. P., & Libby MD PhD, P. (2018). *Braunwald's Heart Disease: A Textbook of Cardiovascular Medicine, 2-Volume Set* (11th ed., p. 2128). Elsevier.

Zsigmond, E., Fuke, Y., Li, L., Kobayashi, K., & Chan, L. (1998). Resistance of chylomicron and VLDL remnants to post-heparin lipolysis in ApoE-deficient mice: the role of apoE in lipoprotein lipase-mediated lipolysis in vivo and in vitro. *Journal of Lipid Research*, *39*(9), 1852–1861. Sciwheel inserting bibliography...